UCRL 9579

UNIVERSITY OF CALIFORNIA

Ernest O. Lawrence

Radiation Laboratory

INORGANIC MATERIALS DIVISION ANNUAL REPORT, 1960

DISCLAIMER

Research and Development

UCRL-9579
UC-4 Chemistry
TID-4500 (16th Ed.)

UNIVERSITY OF CALIFORNIA
Lawrence Radiation Laboratory
Berkeley, California

Contract No. W-7405-eng-48

INORGANIC MATERIALS DIVISION ANNUAL REPORT, 1960

February 21, 1961

Printed in USA. Price $2.50. Available from the
Office of Technical Services
U. S. Department of Commerce
Washington 25, D.C.

INORGANIC MATERIALS DIVISION ANNUAL REPORT, 1960

Contents

METALLURGY AND CERAMICS

INORGANIC MATERIALS DIVISION ANNUAL REPORT, 1960

Kenneth S. Pitzer in charge

Lawrence Radiation Laboratory, Department of Chemistry,
and Department of Mineral Technology,
University of California, Berkeley, California

February 21, 1961

INORGANIC MATERIALS DIVISION PROGRAM: GENERAL INTRODUCTION

The inorganic materials program is concerned with the material environment in which atomic energy processes can be carried out most effectively. In many cases the nuclear reactions are now sufficiently well understood that the limiting factor in effective applications arises from materials in fuel system, moderator, structure, etc. The research in this division is directed primarily toward basic knowledge out of which new or improved solutions to these materials problems will arise. Considerable emphasis is being placed on investigations of selected substances at very high temperatures. This is a relatively unexplored area in which the potential for major scientific advance is great. Also higher temperature is a major factor in the more effective utilization of nuclear energy.

Our investigations are directed primarily toward the mechanical and chemical properties of materials and toward the atomic factors which determine these properties. General principles are sought from which these properties may be predicted for large groups of substances over wide temperature ranges and in different states of fabrication. Thermal, electrical and other properties are also being investigated.

The program in the inorganic materials area has the dual purpose of basic research of direct or indirect interest to the AEC and of research training in the inorganic materials area for graduate students and young postdoctoral appointees. The future progress in this area will be forwarded not only by the knowledge gained directly through this program but also by the utilization of the increased supply of able research men by employment in AEC projects elsewhere.

This report is organized into three sections on the basis of the AEC program categories under which the work is budgeted. This classification conforms substantially with the academic departments with which the professorial members of our staff are affiliated.

The first section comprises the program in chemistry which has been traditionally a part of the Lawrence Radiation Laboratory and has been under AEC financing for some time. This section includes activities in high-temperature and general inorganic chemistry and in the physics and chemistry of the solid state.

The second general section concerns work in the fields of ceramics and metallurgy. Activities in this field are at present in the course of transfer to AEC budgeting through the Lawrence Radiation Laboratory. Most of the work described in this section was financed by funds from other agencies or from the AEC through other contracts, but is included to give a partial picture of the previous program in this field.

A third section concerns materials investigations in nuclear engineering which are financed under the reactor technology category. This work was started July 1, 1960 and is therefore just barely under way at present. In future years the program in reactor technology is expected to link practical reactor problems with the remainder of the program and to constitute a means by which certain basic discoveries may be carried into the initial states of practical application.

CHEMISTRY

I A. HIGH-TEMPERATURE CHEMISTRY

1. DISSOCIATION ENERGIES OF GASEOUS METAL DIOXIDES*

Leo Brewer and Gerd M. Rosenblatt

A considerable amount of equilibria data involving gaseous metal dioxides has become available in recent years. However, it has been difficult to treat these data thermodynamically. Temperature-dependent errors have limited the reliability of enthalpies obtained by use of the second law of thermodynamics. The use of the third law of thermodynamics has been handicapped by the fact that no spectroscopic data are known which would allow fixing of the electronic, vibrational, or rotational partition functions. Nevertheless the data have generally been treated by a third-law method, with each author using a different set of assumptions for calculating the free energy functions of the gaseous molecules. The resultant enthalpies obtained through use of free energy functions based on different calculation procedures have not been self-consistent. The prediction of high-temperature chemical behavior in rocket exhausts, in high-temperature nuclear reactors, and in other high-temperature systems where a variety of elements must be considered requires the use of data that are self-consistent so that comparisons can be made even though absolute accuracy may be poor.

A simple and straightforward procedure for calculating free energy functions has been developed so that the high-temperature equilibria data may be treated in a consistent manner. The electronic partition functions for the gaseous metal dioxides have been estimated by assuming them to be the same as the electronic partition functions for the free gaseous 4+ ions.[1] The rotational partition functions have been calculated by using the same internuclear distances observed for the corresponding diatomic oxides.[2] Likewise, the vibrational frequencies have been obtained from the force constants of the diatomic molecules,[3] assuming a fixed ratio between bending- and stretching-force constants. It has been assumed that all the metallic dioxides have a linear structure. In a few cases in which no data exist from which to calculate the electronic contribution, the free energy functions could be calculated from vapor pressure measurements and the second law of thermodynamics. These experimental free energy functions have been joined smoothly to the calculated ones to yield interpolated values for oxides

*Condensed form of a paper (same authors and title) to be published in Chem. Rev., 1961 (UCRL-9437, Oct. 1960).

[1] C. Moore, Atomic Energy Levels, National Bureau of Standards Circular 467, Vols. I, II, III (1949-58).

[2] L. E. Sutton, Tables of Interatomic Distances and Configuration in Molecules and Ions, Special Publication No. 11, (The Chemical Society, London, 1958).

[3] B. Rosen, Donneés Spectroscopiques Concernant les Molecules Diatomiques (Hermann and Cie, Paris, 1951).

of intermediate elements. The entropy and enthalpy data tabulated by Kelley[4] and Kelley and King[5] for the condensed oxide phases have been used together with this set of consistent free energy functions for the gaseous molecules to treat the available equilibria data and to obtain enthalpies of formation and dissociation energies of the gaseous metal dioxide molecules. These have been found to vary in a rather smooth fashion across the periodic table, thus allowing the prediction of missing values. The final tables of thermodynamic data list free energy functions for twenty-two gaseous metal dioxides and enthalpies of dissociation for twenty-eight gaseous dioxides.[6]

[4] K. K. Kelley, Contributions to the Data on Theoretical Metallurgy. XIII, Bureau of Mines Bulletin 584 (1960).

[5] K. K. Kelley and E. G. King, Contributions to the Data on Theoretical Metallurgy. XIV, Bureau of Mines Bulletin (in press).

[6] The description of the calculation procedures and the final tables of thermodynamic data are to appear in Chemical Reviews in 1961, but an advance copy of the paper is being distributed as UCRL-9437.

2. DISSOCIATION ENERGIES OF GASEOUS DIATOMIC ALKALI HALIDES

Leo Brewer and Elizabeth Brackett

The literature values of internuclear distances and vibrational frequencies of the alkali halide diatomic molecules have been reviewed. Missing values have been estimated, and complete tables of free energy functions between 298 and 2000 °K have been tabulated. In a similar fashion heat-capacity data and enthalpies of fusion have been used to calculate free energy functions for the condensed phases of the alkali halides.

All available vapor pressure data for the alkali halides have been treated by an approximate third-law method to provide a sensitive method of comparison of various determinations and to allow establishment of a best total vapor pressure curve for each alkali halide.

The total vapor pressure values have been converted to fugacities of the diatomic molecule through use of vapor density measurements, velocity selection measurements, and mass spectrometer measurements which yield data on the degree of imperfection of the gas or the extent of polymeric species in the vapor. After correction for imperfection of the vapors, the resultant fugacities were combined with the calculated free energy functions to yield enthalpies of sublimation. A Born-Haber-type cycle was then used to calculate dissociation energies of the gaseous diatomic molecules to free gaseous ions. Comparison of these dissociation energies with those calculated on the basis of a simple electrostatic model with dipole polarization[1] showed excellent agreement. It is concluded that the heats of sublimation as well as

[1] J. Berkowitz, J. Chem. Phys. 29, 1386 (1958).

all the auxiliary thermodynamic data for the alkali halides are known to the order of 1 kcal/mole. In spite of the excellent agreement between the experimental and theoretical dissociation energies it is concluded that the electrostatic model must be used with some caution, as there surely must be some cancellation of errors in the theoretical model to obtain the excellent agreement that has been observed.

3. THE ULTRAVIOLET SPECTRA OF MgOH AND MgO

Leo Brewer and Sandor Trajmar

In spite of the importance of MgO as a refractory material the vaporization processes of MgO are still not firmly established.[1] Magnesium oxide vapor characteristically shows a number of spectra bands in emission or absorption. A number of these bands have been analyzed[2, 3, 4] and have been shown to be due to the diatomic molecule MgO. A rather complex band around 3800 A has not been susceptible of analysis in the past,[5] and there have been indications[5, 6] that the band is due to a mixture of two band systems, one associated with MgOH, and the other with some oxide of Mg. This band system has been studied in the King furnace and in a vacuum arc with elimination of water which is normally associated with magnesium oxide and with addition of hydrogen or oxygen. These variations have shown that the band system is indeed a composite of two separate systems: one of these, which is undoubtedly due to the molecule MgOH, virtually disappears if the magnesium oxide is thoroughly dried and all sources of water and hydrogen are minimized. Addition of hydrogen shows approximately the square-root dependence of intensity upon hydrogen pressure that one would expect for the MgOH molecule. The MgH spectrum can be observed at the same time. The hydroxide and the MgH spectra are observed to vary together as hydrogen partial pressure is varied. Comparison of the spectra with the known MgO spectra shows that they vary together when the magnesium oxide activity is varied.[7] Thus, there is rather good evidence to fix the formula of the hydroxide emitter as MgOH. Because of the difficulty of observing the oxide spectrum free of contamination by the hydroxide spectra, it has not been possible to carry out accurate mass-law experiments to fix the number of magnesium and the number of oxygen atoms per molecule. The spectrum appears complicated enough so that it might well be due to a polymer such as Mg_2O_2. On the other hand, some triplet systems of the diatomic molecule MgO might have similar complexity. It is planned to take an exposure of

---

[1] L. Brewer and A. W. Searcy, Ann. Rev. Phys. Chem. 7, 259 (1956).

[2] P. C. Mahanti, Indian J. Phys. 9, 455 (1935).

[3] R. F. Barrow and D. V. Crawford, Proc. Phys. Soc. (London) 57, 12 (1945).

[4] A. Lagerquist and V. Uhler, Arkiv. Fysik 1, 459 (1949).

[5] A. G. Gaydon and D. Pesic, Proc. Phys. Soc. (London) A 73, 244 (1959).

[6] E. M. Bulewicz and T. M. Sugden, Trans. Faraday Soc. 55, 720 (1959).

[7] L. Brewer and R. Porter, J. Chem. Phys. 22, 1867 (1954).

the oxide band under hydrogen-free conditions on the 21-ft spectrograph. Professor John Phillips of the Department of Astronomy has offered to process such a plate with his line-measuring equipment and to supply the resulting measurements to the high-speed computer for possible analysis. Although a few more experiments will be carried out in an effort to obtain more accurate mass-law measurements, we have essentially reached the limit of our equipment, and it will probably not be possible for us to fix the exact formula of the oxide species.

4. THERMODYNAMICS OF THERMOCELLS WITH FUSED OR SOLID ELECTROLYTES*

Kenneth S. Pitzer

The thermodynamic principles related to thermocells are applied to cells with pure metal electrodes and simple MX_ν electrolytes, where X is a halogen or nitrate. The definitions and terminology of Agar and Breck are followed.[1] The EMF of the cell E is defined as the electrical potential of a wire attached to the hot electrode less the potential of a similar wire attached to the cold electrode. The electrical work for ν equivalents of electricity is determined by the entropy absorbed from the heat reservoir surrounding the hot electrode when this positive electricity passes through the cell from the cold to the hot electrode. This entropy is equal to the sum of the entropy absorbed in the electrode reaction, in this case $\underline{S}_M - \bar{\underline{S}}_{M^{+\nu}} - \nu\bar{S}_{e^-(M)}$, and the entropy transported away from the hot electrode region, in this case $-\underline{S}^*_{M^{+\nu}} - \nu S^*_{e^-(M)}$. Here $\underline{S}_M$ is the molal entropy of the metal, $\bar{\underline{S}}_{M^{+\nu}}$ and $\underline{S}^*_{M^{+\nu}}$ are the partial molal entropy and the entropy of transfer, respectively, of the $M^{+\nu}$ ion, and $\bar{S}_{e^-(M)}$ and $S^*_{e^-(M)}$ are the corresponding properties of the electron in the metal M. These terms may be combined to yield

$$\nu F \frac{dE}{dT} = S_M - \bar{\underline{S}}_{M^{+\nu}} - \nu\bar{\underline{S}}_{e^-(M)} , \qquad (1)$$

where $\bar{\underline{S}}_{M^{+\nu}}$, the total "transported entropy" of the ion $M^{+\nu}$, is the sum of the partial molal entropy of the ion and the entropy of transfer. The quantity $\bar{\underline{S}}_{e^-(M)}$ is, similarly, the "transported entropy" of electrons in the metal M. Note that the transference number does not appear in Eq. (1).

In Eq. (1) the first quantity on the right is just the molal entropy of the metal, which is available from heat capacity data and the third law.[2] Recently

*Brief form of published paper, J. Phys. Chem. 65, 147 (1961).

[1] J. N. Agar and W. G. Breck, Trans. Faraday Soc. 53, 167 (1957).

[2] D. R. Stull and G. C. Sinke, Thermodynamic Properties of the Solvents (American Chemical Society, Washington, D. C., 1958).

Tempkin and Khoroshin have given values for $\bar{S}_{e^-}$ in several metals;[3] these values are zero within the uncertainty of presently available thermocell data. Thus Eq. (1) yields $\bar{S}_{M^{+\nu}}$ from experimental thermocell potentials. Several values obtainable from the literature for fused salts are listed in Table I.

Table I. Thermocells with fused salt electrolytes

Electrolyte	Ref.	T (°K)	S_M	$-\nu F \frac{dE}{dT}$	$\bar{S}_{M^{\nu+}}$	$\bar{S}_{M^{\nu+}}$	$S^*_{M^{\nu+}}$
$AgNO_3$	6, 7	500	13.37	7.6	21.0	19	2
AgCl	5, 6, 8	800	16.43	9.3	26	22	4
AgBr	5, 8	750	16.00	11.	27	22	5
AgI	5, 8	850	16.84	10.	27	24	3
$ZnCl_2$	4	≈ 600	14.41	-6	8	14	-6
$SnCl_2$	4	≈ 600	20.59	+1	22	16	+6

Although it is not yet experimentally feasible to measure directly the partial molal entropies of individual ions, a rather convincing theoretical calculation seems possible in favorable cases. Consider first a fused salt wherein the positive and negative ions are identical in every respect except for the sign of the net electrical charge on each. In this case clearly the symmetry of the situation allows one to divide the measured molal entropy equally between the positive and negative ions.

Next consider the effects of various differences between the ions. The mass effect on the translational entropy is well known, and gives a difference $(3/2)\ R \ln (M_2/M_1)$ between the entropies of species of molecular weights M_2 and M_1. Moderate differences in the short-range forces that determine ion size should have no effect, since ions of the same sign seldom contact one another. Consequently the entropy of the metal ion in a simple binary salt is given by the expression

$$\bar{S}_{M^+} = \frac{1}{2}\left(S_{MX} + \frac{3}{2} R \ln \frac{M_M}{M_X}\right). \qquad (2)$$

The entropies of free rotation and of vibration of polyatomic ions are readily calculated by standard methods and can be subtracted from the total entropy before apportionment of the translation entropy. In actual cases, however, the rotation is usually somewhat restricted. If a reasonable estimate can be made of the potential barrier restricting the rotation, then the net internal entropy can also be estimated.

[3] M. I. Tempkin and A. V. Khoroshin, Zhur. Fiz. Khim. 26, 500 (1952).

[4] L. Poincare, Ann. chim. phys. [6] 21, 289 (1890).

[5] H. Reinhold and A. Blachny, Z. Elektrochem. 39, 290 (1933); H. Reinhold, Z. anorg. allgem. chem. 171, 181 (1928).

[6] H. Holtan, Thesis, Utrecht, 1953; Tidssk. Kjemi, Bergvensan Met., 12, 5 (1952).

[7] B. R. Sundheim and J. Rosenstreich, J. Phys. Chem. 63, 419 (1959).

[8] B. F. Markov, Doilady Akad. Nauk SSSR 108, 115 (1956).

If one type of ion is very much larger than the other, then there are direct short-range repulsive contacts of the large ions. In such cases one expects the freedom of translational motion of the large ions to be less than that of the small ions.

If we apply these methods to $AgNO_3$ at 500 °K and assume a 4.5-cal/deg mole reduction in rotational entropy of NO_3^- from restriction of rotation, the net internal entropy of NO_3^- is 19.7 cal/deg mole. The heat capacity of silver nitrate has been measured and the data as summarized by Kelley[9] yield the entropy value 54.04 cal/deg mole at 500 °K. With the mass correction of Eq. (2) one then finds $\bar{S}_{Ag^+}$ = 19.0 cal/deg mole in fused $AgNO_3$ at 500 °K.

The calculation of the partial molal entropy of silver ion in the fused halides follows the same principles but is simplified by the absence of internal entropy for the anions. The results, based upon Kelley's tables, are given in Table I. No correction has been made for anion-anion repulsions in these values; such effects would further restrict anion motion and reduce the anion entropy. Consequently, the cation entropies would be increased by this effect, which may or may not be significantly large.

The last column in Table I gives the values of the entropy of transfer which follow from the experimental data and our calculation of the absolute ion entropies. In a simple MX salt in the liquid state all the ions are presumably free to migrate without large activation energy. Nothing in the nature of the fused salt seems to indicate any other source of significant heat of transfer. Consequently, we expect the heat and entropy of transfer to be small for the various silver salts. The values of $\underline{S}^*$ in Table I are indeed small and may be further reduced by a modest correction to $\bar{S}$ for anion-anion repulsion effects.

The information on thermocells with solid electrolytes is treated in an analogous fashion with consideration of the more complex transport mechanisms in the solid state.

---

[9] K. K. Kelley, U. S. Bureau of Mines Bulletins 477 and 584 (U. S. Government Printing Office, Washington, D. C., 1950 and 1960).

5. EQUILIBRIUM PROPERTIES OF HYDROGEN GAS FROM 5,000 TO 20,000 °K*

Oktay Sinanoglu, M. S. Vardya,† and Earl M. Mortensen

The equation of state and thermodynamic properties of hydrogen gas from 5000 to 20,000 °K and up to about 50 to 100 atm are well represented by those of monatomic hydrogen with imperfections given by the second virial coefficient, B(T). Only the $^1\Sigma$ and $^3\Sigma$ states of H_2 are important. Calculations were made on this basis. The contribution of $^1\Sigma$ to B(T) is computed from the theory of Sinanoglu and Pitzer for the Rydberg potential which is good for this state. The contribution of the $^3\Sigma$ state is calculated by using the potential energy given by James, Coolidge, and Present[2] for interatomic separations of 0 to 2 au, the calculations by Hirshfelder and Linnett[3] in the range 2 to 12 au, and the results of Pauling and Beach[4] for distances greater than 12 au. Results are given at 200° intervals between 5000 and 20,000 °K for B(T), and include corrections from ideal behavior for the enthalpy, heat capacity, and entropy.

*A paper is now in preparation on this work.

†Astronomy Department, University of California, Berkeley.

[1]O. Sinanoglu and K. S. Pitzer, Equation of State and Thermodynamic Properties of Gases at High Temperatures. I. Diatomic Molecules, UCRL-8685, March 1959.

[2]H. M. James, A. S. Coolidge, and R. D. Present, J. Chem. Phys. 4, 187, 193 (1936).

[3]J. O. Hirschfelder and J. W. Linnett, J. Chem. Phys. 18, 130 (1950).

[4]L. Pauling and J. Y. Beach, Phys. Rev. 47, 686 (1935).

6. FURTHER CALCULATIONS OF THE PROPERTIES OF C_2

Enrico Clementi and Kenneth S. Pitzer

The wave function previously developed[1] for the molecule C_2 has been applied to a number of related problems.

The probabilities for nine electronic transitions among low excited states in the C_2 molecule have been calculated,[2] and are given in form of the oscillator strength, or f values. Particular emphasis is given to the computation of the amount of hybridization in the σ_u 2s and σ_g 2p molecular orbitals. For the Swan transition an f value of 0.048 is calculated, which may be compared to the experimental values of 0.037 reported in literature.

[1]E. Clementi and K. S. Pitzer, J. Chem. Phys. 32, 656 (1960).

[2]E. Clementi, Astrophys. J. 132, 898 (1960).

Recent theoretical and experimental data on the C_2 molecule make feasible a critical recalculation of the molecular abundance S of the C_2 molecule in the solar reversing system.[3] The molecular excitation temperature adopted is 4500 °K. The required partition functions were calculated with inclusion of all the low-lying excited states. By using an oscillator strength f = 0.04, we obtained log S = 12.84. (A table of thermodynamic functions in the temperature range 2000 to 6000 °K has been prepared.)

The spin-orbit perturbation is shown to be responsible for the Ballik and Ramsay rotational perturbation between the $^1\Sigma_g^+$(a) ground state and the excited $^3\Sigma_g^-$(c) state. It is shown that one must take into consideration the configuration interaction between the $^1\Sigma_g^+$(a) and the $^1\Sigma_g^+$(c) states, whereupon the calculated perturbation compares satisfactorily to an estimated experimental perturbation of 2 cm^{-1}.

The oscillator strength and the lifetime for the $^3\Pi_u$(b) - $^1\Sigma_g^+$(a) transition are calculated.

Not only the one-center integrals but also the two-center integrals in the spin-orbit coupling have strong Z dependency. This provides a better theoretical basis for the "Z effect" in phosphorescence mechanism.

---

[3] E. Clementi, Astrophys. J. (Jan. 1961).

7. CURRENT INVESTIGATIONS ON HIGH-TEMPERATURE CHEMISTRY, 1961

A. Under Supervision of Leo Brewer

1. The development of an apparatus for the determination of radiative lifetimes of excited electronic states of high-temperature molecules is continuing, and the apparatus should be ready for measurements in 1961. (With R. A. Berg, Gerd M. Rosenblatt, and Sandor Trajmar.)

2. Absolute light-intensity measurements of emission from the King furnace are being carried out in preparation for the use of radiative lifetimes for the determination of enthalpy of formation of values through third-law calculations. (With Lucy Hagan.)

3. The vapor pressure data for metallic dihalides are being treated by a third-law method through use of calculated free energy functions to obtain enthalpies of formation for the gaseous metal dihalide molecules. (With G. R. Somayajulu.)

4. The vapor pressure data for diatomic oxides of the elements are being treated by a third-law method using calculated free energy functions to obtain enthalpies of formation of the gaseous diatomic oxides. (With Gerd M. Rosenblatt.)

B. Under Supervision of K. S. Pitzer

1. Spectral studies of high-temperature vapor species trapped in inert matrices at low temperatures.

2. Theoretical studies of high-temperature systems.

3. Investigation of the transition between metallic and nonmetallic binding through experimental--principally spectroscopic--measurements, appropriate systems, and theoretical studies.

4. Nuclear magnetic resonance and electron spin resonance measurements on systems related to the preceding topics.

C. Under Supervision of John A. Howe

1. The high-temperature microwave spectrometer is complete except for the absorption cell, which is currently under construction.

I B. SOLID-STATE PHYSICS AND CHEMISTRY

1. HEAT CAPACITY OF FERROMAGNETIC SUPERCONDUCTORS*

Norman E. Phillips

Recently, solid solutions of elements and intermetallic compounds have been discovered in which superconductivity and ferromagnetism appear to coexist.[1] A question of central interest which cannot be answered by magnetic susceptibility measurements is whether the whole sample is both superconducting and ferromagnetic or whether, for example, superconductivity is confined to small regions of the sample.[2] This note presents results of some preliminary calorimetric measurements which show both a superconducting transition in a ferromagnet and a spin alignment taking place in a superconductor. The measurements also indicate that superconductivity and ferromagnetism exist simultaneously throughout the whole sample.

Figure I B. 1-1 shows the heat capacity of two samples belonging to the system $Y_{1-x}Gd_xOs_2$, between 1.1 and 4.2 °K. In this range it is considerably in excess of that to be expected for the lattice and conduction electrons alone. The observed entropy is in each case only 50% of the xRln8 that would be expected for the complete ordering of the gadolinium spins, but the shape of the curves is consistent with association of an entropy of that amount with the total heat capacity anomaly. Susceptibility measurements on similar samples show that the ferromagnetic Curie point, T_c, for the $Gd_{0.075}$ sample is 3.1 °K. For the $Gd_{0.04}$ sample the presence of superconductivity makes the measurement of T_c by that technique difficult, but an extrapolation from higher gadolinium concentrations gives 1.4 °K. The heat capacity maxima are, respectively, 2.5 °K and below 1.1 °K. This correlation must be considered satisfactory in view of the width of the transition and the different nature of the two measurements. At temperatures above the Curie point both samples have a heat capacity which increases with increasing magnetic field, as expected for paramagnetic materials. The one exception occurs for the $Gd_{0.04}$ sample near 3.6 °K, which is the superconducting transition temperature observed in the susceptibility measurements. Here the heat capacity decreases in small fields in the way expected for a superconductor just below its transition temperature, but then starts to increase in larger fields. The maximum decrease with field, 8 millijoules/mole-deg, gives a lower limit for the difference in heat capacity between the normal and superconducting states. For a pure metal with electronic heat capacity γT this difference is about 1.4 γT_s at the superconducting transition temperature, T_s. In the present case the transition is spread over a 10% range of temperature in the way typical of solid solutions and, although the maximum difference depends to a certain extent on the shape of the distribution, it can be expected to be approximately γT_s. The assumption that the whole sample becomes superconducting leads then to a minimum value for γ of 2.3 millijoules/mole-deg^2, which is of the usual order of magnitude. For example, pure Os has a γ of 1.1 millijoules/mole-deg^2.

---

*This work, carried out in collaboration with Dr. B. T. Matthias of the Bell Telephone Laboratories, Murray Hill, New Jersey, has been reported in Phys. Rev. 121, 105 (1961).

[1] Suhl, Matthias, and Corenzwit, J. Phys. Chem. Solids 11, 346 (1959).

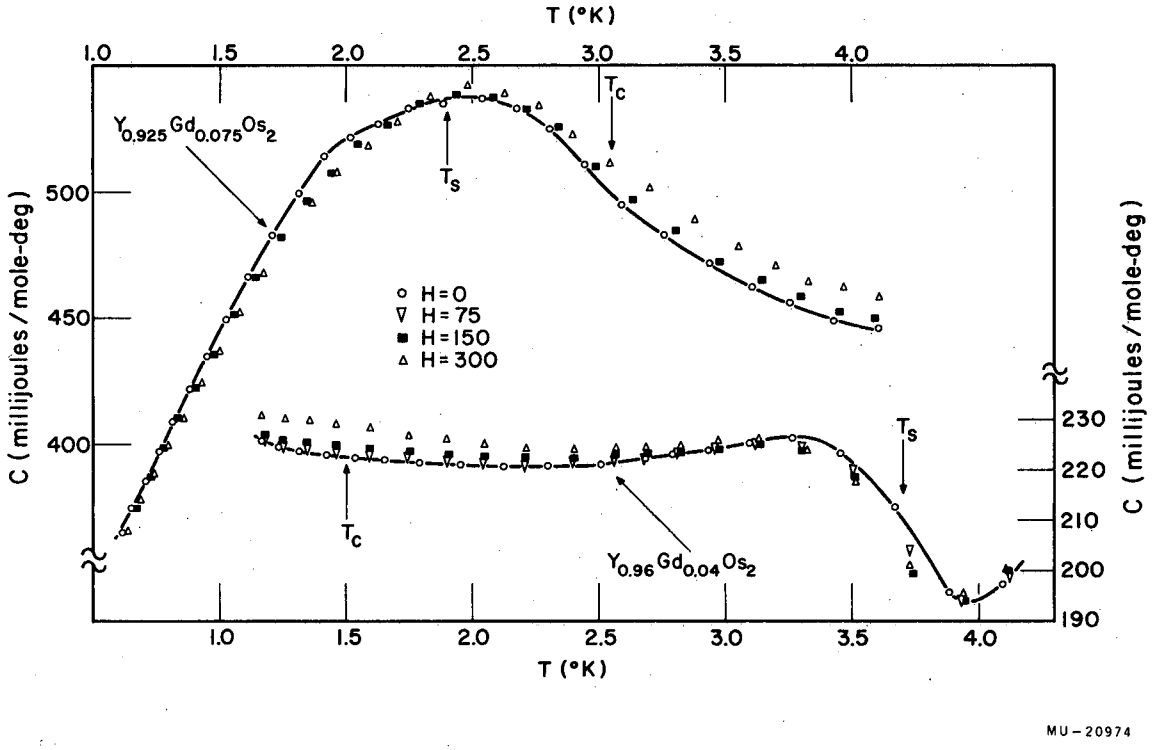

Fig. IB. 1-1. Heat capacity of solid solutions of $GdOs_2$ in YOs_2. T_c and T_s are respectively the ferromagnetic Curie point and superconducting transition temperature obtained by magnetic susceptibility measurements.

For the $Gd_{0.075}$ sample the superconducting transition occurs below the ferromagnetic Curie point. In this case there is a bump about 2% in the zero-field heat capacity relative to that in fields of 150 and 300 gauss. The heat capacity seems to approach a constant value as the field is increased, and the apparent value of γ is 4.0 millijoules/mole-deg^2. This result shows that superconductivity is not confined to a small fraction of the sample, as seemed possible from the susceptibility measurements,[2] but probably occupies the whole volume.

It is interesting that external fields of a few hundred gauss can destroy superconductivity in a ferromagnet for which the field associated with the saturation moment is several times as great. This observation is consistent with the fact that the energy of interaction of the saturation moment with the external field is greater than the superconducting energy, and with the result of Anderson and Suhl that the range of ferromagnetic ordering in a superconductor must be small compared with the coherence length.[3]

Figure I B, 1-2 shows the heat capacity of two solid solutions of gadolinium in lanthanum. The measurements below 1.1 °K were made in an adiabatic demagnetization calorimeter. The behavior of the 0.7% gadolinium sample at temperatures between 0.3 and 1.1° is complicated by thermal hysteresis and a spontaneous evolution of heat following some of the heating periods and lasting for several minutes. In some cases the temperature of the sample suddenly jumped by several tenths of a degree. We believe that these effects are all associated with the exposure of the sample to a magnetic field during cooling: no such effects were observed above 1.1 °K. Between 0.6° and 1.1 °K it was possible to make measurements without having exposed the sample to the field of the main magnet, and results obtained this way are generally higher, show no spontaneous heating, and are the only ones that join the measurements at higher temperatures. On the assumption that the correct heat capacity between 0.3 and 1.1 °K is that obtained when no spontaneous heating was evident, the heat capacity is very similar to that for $Y_{0.96}Gd_{0.04}Os_2$. With the extrapolation to T = 0 shown in the figure, the entropy in excess of that for pure lanthanum at 4.2 °K is 95% of the expected 0.007 Rln8. The superconducting transition is spread out between 1.4 and 1.8 °K. The maximum decrease in heat capacity on application of a magnetic field is 8 millijoules/mole-deg and is consistent with the value 6.7 millijoules/mole-deg^2 for γ for pure lanthanum. For each of the lanthanum-gadolinium samples the heat capacity maximum is in good agreement with an extrapolation of the T_c-vs-composition curve from above the point at which it crosses the T_s curve. Both samples are known to be superconducting at and below the maxima.

---

[2] B. T. Matthias and H. Suhl, Phys. Rev. Letters 4, 51 (1960).

[3] P. W. Anderson and H. Suhl, Phys. Rev. 116, 898 (1959).

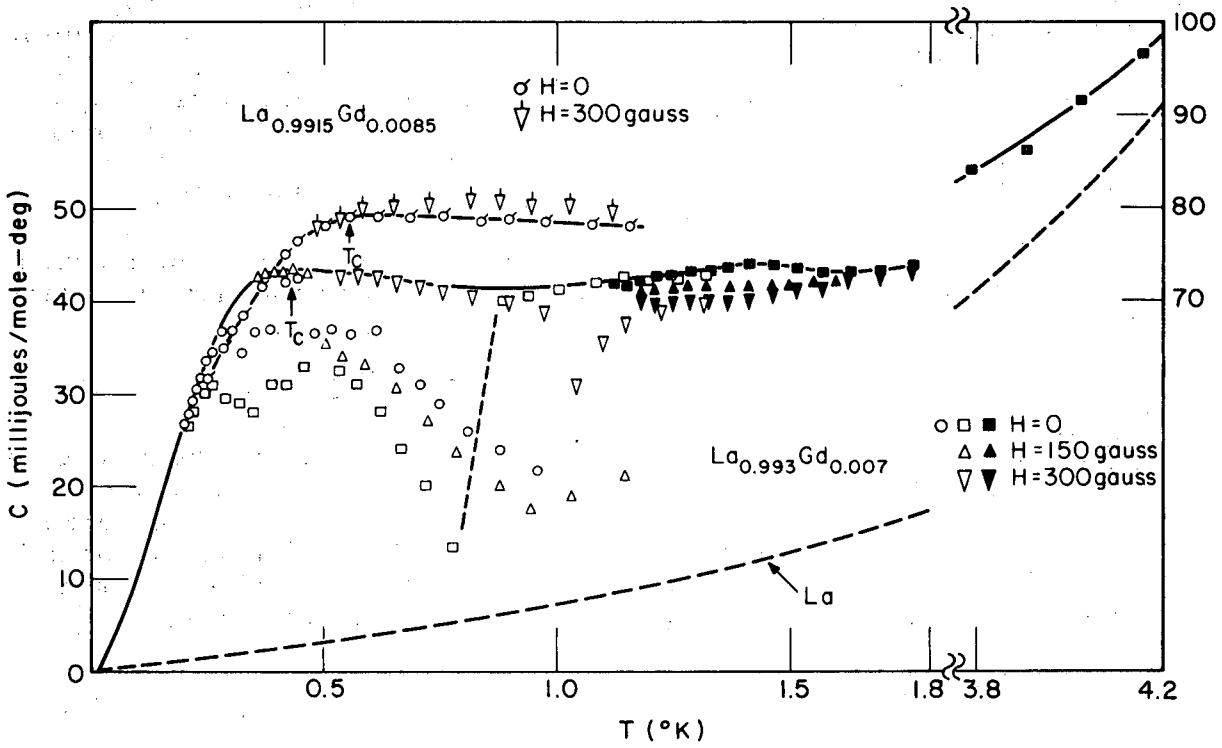

Fig. IB. 1-2. Heat capacity of solid solutions of gadolinium in lanthanum. Magnetic susceptibility measurements indicate a superconducting transition in the 0.7 % gadolinium sample at about 2.1 °K, and ferromagnetic Curie points at temperatures indicated by T_c. Each symbol designates a single series of consecutive measurements: the open symbols represent points obtained in the adiabatic demagnetization calorimeter.

2. HEAT CAPACITY OF ANTIFERROMAGNETIC $CuCl_2 \cdot 2H_2O$ IN THE SPIN WAVE REGION*

R. G. Petersen and Norman E. Phillips

Spin wave theory predicts a T^3 temperature dependence for the magnetic heat capacity of an isotropic antiferromagnet. The presence of anisotropy modifies this result to give an exponential temperature dependence at temperatures small compared with the geometric mean of the exchange and anisotropy energies.[1] $CuCl_2 \cdot 2H_2O$ was chosen as an example in which to look for these effects because the anisotropy field and the T^3 lattice heat capacity are both known. We have so far been unable to obtain a single crystal large enough for the measurements, but report here some preliminary results obtained with a compressed polycrystalline sample. See Fig. I B. 2-1. The relatively long thermal equilibrium times encountered in this sample may have introduced systematic errors below 0.3 °K. Temperature measurements were based on an extrapolation of the susceptibility of copper potassium sulfate from above 1 °K according to a Curie-Weiss law.

Nakamura has shown that, in the long-wave-length limit, the frequencies $\omega_i(k)$ of the spin wave modes in an orthorhombic antiferromagnet are related to their propagation vectors k by an expression of the form

$$\hbar\omega_i(k) \cong 2z\,|J|S[bk^2 + 2a_i]^{1/2}, \quad \text{for } i = 1, 2, \qquad (1)$$

in which b, z, J, and S are, respectively, a structure factor, the number of nearest neighbors, the exchange integral and the spin;[2] a_1 and a_2 are proportional to the anistropy fields and can be deduced from the antiferromagnetic resonance frequencies or the critical fields for flipping of the spins. Eisele and Keffer have shown that for $CuCl_2 \cdot 2H_2O$ Eq. (1) gives, at temperatures small compared with T_c(4.3 °K), a magnetic heat capacity C_M which satisfies

$$C_M/RT^3 = (2\pi^2/3)(k_B/2z\,|J|S)^3 C'_M(T, a_1, a_2), \qquad (2)$$

in which k_B is Boltzman's constant and R is the molar gas constant.[1] The C'_M is strongly temperature-dependent at low temperatures, but approaches unity for $kT \geq 2z\,|J|S(2a)^{1/2}$; C_M/RT^3 predicted by Eq. (2) is shown as the solid curve in Fig. I B. 2-2. Here J/k_B is taken as 5.4 °K to give order-of-magnitude agreement with the experimental result.

Below 0.55 °K the total heat capacity can be resolved into components varying as T^{-2} and T^3, as shown in the figures. The lattice heat capacity[3] accounts for 7% of the T^3 term, leaving $2.25\times10^{-3}\ RT^3$ for C_M and $5.25\times10^{-5}\ RT^{-2}$ for nuclear alignment effects. The latter part probably arises principally from the magnetic hyperfine interaction between the copper nuclei and the electron spins. Upper limits of 132 Mc/sec are thus established for the separation of the levels of Cu^{63} and Cu^{65} respectively.

---

*Brief version of paper to be published in J. Chem. Phys.

[1] J. A. Eisele and F. Keffer, Phys. Rev. 96, 929 (1954).

[2] T. Nakamura, Progr. Theoret. Phys. (Kyoto) 7, 539 (1952).

[3] S. A. Friedberg, Physica 18, 714 (1952).

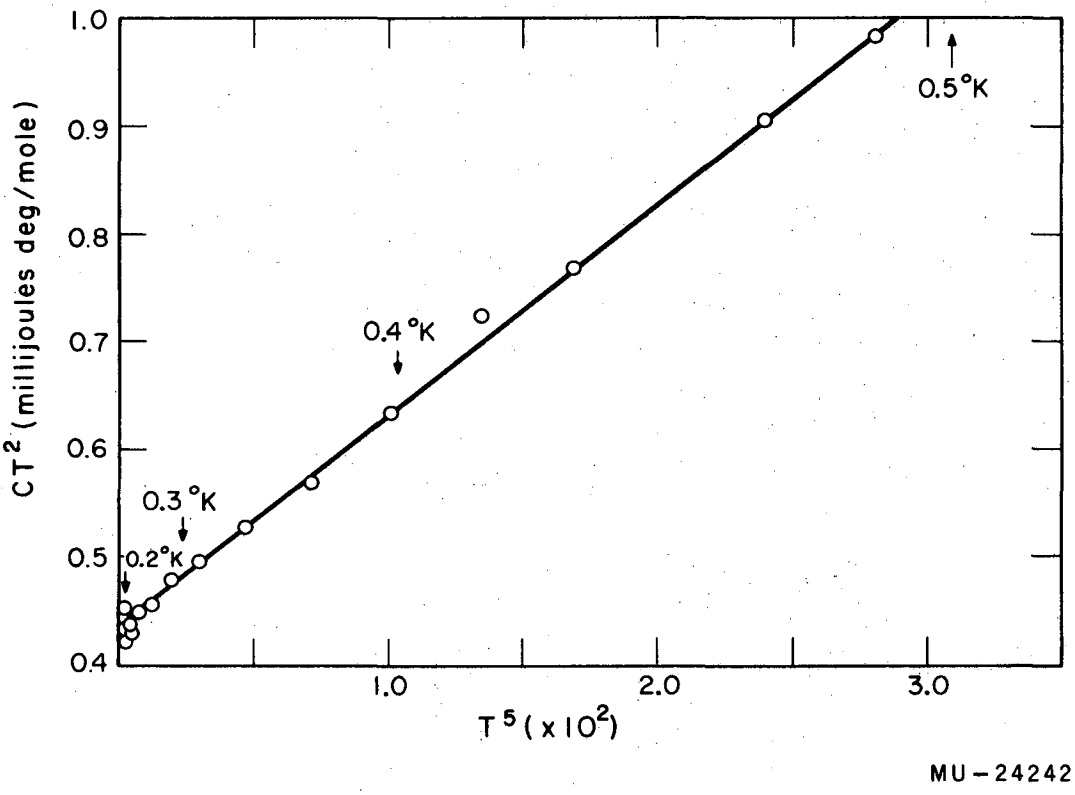

Fig. IB. 2-1. The total heat capacity, C, of $CuCl_2 \cdot 2H_2O$. Higher temperature points show a positive deviation from the straight line and are omitted from this plot.

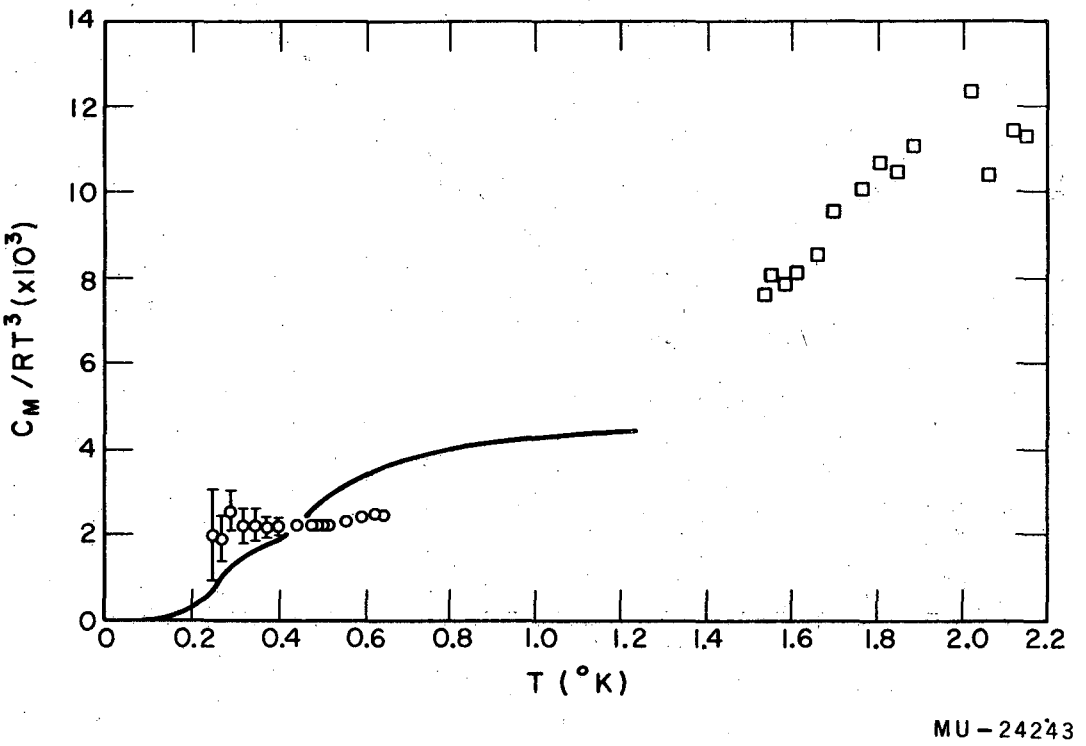

Fig. IB. 2-2. The magnet heat capacity, C_M, of $CuCl_2 \cdot 2H_2O$. The indicated errors correspond to an estimated error of 2% in the total heat capacity. The points designated by squares are from the measurements by Friedberg (see Ref. 3). The solid curve represents the calculation by Eisele and Keffer (Ref. 1).

The T^3 temperature dependence for C_M is not in agreement with Eq. (2). Apart from the possibility of an unexpectedly large error in the T^{-2} term or of particle size effects, the discrepancy may arise from the phenomenological way in which anisotropy is treated in spin-wave calculations. A similar situation exists with respect to the parallel susceptibility of MnF_2. Griffel and Stout[4] have observed the T^2 temperature dependence, predicted by spin wave theory for an isotropic antiferromagnet,[5] at temperatures for which the anisotropy should have brought about a more rapid temperature variation.[1]

[4]M. Griffel and J. W. Stout, J. Chem. Phys. 18, 1455 (1950).

[5]R. Kubo, Phys. Rev. 87, 568 (1952).

3. THE HEAT CAPACITY OF POTASSIUM, RUBIDIUM, AND CESIUM FROM 0.1 °K TO 4.2 °K*

William H. Lien and Norman E. Phillips

Unlike lithium and sodium, the heavier alkali metals do not undergo a martensitic transformation on cooling, and therefore a direct comparison of the electronic heat capacity with theories of the electronic structure is possible. Measurements below 1 °K are necessary to separate the electronic heat capacity from the total. Above 1 °K the lattice heat capacity dominates and, in combination with values of the elastic constants which are being measured in another laboratory, the measurements will provide a test of the various lattice dynamic calculations for the bcc structure.

The heat capacity data reported here have been calculated on the "1958 helium vapor pressure scale" above 1 °K and on the temperature scale described in the preceding report below 1 °K. See Fig. I B. 3-1.

In each case, at temperatures above 0.2 °K, the heat capacity approaches the usual temperature dependence: $C = \gamma T + (12\pi^4 R/5)(T/\theta_0)^3$ In Table I the values of γ and θ_0 are collected and m^*/m, the effective mass ratio, is compared with band theory calculations.

Table I. Heat capacity data

	K	Rb	Cs
θ_0(°K)	90.8	55.0	39.8
γ(millijoules/mole-deg^2)	2.11	2.45	3.46
m^*/m experimental	1.26	1.28	1.55
m^*/m theoretical (Brooks[1])	0.94	0.87	0.83
m^*/m theoretical (Cohen and Heine[2])	0.98	0.93	0.90

*A preliminary report of this work was presented at the International Conference on Low Temperature Physics (Toronto, 1960), and a more complete report will be submitted to the Physical Review.

[1]H. Brooks, quoted in C. Kittel, Introduction to Solid State Physics, (John Wiley and Sons, New York, 1956).

[2]M. H. Cohen and V. Heine, Advances in Physics 7, 395 (1958).

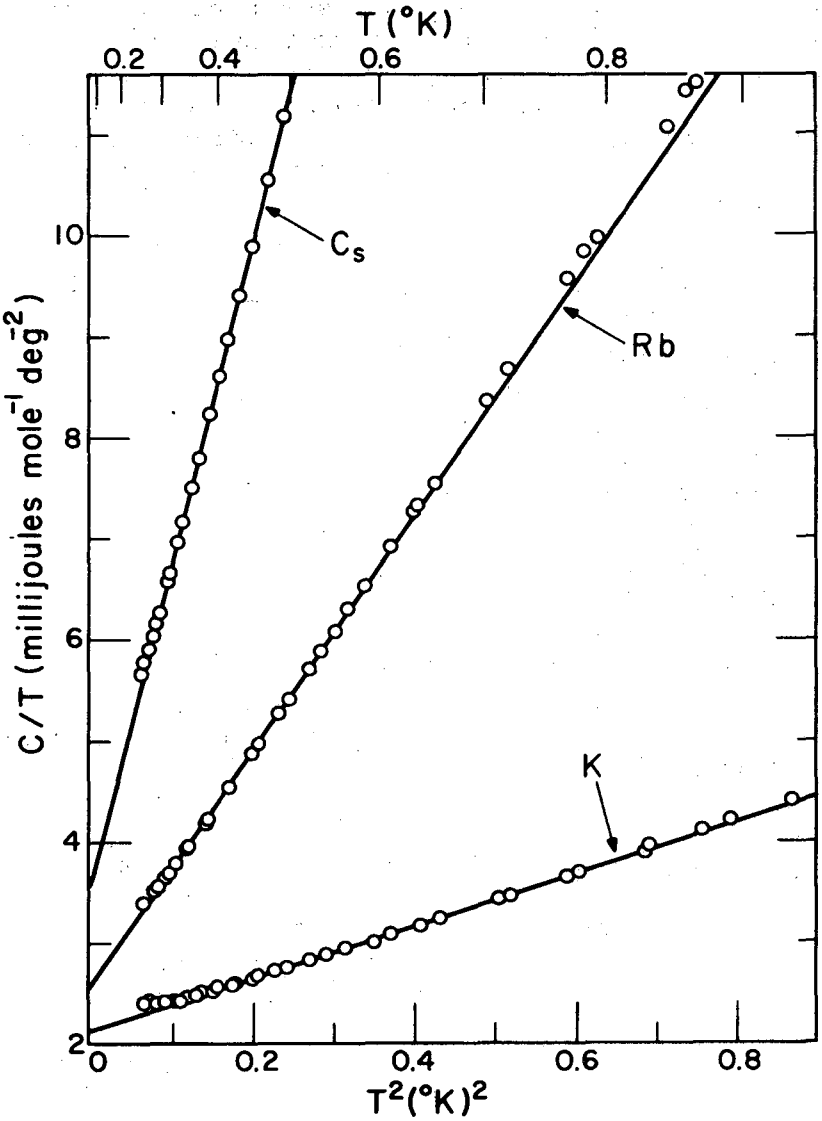

Fig. IB. 3-1. The heat capacity of potassium, rubidium, and cesium.

The deviation of the experimental effective mass ratio from unity includes the effect of electron correlations and electron-phonon interaction as well as that of the lattice potential. The first two of these effects are probably not large and would not be expected to produce the observed trend in m^*. Band theory calculations show that in potassium the electrons are nearly free, in which case the observed m^* is a measure of the effect of correlations and the electron-phonon interaction. If it were assumed that these two effects can be treated separately the experimental result could be taken as support for the calculations by Pines[3] and by Buckingham and Schafroth,[4] which predict, respectively, no change in γ from electron correlations, and approximately a 20% increase in γ from electron-phonon interactions. It seems probable that the observed trend in m^* between potassium and cesium is an indication of the increasing distortion of the Fermi surface. This view is consistent with recent interpretations of transport properties of these metals.[2, 5]

Below 0.2 ^{o}K the heat capacity is as much as 3% higher than a linear extrapolation of C/T vs T^2 from higher temperatures. The possibility that this is related to remaining temperature-scale errors cannot be ruled out, but it is also possible that it is a nuclear quadrupole effect. Unlike the other metals on which measurements have been made, the samples were strained polycrystals. The large Sternheimer factors for these metals would give a large splitting of the nuclear energy levels in the neighborhood of defects.

---

[3] D. Pines, Solid State Physics, Vol. 1 (Academic Press, Inc., New York, 1955, pg. 367).

[4] M. J. Buckingham and M. R. Schafroth, Proc. Phys. Soc. (London) A67, 828 (1954).

[5] J. M. Ziman, Phil. Mag. 4, 371 (1959).

4. THE MAGNETIC TEMPERATURE SCALE FOR COPPER POTASSIUM SULFATE. THE HEAT CAPACITY OF COPPER BETWEEN 0.1 AND 4.2 °K*

Norman E. Phillips

Heat capacity measurements on a number of metals for which C/T was expected to be linear in T^2 have shown deviations from this behavior at temperatures below 0.3 °K.[1] The deviations have always been in the same proportion to the total heat capacity, suggesting that they are produced by errors in the temperature measurements and are not properties of the various metals. The temperature measurements in these experiments were based on an extrapolation from above 1 °K of the susceptibility of copper potassium sulfate according to a Curie-Weiss law. The Weiss constant, Δ, was taken as 0.033°. Magnetic measurements on this salt by Garrett[2] suggested that the temperature defined in this way was a good approximation to the thermodynamic temperature.

In principle it is possible to derive a correction to the temperature scale from heat capacity measurements on a substance of known heat capacity covering the range in question and extending into a region in which the temperature is well known. For this purpose the heat capacity of copper has been measured between 0.1 °K and 4.2 °K with a precision of 0.2% over most of the range. Above 1 °K the measurements are in good agreement with several other recent determinations, and C/T is linear in T^2, permitting an extrapolation to below 1 °K. The experimental points just below 1 °K are in agreement with the extrapolation, but at the lowest temperatures they show the usual deviations. A corrected magnetic temperature scale for copper potassium sulfate has been derived from the measurements and is given in Table I in terms of a temperature-dependent Weiss constant. Temperatures below 1 °K are then determined by fitting susceptibility measurements above 1 °K to a Curie-Weiss law with $\Delta = 0.033°$ but using the values of Δ from Table I to calculate the temperature from the susceptibility at temperatures below 1 °K.

Table I. The effective Weiss constant for copper potassium sulfate

T	Δ
≥ 0.40	0.033
0.30	0.032
0.25	0.031
0.20	0.029
0.15	0.026
0.10	0.019

*To be submitted to Phys. Rev.

[1] N. E. Phillips, Phys. Rev. 114, 676 (1959).

[2] C. G. B. Garrett, Cermonies Langevin-Perrion (Collège de France, Paris, 1948).

The temperature scale of Table I has been used to recalculate the heat capacity measurements on Al, Zn, Cd, and Ga. For the first three of these C/T was then found to be linear in T^2, as expected. Approximately half of the heat capacity of Ga at 0.1 °K arises from a nuclear quadrupole interaction and is proportional to T^{-2} with a proportionality constant determined by the known resonance frequency. In this case also the corrected temperature scale gives the expected heat capacity.

Cooke, Meyer, and Wolf[3] have compared the susceptibility of copper potassium sulfate with that of cerium magnesium nitrate, for which there is good evidence that $\Delta = 0$. They also find appreciable deviations from a Curie-Weiss law for the copper salt. The temperature scale of Table I is intermediate between their result and that of Garrett, but is much closer to the former.

[3] Cooke, Meyer, and Wolf, Proc. Roy. Soc. (London) 233A, 536 (1956).

5. HEAT CAPACITY ANOMALY IN SOLID AIR*

William H. Lien and Norman E. Phillips

We have recently had occasion to make heat capacity measurements on several "empty" calorimeters, made almost entirely of copper and weighing approximately 180 g. In two separate sets of measurements between 1 °K and 4 °K unexpectedly high results were obtained: below 3 °K the heat capacity was 40% to 80% higher than estimated. Investigation showed that the high heat capacity was caused by the presence of approximately 0.1 g of air sealed into the calorimeters. After the second of these runs the calorimeter seal was cracked to permit the escape of the air and the measurement repeated without otherwise changing the apparatus. The heat capacity was then found to be close to that estimated for the calorimeter. The heat capacity of the air is shown in Fig. I B. 5-1. There is an uncertainty of 5% in the amount of air present and therefore in the values plotted in the figure. In this temperature range the heat capacity of solid air is as much as 400 times that of solid oxygen.[1]

It seems probable that the large heat capacity is associated with an antiferromagnetic ordering of the electron spins of the oxygen molecules at about 3 °K. From a comparison of the spectroscopic entropy of oxygen gas with calorimetric measurements on the condensed phases, Giauque and Johnston showed that in pure solid oxygen the spins are largely aligned at liquid

* Brief version of published paper, J. Chem. Phys. 34, 1073 (1961).

[1] M. O. Kostriukova and P. G. Strelkov, Doklady Akad. Naukk S. S. S. R. 90, 525 (1953).

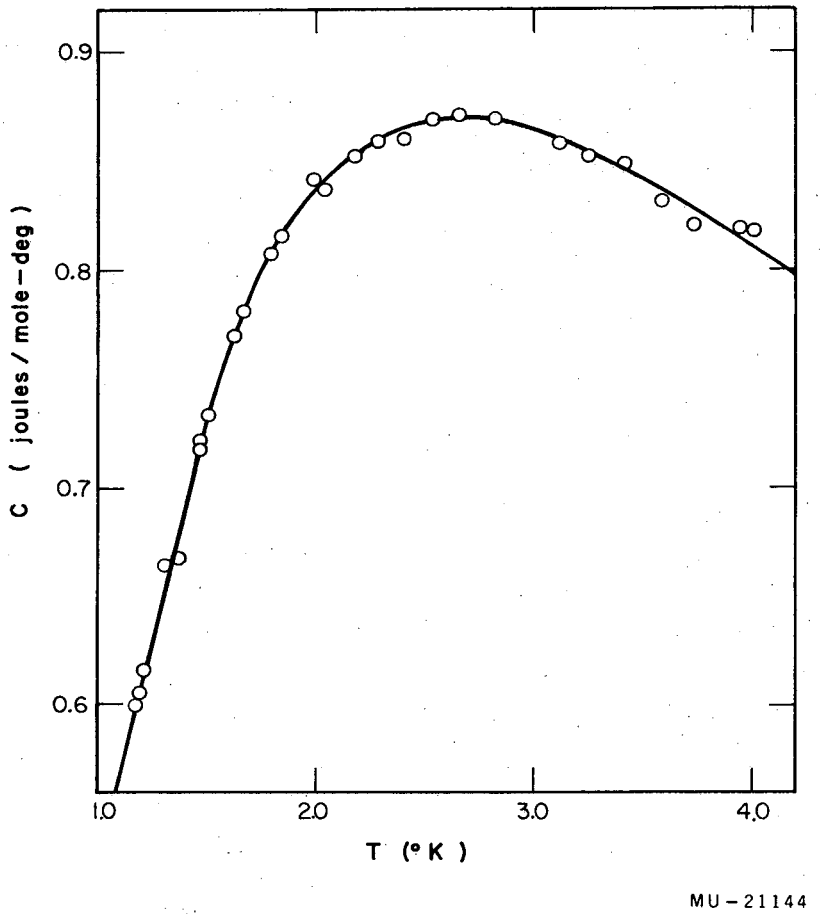

Fig. IB. 5-1. The heat capacity of solid air.

hydrogen temperature.[2] Calorimetric[2, 3] and magnetic[3, 4] susceptibility data suggest that a transformation to an antiferromagnetic state is coincident with the γ-β crystallographic transition at 43.8 °K. Dilution of an antiferromagnet with a diamagnetic material reduces the energy of interaction between the spins. Consequently, the alignment of the spins in solid air can be expected to take place at a lower temperature than in pure oxygen. Further support for this point of view comes from magnetic susceptibility measurements on liquid oxygen–nitrogen solutions. Between 64 and 77 °K these solutions follow a Curie-Weiss law with antiferromagnetic Weiss constants.[5] The Weiss constant for a composition corresponding to the present sample would be about 7 °K, within the usual range of values that might be expected for a material with a Neel temperature of 3 °K. That the heat capacity does not have the sharp peak characteristic of antiferromagnetic transitions in pure compounds is to be expected on general grounds, and also by comparison with magnetic measurements on solutions.[6]

[2] W. F. Giauque and H. L. Johnston, J. Am. Chem. Soc. 51, 2300 (1929).

[3] Borovik-Romanov, Orlova, and Strelkov, Doklady Akad. Nauk S.S.S.R. 99, 699 (1954).

[4] Kanda, Haseda, and Otsubo, Physica 20, 131 (1954).

[5] A. Perrier and H. K. Onnes, Leiden Com. 139d (1914).

[6] H. Bizette and B. Tsai, Compt. rend. 217, 444 (1943).

6. PHASE DIAGRAMS OF TRANSURANIUM ELEMENTS

Peter Montgomery and Harold Stromberg

A modification of the anvils has been built which permits the study of as little as 400 micrograms of metal from a pressure of about 2 to 30 kilobars, and from room temperature to 400 °C. The apparatus was checked by the phase diagram of bismuth and lanthanum. Pressure-temperature studies have been made on neptunium, plutonium, and americium.

The neptunium was obtained from Professor Burris Cunningham's group. The sample was well behaved. The α-β transition was the only one studied. The P-T data are given in Table I.

Table I. α-β transitions in neptunium

Pressure (kbars)	Temperature (°C)
4.4	278
5.5	286
6.6	290
8.8	304
11.0	334

The plutonium was obtained from the Los Alamos Scientific Laboratory. It was of the highest purity available. Many of the features have been determined.

The americium was supplied by Professor Cunningham's group. The purity of the samples was not as great as desirable. They were roughly 95 mole % americium. Each sample weighed about 500 micrograms.

Because of the nature of americium no features of the phase diagram were established. Several pages could be filled with its odd behavior. The difficulty appears to be that the behavior is very highly dependent on the past history as well as the purity of the sample. The same behavior could not be obtained twice in the same sample, let alone from two different samples. Only one feature seems to be reproducible from sample to sample. In an isobaric heating, the resistance of the metal would rise by a factor of 100. At about 400 ^{o}C the resistance sharply decreased to its initial value. Once this nonmetallic state was produced and destroyed in the sample, it would not reappear in the same sample again.

Several man-years of labor appear to be essential to resolve the difficulties inherent in this problem.

7. THE USE OF BRIDGMAN ANVILS FOR THE DETECTION OF PHASE CHANGES OF INSULATING MATERIALS

George Jura

In all the previous work with Bridgman anvils, the measurements have been restricted to the determination of the electrical resistance of the material under study. This has limited their utility primarily to metals and some of the semiconductors. A method is here described whereby phase transitions of any material can be obtained with the anvils.

Normally, a first-order phase change is observed in the piston-cylinder apparatus by a discontinuity in the motion of the piston, which entails a discontinuous volume change. In the anvils a volume change must also occur when a first-order change occurs. Thus if a sufficiently sensitive means of determining the motion of the anvils could be found, phase changes could be detected without recourse to electrical resistance. In the previous section of this report it was pointed out that there exists a radial pressure gradient in the anvils. This would be expected to make any transition observed by volume change very broad, since the entire face of the anvil must be filled with the material under study. This is found to be true.

The method for the determination of the motion of the anvils is as follows. The measurement that is actually made is the distance between two anvils, at a fixed distance from the edge, on the tapered support of the faces. This is done by two arms, one of which is fixed, the other resting on a knife edge. The change in distance causes a motion of the movable arm. The motion of this arm is measured by a Sheffield Accutron gauge. It is possible to detect changes of as little as 10^{-6} inch with this arrangement. If necessary, this could be increased by a factor of ten by adding a lever system to the movable arm. At present this is not warranted.

The system must be used differentially. The range of the instrument with this sensitivity is not great enough to directly obtain the integrated motion. The maximum pressure change that can be used is about 7 kbars. The motion of the anvils is very complex, and not yet completely analyzed. However, enough work has been done to show that phase changes can be found with this method. Those that have been established are given in Table I. Because of the pressure gradient, the transition is expected to occur at a pressure well below load. So far, the loads form a well-behaved curve when plotted against the pressures obtained by Bridgman by the conventional technique.

Table I. Loads (in kilobars) for various transitions.

Solid	This work	Bridgman
Bi 4-5	55	60
Bi 6-8	79	90
AgCl	75	90
Sb	69	85
$NaNO_3$	50	55

It is hoped the method cannot only be used to detect phase changes, but also can be extended to the determination of relative compressibility.

8. THE DETERMINATION OF PRESSURES IN BRIDGMAN ANVILS

George H. Jura, Peter Montgomery, and Harold Stromberg

The Bridgman anvils[1] are the pressure-generating apparatus used in our work. Kennedy has pointed out that above 30 kbars, the apparent transition pressures in Bridgman anvils are about 30% higher than those observed for the same transition in the piston-cylinder apparatus.[2] Since the piston-cylinder measurements can be checked by dead-weight gauges, they must be taken as absolute, and the anvil measurements must be considered to be in error. Earlier, we have studied the external deformation of the anvils radiographically.[3] The external deformation cannot account for the discrepancy, since at a load of 400 kbars the average pressure can be at most only 12% less than the applied load. The internal deformation must be the cause of this discrepancy. The internal deformation cannot be studied radiographically. When the energy of the radiation is sufficiently high to penetrate the carbides, the edges are so diffuse that meaningful observations are not possible.

[1] P. W. Bridgman, Proc. Am. Acad. Arts Sci. 81, 165 (1952).

[2] G. Kennedy, Report, Lake George Conference on High Pressures, June 1960.

[3] R. J. Vaisnys, Ph. D. Thesis, University of California, 1959.

In the usual method of making measurements in the anvils, a thin strip of the material is imbedded in AgCl, and leads from each end of the sample are brought into contact with the carbide surfaces. Connections are then made from each anvil to the external measuring circuit. The reason for this geometry is to make the contact resistances small compared with that of the sample. The object, relative resistance measurements as a function of pressure. It is evident that these resistance-pressure measurements are not valid. Also, it is essential to study the internal pressure distribution in the anvils.

For studying the internal pressure gradient, the old geometry of the sample cannot be used, since a radial pressure gradient in the sample permits different parts of the sample to be at different pressures. To minimize the radial pressure gradient, we have used a wire 0.008 in. in diameter. The wire is placed in a hole of the same size in a silver chloride disk. This geometry leads to very large end corrections, and relative resistances cannot be obtained by this method. However, the discontinuities in the resistance are still detectable, so that the phase boundaries can be determined by this method. The above geometry was used in all the experiments described.

Anvil faces of 1/4, 3/8, and 1/2 in. were used. The pyrophylite retaining rings were 0.010 in. thick, and the width was 1/32 in. for faces of all diameters. The thickness of the silver chloride varied from 0.008 to 0.0085 in., except when the studies of silver chloride thickness were being made.

To determine the effect of silver chloride thickness, a bismuth wire was mounted in the center of a silver chloride disc in 3/8-in. -faced anvils. The results are shown in Table I. It is evident that as long as the silver chloride thickness is greater than 0.0075 in. the results are essentially independent of the thickness. It is presumed that this relationship holds for faces of other diameters.

Table I. Effect of AgCl thickness on bismuth transitions

AgCl thickness (in.)	Load for Bi transitions (kbars)		
	1-2	2-3	6-8
0.009	25	27	100
0.0085	25	28	100
0.008	25	27	98
0.007	26	30	103
0.006	32	34	125

The next series of experiments studied the same transitions as above. In these experiments, the wire was mounted in the center of the silver chloride disc, and the transition loads were determined as a function of the face diameter. Here it was found that the load at which the transition occurs is a strong function of the face diameter. The results are shown in Table II.

Table II. Effect of face diameter on bismuth transitions

Face diameter (in.)	Load for Bi transitions (kbars)		
	1-2	2-3	6-8
1/4	24	26	83
3/8	27	29	100
1/2	30	--	120

Since a given transition occurs at a given pressure, the above table shows that there is a marked difference between load and pressure. The 1/4-in. anvils are the closest to the accepted results for the 1-2 transition. The figures also show that a pressure gradient must exist in the anvils, since there is no loss of the applied thrust by friction.

The work in determining the gradient is now under way. Results for the 3/8-in. faces are the most complete, and are given in Table III for the bismuth 1-2 transition. Since it is reasonable to assume that the pressure gradient is radial, the results are given in terms of r/r_0, where r is the distance from the center of the disc, and r_0 the diameter of the face, 0.375 in. in this particular system.

Table III. Radial pressure gradient in 3/8-inch anvils at 25 kbars

r/r_0	Load for Bi 1-2 transition (kbars)
0.000	27
0.234	25
0.399	33
0.632	23
0.761	18

Within the error of the present measurements, this gradient is linear with respect to r/r_0. It will be observed that at the center the pressure is less than the load, while at the edge the pressure is higher than the load. The difference in pressures is so great that it is possible to place two samples in the same disc, one at the center, the other at the edge, and all the bismuth transitions can be observed to occur separately in each location.

The above shows that previous data on relative resistances are incorrect. First, the samples were located in the center of the anvil, where the pressure is lower than the load; and second, the sample is not at uniform pressure. The probable cause of this large pressure gradient can be explained in the following manner. At the edges, the pyrophylite ring extrudes, leaving the face unsupported, or with less support than at the center. This causes the face to move downward at the edge, thus cupping the face. The silver chloride is not hydrostatic, and the internal friction supports this gradient.

The above situation, which appears disconcerting at first glance, actually does not invalidate the usefulness of the apparatus. It merely points out the correct method of use. First, it is now possible to construct an absolute pressure scale to as high as 400 kbars, as long as a first-order transition can be found. The method of doing this is to determine the load at the center and edge of anvils of different sizes, and extrapolate the upper and lower loads to zero anvil size. This has been partially done for the bismuth 6-8 transition. The best figure for this transition if 86 ± 3 kbars. This is to be compared to the 90 kbars obtained by Bridgman in a piston-cylinder apparatus. Bridgman's value may be in error because of the impossibility of making proper corrections for friction in his apparatus. His value could be high by as much as 5%.

The anvils still can be used for relative resistance measurements. The geometry cannot be that which has been previously used. A wire must be used, and bent in a circular arc. This arc if properly placed should be at constant pressure.

9. GAPS TO 500 KILOBARS

R. J. Vaisnys, Harold Stromberg, and George Jura

In our earlier work, gaps were determined thermally to a pressure of 200 kbars.[1] This has been extended to 500 kbars for anthracene, selenium, and iodine. The techniques are unchanged from those used at lower pressures. The temperature range used was from 50 to 180 °C over the entire pressure range.

Anthracene

The anthracene was recrystallized several times. Its exact purity is not known. Because of its high resistance, these measurements are the poorest of the series. There is no assurance that the conductivity observed was not due to the surface rather than through the bulk. If it was a surface conductivity, then the gap measurements are invalid. The gap was found to be 1.0 v at 50 kbars and 0.6 v at 200 kbars; the gap decreased to 0.5 v at 500 kbars. It appears that the hydrocarbons will all have high resistivities to these pressures.

Selenium

The selenium used was supposedly 99.999% pure. The material was purchased from the American Smelting and Refining Co., South Plainfield, N. J.

The interest in selenium stems from the possibility that it will undergo a metallic transition similar to that of tellurium. The tellurium transition occurs at about 50 kbars.[2] The previous work to 200 kbars and the present extension to 500 kbars do not show this transition.

[1] R. J. Vaisnys, Ph. D. Thesis, University of California, 1959.

[2] P. W. Bridgman, Proc. Am. Acad. Arts and Sci. 81, 165 (1952).

The gap decreased to about 0.04 v at 300 kbars. It was not possible to determine gaps lower than this by the thermal technique. The specific resistance decreased slowly with increases in pressure. The lowest specific resistance observed is 3000×10^{-6} ohm cm. From the sign of the thermoelectric power, selenium is of p type over the entire region studied. Its semiconducting properties at the highest pressures are very much like those of gray tin.

Iodine

The iodine was highly purified. The location of the Fermi surface, as deduced from the thermoelectric behavior, was halfway between the band edges, indicating that the intrinsic conductivity was being observed. The initial resistances and gaps indicated that no measurable hydrolysis of the sample had occurred.

The rapid decrease of the gap with pressure observed to 200 kbars, 1.6 to 0.17 v, continued to about 325 kbars, where the gap had decreased to 0.085 v. The gap decreased only to 0.080 v at 500 kbars. The specific conductivity was reduced to 500×10^{-6} ohm cm, a very low value considering the size of the gap. From the thermoelectric measurements, the sample is of p type at all pressures. The specific resistance is slightly more than twice the maximum resistance observed for caesium at 50 kbars. [2]

Alder, from his shock measurements, predicts that there should be a first-order change to the metallic state at about 200 kbars. [3] Our work shows no sign of this transition. Normally, this kind of discrepancy could be explained in kinetic effects. The very high temperatures in shock would increase the rate to the degree that it becomes observable. If the transition observed by Alder is the metallic transition, it seems reasonable to assume that a lattice of monatomic iodine has been formed. The breaking of the bonds should not require the high temperature, merely overlap between the neighboring molecules.

[3] Berni J. Alder (Lawrence Radiation Laboratory), private communication.

10. METALLIC CONDUCTIVITY OF PHOSPHORUS AND SILVER OXIDE AT HIGH PRESSURES

Robert E. Harris, R. J. Vaisnys, Harold Stromberg, and George Jura

The specific resistance of phosphorus and silver oxide have been measured to 200 kbars. Phosphorus exhibits true metallic conduction at loadings of 170 kbars and higher. Its specific resistance at 200 kbars is $50 \pm 20 \times 10^{-6}$ ohm cm. There is no observable first-order transition of the semiconducting black to the metallic form of this element. Freshly prepared silver oxide also possesses metallic conduction in the same pressure region as phosphorus. Its specific resistance at 200 kbars was found to be $60 \pm 20 \times 10^{-6}$ ohm cm. Aged oxide does not become metallic even at loads as high as 400 kbars. The change to continued semiconduction at the higher loads appears to be related to the formation of the carbonate on the surface of the oxide.

11. RESISTANCE MEASUREMENTS TO 400 KILOBARS*

J. R. Vaisnys, Harold Stromberg, and George Jura

A modification of the Bridgman anvils permits studies to be made to a load of 400 kbars, about twice that previously available. The external deformation of the anvils has been studied for 1/4-in. faces of 1-in. -diam carbides. Thus, a lower limit of the pressure can be stated provided internal deformations are neglected. It is shown that silver chloride is an insulator to the highest loads, and selenium is a semiconductor to a load of 270 kbars.

*Brief version of report (same authors and title), UCRL-9469, Nov. 1960.

12. RESISTANCE AND THERMAL GAP MEASUREMENTS TO 400,000 ATMOSPHERES*

Robert E. Harris, R. J. Vaisnys, Harold Stromberg, and George Jura

The published work on high pressure by static methods extends to a pressure of 200,000 atm. In this paper we summarize our work to a pressure of 400,000 atm. We have exceeded this last figure, but our knowledge is as yet too uncertain even for an informal public discussion. Bridgman-type anvils have been used for this work. The modifications that we have made in the construction of the anvils are described. We have made resistance measurements to a pressure of 400,000 atm, and temperature coefficients of resistance to 200,000 atm. We have been able to determine the sign of the thermoelectric power. Finally, there is an attempt to determine the pressure scale that has some significance other than loading to this pressure region.

*Abstract for Proceedings of the Conference on Very High Pressure, Lake George, N. Y., June 1960.

13. CURRENT INVESTIGATIONS ON SOLID-STATE PHYSICS AND CHEMISTRY, 1961

Norman E. Phillips

1. Heat capacity measurements on "ferromagnetic superconductors" are being extended to temperatures above 4 ^{o}K and below 1 ^{o}K in a "He^3 calorimeter" in which the sample is not exposed to magnetic fields or cooling.

2. An adiabatic demagnetization calorimeter, which employs one paramagnetic salt for cooling and a second for temperature measurement, is nearly complete. It will be used first for measurements of the lattice heat capacity of superconducting I_n and S_n.

3. Further heat capacity measurements on antiferromagnetic materials are being made at temperatures in the spin-wave region.

4. A more detailed investigation of the heat capacity of Al in the vicinity of its superconducting transition has been initiated.

George Jura

1. Equipment has been designed and built for measuring the magnetic permeability under pressure. It is expected that, if the apparatus performs according to expectations, it will be possible to obtain Curie points as a function of pressure as well as temperature. Also, there is a possibility that ferromagnetic-antiferromagnetic transitions will be observed. The one possibility for this transition is iron, the second the Heuser alloys.

2. The equipment has been built for the determination of Hall coefficients under pressure. The use of this technique for the study of semiconductors is apparent.

I C. REACTION KINETICS

1. REACTIVE SCATTERING IN CROSSED MOLECULAR BEAMS: K ATOMS WITH CH_3I AND C_2H_5I

Dudley R. Herschbach, George H. Kwei, and James A. Norris

Angular distributions of reactively scattered KI have been measured at the intersection of a K atom beam with beams of CH_3I and C_2H_5I.[1] In these reactions kinematical features are particularly favorable for a study of the recoil spectrum of the product molecules.[2] An analysis which relies only upon conservation laws shows: (a) the final relative velocity vector has a quite anisotropic distribution, strongly peaked about the direction of the initial relative velocity vector; (b) about 50 to 70% of the 25 kcal/mole energy of reaction goes into internal excitation of the products.

The beams are formed by thermal effusion from ovens mounted on a turntable which is rotated to sweep the angular distribution past surface ionization detectors. Vertical adjustment of the detector position allows the scattering to be measured out of the plane (angle ϕ, accessible over 0 to 30 deg) as well as in the plane of the incident beams (angle θ, accessible over -20 to 130 deg from the K beam). The KI can be distinguished from elastically scattered K by use of two detectors: one a W filament, about equally sensitive to K and KI; the other a Pt-W alloy,[3] about ten times as effective for K as for KI. Although this differential detection was used, it proved unnecessary for these reactions, as the KI distributions are displaced far from the K beam and appear on the W detector as pronounced peaks well above the smoothly varying background from elastic scattering. Typical conditions are: K beam at 725 °K in perpendicular collision with CH_3I at 375 °K, peak of the KI distribution at θ = 93 deg, ϕ = 0, with half-intensity at θ = 71 to 107 deg. Under the same conditions C_2H_5I gives similar results except that the peak of the KI distribution is shifted to about θ = 100 deg.

The principal qualitative features of the analysis may be seen in Fig. I C. 1-1. Here $\vec{v}$ denotes the initial relative velocity vector and c the center of the mass vector. The recoil velocity that carries the KI away from the center of mass can have any direction, but conservation of momentum and energy determine its magnitude as

$$v_4' = [(2/M)(M_3/M_4)(E + Q)]^{1/2},$$

where $M_4 \leftrightarrow$ KI, $M_3 \leftrightarrow CH_3$; E is the initial relative energy and Q the internal energy converted into translational energy of separation of the products. (Figure I C. 1-1 corresponds to E = 3 kcal/mole, but the conclusions are found not to be significantly affected by averaging over the initial velocity distributions.) Thus the possible spectrum of recoil vectors for KI is

---

[1] G. H. Kwei, J. A. Norris, and D. R. Herschbach, Bull. Am. Phys. Soc. 5, 503 (1960); to be submitted to J. Chem. Phys.

[2] D. R. Herschbach, Theoretical Analysis of Cross Sections for Chemical Reactions as Measured in Molecular Beam Experiments, UCRL-9379 Abstract, April 1960.

[3] E. H. Taylor and S. Datz, J. Chem. Phys. 23, 1711 (1955).

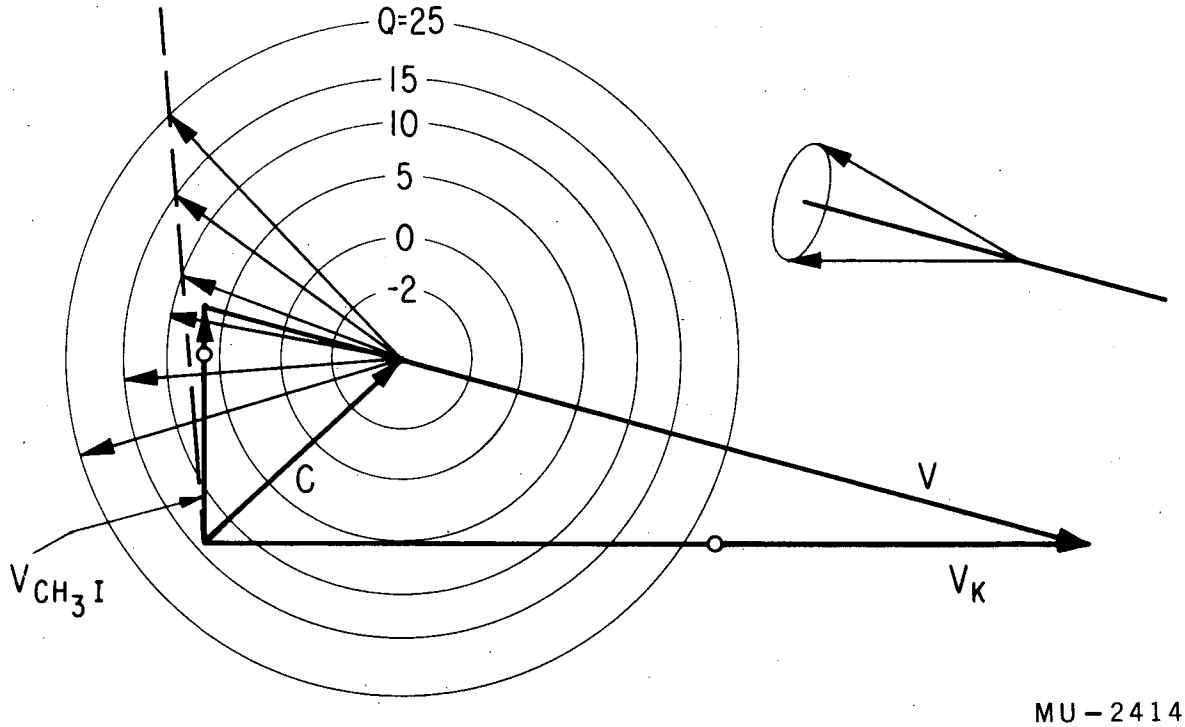

Fig. IC. 1-1. Analysis of reaction $K + CH_3I \rightarrow CH_3 + KI$; K at 725 °K, CH_3I at 375 °K.

represented by a set of spheres, one for each value of Q up to the maximum of 25 kcal/mole (the difference in bond energy of K-I and C-I). It is seen that the peak observed at 93 deg in the laboratory frame corresponds to scattering in which an observer stationed at the center of mass would see the KI recoil backwards (and the CH_3 forwards) with respect to the incoming K beam. Also, at the peak $Q \gtrsim 9$ kcal/mole. Large Q values can appear only if the recoil velocity deviates considerably from the direction of v, as indicated in Fig. IC. 1-1. The scattering must have cylindrical symmetry about v, since the incident beams contain all possible molecular orientations and impact parameters. Therefore the measurements of out-of-plane scattering, which show substantial peaking about $\phi = 0$, directly demonstrate the absence of appreciable contributions from large Q values. This is also shown by the lack of additional in-plane scattering at the angles indicated in Fig. IC. 1-1.

The observed small shift in the KI distribution for the C_2H_5I reaction is just that expected from the mass change.

For both reactions a preliminary value of the activation energy, $E^* = 2$ to 3 kcal/mole, is obtained from the temperature variation of the collision yield, and the total reaction cross sections are roughly 10 to 15 A^2.

One other reaction, $K + HBr \rightarrow H + KBr$, has previously been studied in crossed molecular beams.[3,4] However, the angular distribution is not comparable to those studied here. In this reaction there is a very large disparity in the masses of the products and Q_{max} is only 6 kcal/mole; consequently the recoil spectrum of KBr is confined within such a small sphere that the initial velocity distributions smear out any possible anisotropy.[5,6]

---

[4] E. F. Greene, R. W. Roberts, and J. Ross, J. Chem. Phys. 32, 940 (1960).

[5] D. R. Herschbach, J. Chem. Phys. 33, 1870 (1960).

[6] D. R. Herschbach, S. Datz, and E. H. Taylor, Collision Mechanics in Crossed Maxwellian Molecular Beams, UCRL-9378, Aug. 1960; J. Chem. Phys. (to be published).

2. CURRENT INVESTIGATIONS ON REACTION KINETICS, 1961

Dudley R. Herschbach

Several additional reactions of alkali atoms (Li and Cs as well as K atoms) with halogen-containing molecules are under study; a wide range of the kinematical factors is covered in this series of reactions to provide a test of scattering theory. A detector for halogen atoms is being developed; it is already satisfactory for elastic-scattering studies but not yet sensitive enough for reactive-scattering measurements. Apparatus under construction includes a toothed-wheel velocity selector, separately pumped chambers designed for high-temperature ovens (up to 3000 ^{o}K), and a small mass spectrometer which will enhance the sensitivity of the surface ionization detector.

Bruce H. Mahan

1. Measurement of cross sections of gas phase ion-electron recombination reactions in aromatic hydrocarbons.

2. Measurement of the cross sections for electron transfer in the reactions

$$I^{+} + I^{-} \rightarrow 2I,$$

$$Br^{+} + Br^{-} \rightarrow 2Br.$$

3. Investigation of the vacuum ultraviolet emission spectrum of Xe_2^{*} and other excited noble gas diatomic molecules.

ID. INORGANIC CHEMISTRY

1. IDENTIFICATION OF CHLORIDE COMPLEXES OF Ru(III)*

Dwight A. Fine and Robert E. Connick

Ruthenium in the +3 oxidation state forms a variety of complex ions which interconvert, slowly at room temperature in the case of the lower complexes and rapidly with the higher complexes. Rehn and Wilson had tentatively identified several of them on the basis of their ion-exchange behavior.[1] The first complex, $RuCl^{2+}$, subsequently had been unambiguously characterized by Cady and Connick.[2]

In this work the following species were definitely identified: $RuCl_2^+$(cis and trans), $RuCl_3$(cis and trans), and $RuCl_4^-$(cis and trans). In addition, two monomeric species forming at successively higher chloride concentrations were presumed to be $RuCl_5^{2-}$ and $RuCl_6^{3-}$. Still other unidentified chloride complexes are believed to be present in the system.

Each species has a characteristic spectrum, and these were established to make possible their use for identification in chemical studies.

The two $RuCl_2^+$ isomers were separated on an ion-exchange column and their average charge per ruthenium atom determined from their exchange capacity.[2] The total charge per species was found from a double equilibration with the hydrogen ion form of Dowex-50 at two different hydrogen ion concentration.[2]

The $RuCl_3$ isomers were separated on an ion-exchange column by means of their different velocities of migration down the column. The molecular weights were obtained from the freezing-point depressions, with a correction being made for the acid in the solution.

The two $RuCl_4^-$ isomers can be separated on an anion-exchange column and their spectra determined. The formulas were obtained by studying the equilibrium between $RuCl_3$ and $RuCl_4^-$ as a function of the chloride concentration at a total acid concentration of 3.0 M. Trifluoroacetic acid was added to replace hydrochloric acid.

The spectrum of $RuCl_5^{2-}$ was obtained by dissolving $K_2RuCl_5 \cdot H_2O$ in dilute hydrochloric acid. Because of the rapidity with which it dissociates to $RuCl_4^-$, it was necessary to follow the absorption at each wave length as a function of time and to extrapolate to zero time.

---

*A brief form of published paper, R. E. Connick and D. A. Fine, J. Am. Chem. Soc. 82, 4187 (1960). A second paper has been accepted for publication in J. Am. Chem. Soc., and a third is in preparation. This material comprised the thesis of Dwight A. Fine, Chloride Complexes of Ruthenium (III), UCRL-9059, February 2, 1960.

[1] I. M. Rehn and A. J. Wilson, Ruthenium(III) Chloride Complexes in Trifluoroacetic Acid, Hanford Atomic Works, Richland, Washington.

[2] H. H. Cady and R. E. Connick, J. Am. Chem. Soc. 80, 2646 (1958).

The spectrum of Ru(III) in 12 M HCl was assumed to correspond to that of $RuCl_6^{3-}$, although there is no definite evidence that the conversion of $RuCl_5^{2-}$ to the higher complex is actually complete under these conditions.

Very roughly approximate values of equilibrium quotients (expressed in moles per liter) are shown in Table I along with the ionic strength, which was due to hydrochloric acid in all but some of the $RuCl_4^- - RuCl_3$ equilibria.

Table I. Equilibrium quotients

	Q(M)	Ionic Strength (M)
$\frac{(RuCl^{2+})(Cl^-)}{(RuCl_2^+)}$	= 0.035	0.1
$\frac{(RuCl_2^+)(Cl^-)}{(RuCl_3)}$	= 0.37	0.1
$\frac{(RuCl_3)(Cl^-)}{(RuCl_4^-)}$	= 1.2	3
$\frac{(RuCl_4^-)(Cl^-)}{(RuCl_5^{2-})}$	≈ 7	5
$\frac{(RuCl_5^{2-})(Cl^-)}{(RuCl_6^{3-})}$	≈ 7	5

The equilibrium composition of the isomeric mixtures was obtained, only approximately, as shown in Table II. Although there is no conclusive proof, it is believed that in each case the cis isomer is in the numerator.

Table II. Isomeric equilibrium ratios

	cis/trans ?	Statistical
$RuCl_2^+$	2.0	4/1
$RuCl_3$	0.3	2/3
$RuCl_4^-$	4	4/1

In the last column is given the ratio expected statistically. Assuming the identification to be correct, one sees that the observed values are remarkably close to the statistical, and it may be inferred that the electrostatic effect is small. Calculations show that as a consequence the effective dielectric constant must be on the order of that of water.

2. THE PREPARATION OF THE VOLTILE HYDRIDES OF GROUPS IV-A AND V-A BY MEANS OF AQUEOUS HYDROBORATE*

William L. Jolly

The convenience of working with only aqueous solutions stimulated our exploitation of the aqueous hydroborate method for the preparation of volatile hydrides. In general, our aim was to increase as far as possible the yields with respect to the hydroborate consumed. We have assumed that all four hydrogens of the hydroborate ion are potentially available for hydride formation. Thus, for the stibine-producing reaction, we write

$$3BH_4^- + 4H_3SbO_3 + 3H^+ \rightarrow 3H_3BO_3 + 4SbH_3 + 3H_2O.$$

By the dropwise addition of an alkaline solution of hydroborate and either arsenite, antimonite, germanate, or stannite to aqueous acid, good yields of either arsine, stibine, germane, or stannane, respectively, were obtained. Small amounts of diarsine, digormane, and the heretofore unknown distannane[1] formed with the arsine, germane, and stannane, respectively. No silane nor plumbane was obtained by similar procedures using solutions of sodium silicate or sodium plumbite, respectively, and only traces of phosphine were obtained by similar procedures involving phosphite and hypophosphite.

Distannane readily decomposed at room temperature to tin and hydrogen in an observed atom ratio of 1:3. The infrared spectrum of the frozen solid (-180°) is similar to the spectra of digermane and disilane. Absorption maxima were observed at the following frequencies (in cm^{-1}): 690(s), 880(w), 1040(w), 1840(vs), 2010(w), 2220(w), 2280(vw), 2420(vw), 3620(m).

It is particularly interesting that neither the silicate, the hypophosphite, nor the phosphite ion is appreciably reduced by hydroborate. It seems likely that, in each of these species, the central atom is too well protected by its four surrounding atoms to permit approach of a hydride ion. If germanium(IV), tin(II), arsenic(III), and antimony(III) have coordination numbers of four (as do Si(IV), P(I), and P(III)), then the greater size of the central atoms in these cases would explain their greater accessibility to hydride ions. Recent work has shown that sulfite (or sulfurous acid) is readily reduced to hydrogen sulfide by hydroborate.[2] Here the sulfur atom has a coordination number of only three, and is accessible to hydride ions. The sulfate ion, with four coordinated oxygen atoms, is inert to hydroborate. The nitrous acid molecule, with only two oxygen atoms, is readily reduced to ammonium ion by aqueous hydroborate.[3] However, the three oxygen atoms of the nitrate ion are apparently enough to protect the nitrogen atom from attack by hydroborate, inasmuch as nitrate is inert to hydroborate in acid solution.[3]

---

*A detailed account of this work will soon be published in the Journal of the American Chemical Society.

[1] W. L. Jolly, Angew. Chem. 72, 268 (1960).

[2] Unpublished observations by F. Y. Tsang.

[3] M. E. Kramer, Ph. D. Thesis, St. Louis University, 1954.

The inability to detect any plumbane in the reduction of lead (II) by hydroborate may be explained by the extreme instability of plumbane. Since lead metal formed in the reaction flask, it is apparent that reduction took place; but any plumbane that may have formed underwent immediate decomposition to the elements.

3. THE HYDROLYSIS OF AQUEOUS HYDROBORATE

Robert E. Mesmer and William L. Jolly

Because of the widespread use of aqueous solutions of alkali metal hydroborates as reducing agents in analytical and synthetic chemistry, it is important to understand the mechanism of hydroborate reductions. The only available data on the mechanism of these reductions are some conflicting kinetic data on the hydrolysis reaction,[1-5] a few tracer studies on the aqueous hydrolysis and other solvolysis reactions,[6, 7, 8] and a kinetic study on the reduction of aqueous ferricyanide.[9]

All investigators report first-order dependence on hydroborate concentration in the rate expression for the reaction

$$BH_4^- + 4\ H_2O \rightarrow B(OH)_4^- + 4\ H_2.$$

There is agreement with first-order dependence on hydrogen ion concentration below pH 12 as well as with deviation to less than first order above pH 12. However, the reported rate constant[3] for the hydrolysis in highly acid solutions (1 M to 3 M H^+) differs by a factor of 10^6 from that reported above pH 7.

---

[1] R. L. Pecsok, J. Am. Chem. Soc. 75, 2862 (1953).

[2] J. B. Brown and M. Svenson, J. Sci. Labs. Denison University, 44-8, 151 (1958).

[3] M. Kilpatrick and C. D. McKinney, J. Am. Chem. Soc. 72, 5474 (1950).

[4] E. H. Jensen, A Study on Sodium Borohydride with Special References to its Analytical Applications in Organic Chemistry, Nyt. Nordisk Forlag, Arnold Busck, Copenhagen, 1954.

[5] R. E. Davis and C. G. Swain, J. Am. Chem. Soc. 82, 5949 (1960).

[6] P. Girodot and R. Parry, J. Am. Chem. Soc. 73, 2368 (1951).

[7] W. C. Brown, L. Kaplan, and K. Wilzback, J. Am. Chem. Soc. 74, 1343 (1952).

[8] R. E. Davis, C. L. Kibby, and C. G. Swain, J. Am. Chem. Soc. 82, 5950 (1960).

[9] T. Freund, J. Inorg. Nuclear Chem. 9, 246 (1959).

To clarify the hydrogen ion dependence in very basic solutions, the rate law was determined by using pH meter measurements for one set of data and hydroxide concentrations for another. Both sets of data indicate the rate expression

$$\frac{-d(BH_4^-)}{dt} = k_1(H^+)\,(BH_4^-) + k_2(BH_4^-).$$

This was demonstrated by linear plots of $\frac{1}{k'}$ vs $\frac{(H^+)}{k'}$ and $\frac{1}{k'(OH^-)}$ vs $\frac{1}{k'}$ in which $k' = k_1(H^+) + k_2$ or $k' = k_1K_w/(OH^-) + k_2$, respectively. Both sets of data were obtained in the temperature range 10 to 50°. The following table contains the heats and entropies of activation for the two terms in the rate law calculated from both sets of data.

Heats and entropies of activation

	$\Delta H_1^{\ddagger}$	$\Delta H_2^{\ddagger}$	$\Delta S_1^{\ddagger}$	$\Delta S_2^{\ddagger}$
	(kcal/mole)		(cal/deg · mole)	
pH	7.9 ± 1	22.1 ± 2	-4.0 ± 3	-18.4 ± 3
(OH^-)	6.3 ± 1	20.6 ± 2	-8.3 ± 3	22.2 ± 3

The tabulated values from the hydroxide data have been corrected for the heat and entropy of ionization of water. The analytical expressions for the rate constants obtained by averaging the heats and entropies are

$$k_1 = 5.99\times10^{10}\ M^{-1}\ min^{-1}\ T\ e^{-3550/T},$$

$$k_2 = 1.72\times10^{7}\ min^{-1}\ T\ e^{-10,380/T}.$$

The entropy change of -4 to -8 eu for the process having the activated complex $BH_5\times H_2O$ is unusual for a reaction involving oppositely charged ion combination. The entropy changes usually associated with the combination of hydrogen ions and the anions of weak acids are usually around +20 eu. High polarity in the activated complex could explain the low change in entropy. There are a few examples of similar reactions which have essentially no change in entropy, viz, acetoacetate plus hydrogen ion, R^+ plus Cl^-, and NH_4^+ plus CNO^-.

The entropy change for formation of the activated complex $BH_4^- \times H_2O$ is -20 eu. A decrease in entropy for this process would be predicted if the activated complex resembled a hydrated hydride ion and a hydrated $BH_3 \cdot H_2O$ species. Kinetic isotope effects[10] (obtained through the use of BD_4^- and BH_4^-) are consistent with the above data in that they

[10] Unpublished data of Robert E. Mesmer and William L. Jolly (Lawrence Radiation Laboratory).

suggest the mechanism

$$H_2O + BH_4^- \rightarrow [H_2O \cdots BH_3 \cdots H^-]^{\ddagger} \rightarrow \underset{\text{fast reactions}}{H_2OBH_3 + H^-}.$$

A flow technique was used to measure rate constants between pH of 3.5 and 7.0. Half lives of the order of a few milliseconds up to a few seconds were obtained. These results are consistent with our rate constant obtained at high pH, and indicate that the rate constant of 48 M^{-1} min^{-1} reported by McKinney and Kilpatrick is in error. In fact we were able to set a lower limit of 10^4 M^{-1} min^{-1} on the constant by using this technique at 1 M hydrogen ion concentration. Davis and Swain have furnished a satisfactory explanation[11] of the low rate constant obtained by McKinney and Kilpatrick.

[11] See footnote 5 in Reverence 5.

4. SHORT-LIVED CHROMIC ION SPECIES OBTAINED BY ELECTRO-OXIDATION OF CHROMOUS ION

Wayne Mathews and Edwin F. Orlemann

By applying a suitably alternating potential to a small mercury-drop electrode the Cr^{+++}, Cr^{++} system has been alternately reduced and oxidized at various frequencies. Under these conditions the species oxidized and reduced are those formed at the electrode and observed before they have time to diffuse away rather than those found in the body of the solution. The technique can be used to reveal "new" short-lived species, or in various modifications to study the interconversion half lives of species already existing in the solutions.

In the experiments presented here 0.1 M HCl, 0.9 M KCl solutions containing 2.0×10^{-3} M $CrCl_3$ were studied. The cell consisted of a small 0.3-mm-radius mercury drop whose size could be reproduced, and a large mercury pool as the second electrode. Since the latter maintains the potential of a 0.1 M calomel electrode, a potential applied to the cell alters only the potential of the small mercury drop. The potential across this cell was cycled linearly with time from 0 to -1.25 v and back to 0 at frequencies ranging from 0.02 to 100 cps. During the sweep from 0 to -1.25 v, reduction of Cr^{+++} to Cr^{++} is observed in terms of a flow of current corresponding to this process, and in the return to 0 v, a net oxidation of Cr^{++} to Cr^{+++} occurs. The resultant current-voltage curves were recorded on an oscilloscope and were photographed when a steady state was obtained at any particular frequency. The data discussed are those of the steady-state pictures, and the potentials given are half-wave potentials ("half wave" meaning that they represent the potential at which one-half the maximum current due to a particular process was observed). Because of the time dependence of these measurements such potentials are not directly related to polarographic half-wave potentials, and in fact have little fundamental significance. All potentials are referred to a 0.1 N calomel electrode. The temperature is 25.0±.1°C.

At a frequency of 0.02 cps the stable Cr^{+++} species in this solution gives rise to a current whose half-wave potential is -0.98 v. The Cr^{++} formed is oxidized back to Cr^{+++} at a potential of -0.55 v. At 0.04 cps there is still a single current wave corresponding to the oxidation of Cr^{++} at -0.55 v and a reduction of Cr^{+++} at -0.98 v, but a very small reduction current appears at -0.70 v due to the appearance of a new Cr^{+++} species. At 1 cps three Cr^{+++} reductions are clearly seen--the first at -0.45 v, the second at -0.70 v, and the original one at -0.98 v. At 10 cps these three reduction waves are again seen, with the one at 0.45 v somewhat increased in total current but not much. At 100 cps no detail in regard to relative currents can be observed, but it can be seen that three Cr^{+++} species are being reduced.

From an analysis of the frequency dependence of the currents observed it can be concluded the -0.45 v Cr^{+++} species converts directly to the stable Cr^{+++} species with a half life of about 1 sec. The -0.70 v Cr^{+++} species converts to the stable form with a half life of about 20 sec. Since only one Cr^{++} oxidation at -0.55 v is observed at all frequencies, there must be only one Cr^{++} species formed by reduction of the three Cr^{+++} ions, or equilibrium must be established among the Cr^{++} species in less than 10^{-4} sec.

It will be of particular interest in future work to chemically characterize these two Cr^{+++} species and attempt to relate their possible structures to the observed reduction potentials and their rates of conversion to the stable Cr^{+++} species.

5. CURRENT INVESTIGATIONS IN INORGANIC CHEMISTRY 1961

Robert E. Connick

1. Hydrolysis and polymerication of chromic ion.

2. Rates of interconversion of the chloride complexes of Ru(III).

3. Rates of replacement of water molecules in the first coordination sphere of metal ions. (Studied by using the nuclear magnetic resonance of O^{17}.)

4. Rate of formation of triiodide ion. (Studied by nuclear magnetic resonance.)

William L. Jolly

1. The effects of changing experimental conditions on the yields of GeH_4, Ge_2H_6, Ge_3H_8, and GeH_x (polymer) in the reaction of aqueous hydroborate and germanium(IV) are being studied.

2. The kinetic effects of replacing deuterium for hydrogen [in the hydroborate and(or) the water] are being measured to help elucidate the mechanism of the reaction

$$BH_4^- + 4\ H_2O \rightarrow (B(OH)_4^- + 4\ H_2O.$$

3. While on leave in Heidelberg, Germany, one of us (W. L. J.) found a new method for the preparation of S_4N_4, namely the reaction of S_2Cl_2 vapor with solid ammonium chloride:

$$6S_2Cl_2 + 4NH_4Cl \rightarrow S_4N_4 + 8S + 16HCl.$$

This method is presently being further developed to increase the efficiency of the process.

4. A new absorption cell has been built for measuring the infrared absorption spectra of alkali metal–ammonia solutions in the concentration range 0.001 to 0.1 molar.

Edwin F. Orlemann

1. Analysis of single-pulse-potential current-voltage curves as a means of determining the rate of interconversion of complex ions.

2. Analysis of alternating-potential current-voltage curves to characterize short-lived intermediates and short-lived electrode reaction products.

I.E. GENERAL PHYSICAL AND THEORETICAL CHEMISTRY

1. INTERACTIONS BETWEEN MOLECULES ADSORBED ON A SURFACE*

Oktay Sinanoğlu and Kenneth S. Pitzer

Physical adsorption is characterized by relatively weak forces as compared with chemisorption, and it might be considered a process in which both the adsorbed molecules and the adsorbent surface remain quite unchanged. Thus the van der Waals forces that cause physical adsorption can be understood for the most part through the use of quantum mechanical perturbation theory. The theory of these forces between molecules has been reviewed by Margenau,[1] and there are some recent considerations by Pitzer.[2] Extensive reviews on the forces that cause physical adsorption also exist.[3, 4]

Some interesting phenomena such as the formation of monolayers and multilayers on an adsorbent involve the forces between adsorbed molecules themselves as well as with the surface. Such forces can be investigated through the application of statistical mechanics to experimental measurements, especially in physical adsorption, and although this is difficult when the adsorbate is dense, it becomes particularly suitable in the dilute case--i.e., relatively high-temperature adsorption making use of a theory similar to the virial-coefficients treatment of imperfect gases.[5] By such a method it is possible to investigate the adsorption of essentially one molecule, two molecules, etc., at a time on a surface, and the potential energies of interaction involved in each case.[5]

Such experimental evidence has long shown[3, 5b] that two inert gas atoms adsorbed into a monolayer display a rather different potential energy between themselves from their energy when they are in the gas phase, i.e., the presence of the surface apparently causes a new long-range repulsion to appear between the two molecules of the monolayer, and this repulsion tends to counterbalance their usual London attraction. On the other hand, in multilayer formation additional attractions must exist. These observations are not explainable in terms of second-order perturbation theory of long-range forces. This theory predicts that the total interaction between a system of adsorbed molecules and the surface must be pairwise additive; hence the interaction between molecules would be unaltered.[1]

---

*Brief version of published paper, O. Sinanoglu and K. S. Pitzer, J. Chem. Phys. 32, 1279 (1960).

[1] H. Margenau, Revs. Modern Phys. 11, 1 (1939).

[2] K. S. Pitzer, Advances in Chemical Physics, Interscience Publishers, Inc., New York, 1950, Vol. II; or see K. S. Pitzer, UCRL Report No. 8395, 1958.

[3] J. H. de Boer, Advances in Catalysis 8, 29 (1956).

[4] S. Brunauer, The Adsorption of Gases and Vapors, Princeton University Press, Princeton, New Jersey, 1945, p. 180.

[5] (a) W. A. Steele and G. D. Halsey, Jr., J. Chem. Phys. 22, 979 (1954); see also
(b) M. P. Freeman, J. Phys. Chem 62, 729 (1958).

The intermolecular potential energy between two inert gas molecules is considerably altered when these molecules are next to a solid surface as in physical adsorption. In this article, the two-molecule surface potential is derived from quantum mechanical third-order perturbation theory. It is shown that this potential consists of two parts, just as does the energy giving the van der Waals attraction of a single molecule to a surface. The first part exists only when the surface has a net electrostatic field, and this is equivalent to the classical polarization effect. The second part arises from the fluctuations of the surface fields, and is of the same origin as the dispersion forces. The third-order energy, i.e., the new intermolecular interaction caused by the surface, is directly related to the zero-coverage heat of adsorption, and except for this experimental quantity the results do not require specific assumptions about the surface. Thus the theory is applicable to either metal or insulator surfaces. When both the two-molecule-surface and the one-molecule-surface interactions are available experimentally (for example, from the application of virial-coefficients treatment in physical adsorption) the electrostatic field of the surface can be estimated.

The fluctuation or dispersion part of the third-order energy is shown to yield a repulsion between two molecules in a monolayer that amounts to 20 to 40% of the gas-phase Lennard-Jones potential minimum ϵ_0. The same energy yields an additional attraction of about 10 to 20% of ϵ_0 when the two molecules are on top of each other, as in multilayer formation. The theory is applicable also when more than two molecules at a time need be considered on the surface.

2. PERTURBATION THEORY OF MANY-ELECTRON ATOMS AND MOLECULES*

Oktay Sinanoğlu

Perturbation theory with operator techniques is applied to a non-degenerate many-electron system, taking the electron repulsions,

$$\sum_{i>j}^{N} r_{ij}^{-1} ,$$

as the perturbation. The first-order wave function (WF), χ_1, is obtained rigorously in terms of the first-order WF's of independent two-electron systems. The pair functions containing nuclear parameters can be solved for individually by variational or other methods, then used in various atoms or molecules. For example, Li atom is built up completely from the $(1s)^2\ ^1S$, $(1s2s)\ ^1S$ and ^3S states of Li^+. The χ_1 gives the energy to third order and as an upper limit to the exact E. The E_2 is equal to the sum of complete pair interactions plus many-body terms of two types: (a) "cross polarization," which exists even in no-exchange intermolecular forces, and (b) Fermi correlations.

*Abstract of published paper, Phys. Rev. 122, 493 (1961).

3. INTER- AND INTRA-ATOMIC CORRELATION ENERGIES AND THEORY OF "CORE POLARIZATION"*

Oktay Sinanoglu

Atomic and molecular energies depend strongly on the correlation in the motions of electrons. Their complexity necessitates the treatment of a chemical system in terms of small groups of electrons and their interaction, but this must be done in a way consistent with the exclusion principle. To this end, a nondegenerate many-electron system is treated here by a generalized second-order perturbation method based on the classification of all the Slater determinants formed from a complete one-electron basis set. The correlation energy of the system is broken down into the energies of pairs of electrons including exchange. Also some nonpairwise additive terms arise which represent the effect of the other electrons on the energy of a correlating pair on account of the Pauli exclusion principle. All energy components are written in approximate but closed forms involving only the initially occupied H. F. orbitals. Then each term acquires a simple physical interpretation and becomes adoptable for semiempirical usage. The treatment is applied to detail to two particular problems:

(a) The correlation energy between an outer electron in any excited state and the core electrons--e. g., in the Li atom--is represented by a potential acting on the outer one. This potential can be regarded as the mean-square fluctuation of the Hartree-Fock potential of the core, and applies even when the outer electron penetrates into the core. The magnitudes of some of the correlation effects are calculated for Li.

(b) Starting from a complete one-electron basis set of SCF MO's, the energy of a molecule is separated into those of groups of electrons and intramolecular dispersion forces acting between these groups. The assumptions that are usually made in discussing dispersion forces at such short distances are then removed, and generally applicable formulae are given. Some three or more-electron correlation effects and limitations in the use of "many-electron group functions" for overlapping systems are also discussed.

---

*Brief form of published paper, J. Chem. Phys. 33, 1212 (1960).

4. THEORY OF ELECTRON CORRELATION IN ATOMS AND MOLECULES*

Oktay Sinanoglu

Corrections to the Hartree-Fock (H. F.) wave function, ϕ_0, and energy of a many electron system are given. By the use of operator techniques in perturbation theory, the first order W. F., X_1', is obtained in terms of pair functions. These satisfy equations just like those of an actual two electron system except that now each electron moves in the H. F. field of the entire N-electron "medium" added to the field of nuclei. Every pair function must be orthogonalized to each of the two H. F. orbitals associated with it to get the complete X_1'. This X_1' determines both E_2 and E_3. The second order energy, E_2, comes out as the sum of pair interactions and three and four body correlations due to the exclusion principle. The latter may be incorporated into the pair energies if each pair function is orthogonalized also to the remaining H. F. orbitals of ϕ_0. The approach allows the valence and inner shells, etc. to be discussed separately and extends some of the concepts of quantum chemistry based on orbital approximations so as to include correlation.

*Abstract of published paper, Proc. Roy. Soc. (London) A 260, 379 (1961).

5. CORE POLARIZATION IN Li_2

Oktay Sinanoglu and Earl M. Mortensen

Recently a theory was given[1a, b, c] to show how a molecule can be built up from separate groups of electrons. Each group includes electron correlation, yet the separation takes the Pauli Exclusion Principle fully into account. The method justifies, e. g., the separate treatment of σ and π electrons.

In Li_2 the energy separates into the energies of two Li^+ ion cores interacting with dispersion forces, the correlated $(\sigma_g 2s)^2$ shell, and the correlation energy between the outer electrons and cores.[1a] The last is referred to as "core polarization" and has not been considered in previous configuration interaction calculations.[2] It is the entire correlation effect and not just the "orbital average polarization",[1a] or single excitations part, which would vanish after a complete SCF calculation. This core-valence electron correlation energy can be obtained as the expectation value of a Li^+ correlation or "fluctuation" potential[1] over outer Mo's.

[1]Summarized in preceding sections; for full publications see
(a) J. Chem. Phys. 33, 1212 (1960);
(b) Proc. Roy. Soc. (London) A 260, 379 (1961);
(c) Phys. Rev. 122, 493 (1961).

[2]E. Ishiguro, K. Kayama, M. Kotani, and Y. Mizuno, J. Phys. Soc. (Japan) 12, 1355 (1957).

We use Callaway's potential,[3] V_p, resulting from the instantaneous polarization of (Li^+) by a slow electron, the main part coming from the dipole terms. We shall examine the contribution of core polarization to the small binding energy of Li_2 and its sensitivity to the crudeness of the outer MO's used.

For the Li atom, $\langle 2s, V_p 2s \rangle$ is calculated with an analytic Hartree-Fock SCF orbital, $2s_R$, and also with a Slater orbital, $2\overset{o}{s}$, Schmidt orthogonalized to the core. The SCF $2s_R$ is the six-term "best compromise" orbital given by Roothaan, Sachs, and Weiss[4] in their Table Vb. The $2\overset{o}{s}$ is for Slater exponents $\delta_{1s} = 2.65$ and $\delta_{2s} = 0.65$:

$$2\overset{o}{s} = (1/\sqrt{4\pi})[\,0.39915\ r \exp(-0.65r) - 1.5030 \exp(-2.65r)] \qquad (1)$$

For Li_2 $\sigma_g 2s$, $V_p \sigma_g 2s$ is calculated for one core and one outer MO, the result being multiplied by four for the total core polarization.[1a] Two different approximate outer MO's are used:

(a) the analytic "best limited" SCF MO of Ransil,[5]

$$(2\sigma_g)_R = 0.52979\ (2s_a + 2s_b) + 0.11438\ (2p\sigma_a = 2p\sigma_b) \qquad (2)$$

$$- 0.14397\ (1s_a + 1s_b),$$

with Slater exponents $\delta_{2s} = 0.6335$, $\delta_{2p} = 0.7609$ and $\delta_{1s} = 2.6894$; and

(b) an MO formed from 2s Slater AO's Schmidt orthogonalized to <u>both</u> cores,

$$(2\sigma_g)_{OMO} = 0.57222\ (2s_a + 2s_b) - 0.13748\ (1s_a + 1s_b), \qquad (3)$$

with $\delta_{2s} = 0.65$, $\delta_{1s} = 2.65$. Both MO's are for the equilibrium internuclear distance of $R_e = 5.051$ au.

The lowering of the total energies of Li and Li_2 due to core polarization is shown in Table I. Numerical integrations were carried out on an IBM 704. The value obtained for Li with the analytic[4] HF SCF $2s_R$ agrees with Callaway's.[3] He used an earlier numerical HF orbital. The total energy of Li_2 is lowered by about 0.25 ev. This should be compared to the "orbital average polarization" energy, which should be less[6] than 0.019 ev as found by Ishiguro et al.[2] The latter is not a correlation energy and arises as the difference between a complete SCF and a fixed-core–outer-electron SCF calculation.[1a, 2]

---

[3] J. Callaway, Phys. Rev. <u>106</u>, 868 (1957); V_p given in his Table I is in Rydbergs.

[4] C. C. J. Roothaan, L. M. Sachs, and A. W. Weiss, Revs. Modern Phys. <u>32</u>, 186 (1960).

[5] B. J. Ransil, Revs. Modern Phys. <u>32</u>, 245 (1960); his Table I.

[6] The value 0.019 ev is too high for "orbital average polarization" in Li_2, because it results from a very crude approximation[2] to outer MO's in the field of fixed cores.

Penetration effects are neglected in V_p. They were estimated previously[1a] for Li to be less than 0.035 ev for the $1s_\beta 2s_\alpha$ interaction and 0.001 ev for $1s_\alpha 2s_\alpha$. The "exclusion effect"[1] of other electrons on the core-polarization energy of one, as well as three or more electron Coulomb correlations which may be small, are also left out.

The contribution to the binding energy (1.03 ev) of Li_2 is also shown in Table I. We note that the energy is not very sensitive to the crudeness of the orbitals used. Thus where SCF MO's are not available--e.g. for Na_2, K_2, etc.--it would suffice to use OMO's. Note also that though core polarization contributes quite appreciably to the total energies of Li and Li_2, the effects on the two almost cancel, and yield a small contribution to the binding energy. Such a cancellation has often been assumed in semi-empirical theories.

Table I. Core polarization energies

		(-ev)
Li atom		
(a) HF SCF	$2s_R$	0.1018
(b) OAO (Eq. 1)	$2s^o$	0.1066
Li_2 molecule (R_e = 5.051 au)		
(c) SCF MO (Eq. 2)	$(2\sigma_g)_R$	0.2473
(d) OMO (Eq. 3)	$(2\sigma_g)_{OMO}$	0.2520
Contribution to Li_2 binding energy		
(c) -2 (a)		0.0436
(d) -2 (b)		0.0387

6. NUCLEAR MAGNETIC RESONANCE STUDIES OF HYDROGEN BONDING. II. ALCOHOLS*

Jeff C. Davis, Kenneth S. Pitzer, and C. N. R. Rao

The proton magnetic resonance spectra of solutions of methanol, ethanol, i-propanol, and t-butanol in carbon tetrachloride and of ethanol in benzene have been measured over the temperature range 20 to 60° C. The methods were described in Paper I.[1] The shifts δ in very dilute solutions yield values of δ_M for the monomeric alcohols. Finite values of $\partial\delta/\partial x$ at zero mole fraction are obtained which clearly indicate the presence of a dimeric species. The relationships between these data and the equilibrium constants and enthalpies of dimerization are discussed, but the probable presence of both cyclic and open dimers complicates the interpretation. For ethanol in benzene, where open dimers are believed to predominate, the enthalpy of dimerization is found to be 5.1 ± 1 kcal/mole of dimer. Only qualitative comments are made concerning the results in concentrated solution in which many polymeric species are present.

The shift between δ_M for the monomer and the δ value for fully hydrogen-bonded polymer appears to be roughly 280 cps for each alcohol, if we assume some dissociation in the pure liquids and that this dissociation increases with temperature. There appears to be most dissociation in t-butanol and successively less for the smaller molecules.

The values of δ_M show no significant change with temperature, and this result throws some doubt upon the large temperature change of the apparent δ_M values for certain carboxylic acids that we reported previously[1] on a very tentative basis.

The very much smaller dissociation made the δ_M values of the acids much less certain than the present values for the alcohols, but the acids may associate more strongly with the solvent and hence behave differently.

Data from dielectric measurements and other sources are considered in a discussion of the relative abundance of cyclic and open-chain dimeric and polymeric species.

---

*Brief form of published paper, J. Phys. Chem. 64, 1744 (1960).

[1] J. C. Davis and K. S. Pitzer, J. Phys. Chem. 64, 886 (1960).

7. NMR ANALYSIS OF THE $A_3(X_3)_3$ SYSTEM

Juana V. Acrivos

Introduction

The NMR spectra of the symmetric trisubstituted benzenes $(CH_3)_3C_6H_3$ and $(CF_3)_3C_6H_3$ have been studied. The symmetry of these molecules belongs to the operations of the point group $D_3xC_{3v}xC_{3v}xC_{3v}$ when free rotation of the methyl radicals about their threefold axes is taken into account.[1, 2] The spin eigenvalue problem is solved in the light of the study made by Wilson[3] on the homomorphic case of $C_6H_3F_3$. The parameters involved in the problem are given in Fig. IE.7-1.

The nuclear hyperfine coupling constants for the hydrocarbon were calculated by using the Ramsay theory.[4, 5] The values obtained are in fair agreement with the measured ones.

Spectrum Analysis

The spin functions were obtained by applying the symmetry operations, P, of the group to the spin product functions for the equivalent nuclei and the products formed by these. The general expression is given by

$$\psi_i^{\Gamma} = 1/\eta \sum_P \chi_i^{\Gamma}(P)\, P\left[\psi^{\gamma_0}(1,2,3) \times \psi^{\gamma_1}(a,b,c)\right], \qquad (1)$$

where

$$\psi^{\gamma}(i,j,k) = \sum_P \chi^{\gamma}(P)\, P\left[\phi(m_i)\,\phi(m_j)\,\phi(m_k)\right]$$

and

$$\gamma_0 \times \gamma_1 = \Sigma\, \Gamma_i .$$

Here $\phi(m)$ is the spin function for a methyl group or a ring proton where m is the z component of the spin angular momentum. The Γ_i are the reduced species of the product $\gamma_0 \times \gamma_1$ and the $\chi^{\Gamma}(P)$ are the corresponding characters for the species Γ in the irreducible representation, η is the normalization constant.

---

[1] E. B. Wilson, Jr., J. C. Decius, and P. C. Cross, Molecular Vibrations (McGraw-Hill Book Co., New York, 1955).

[2] H. M. McConnell, A. D. McLean, and C. A. Reilly, J. Chem. Phys. 23, 1152 (1955).

[3] E. B. Wilson, Jr., J. Chem. Phys. 27, 60 (1957).

[4] N. F. Ramsay, Phys. Rev. 91, 303 (1953).

[5] H. M. McConnell, J. Chem. Phys. 24, 460 (1956); ibid, 70, 126 (1959); J. Mol. Spectroscopy 1, 11 (1957).

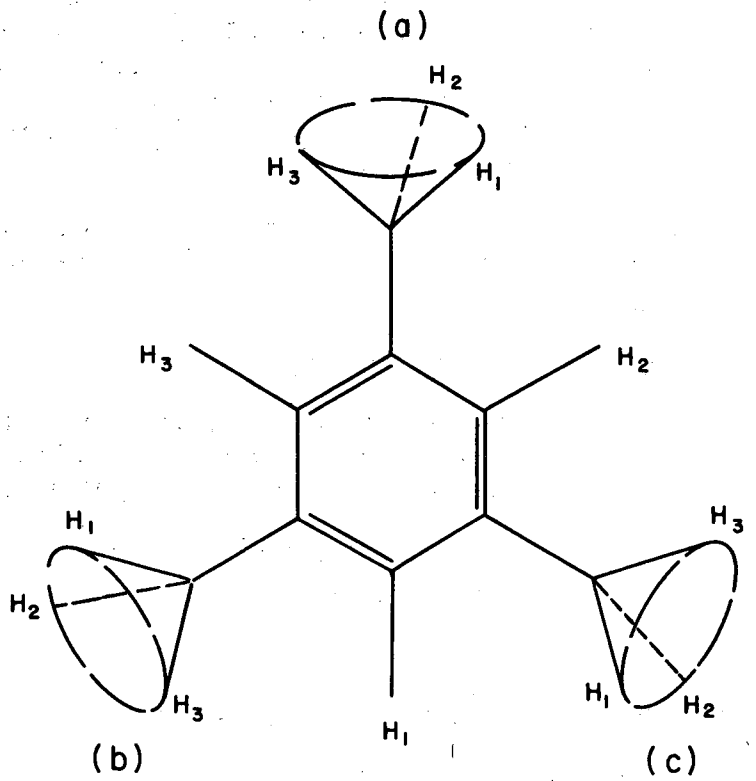

MU-24280

Fig. IE. 7-1. Parameters for spin eigenvalue problem.

Chemical shifts	Coupling constants
$\nu_0 = (\gamma_1/2\pi)\,(1 - \delta_0)\,H^z$	$J_0 = J[P(H_1, H_2)]$
$\nu_1 = (\gamma_1/2\pi)\,(1 - \delta_1)\,H^z$	$J_1 = J[P(H_1, H_{2a})]$, $J_1 = J[P(H_1, H_{1b})]$
	$J = J[P(H_{1b}, H_1)]$, $J' = J[P(H_{1a}, H_1]$

$P \equiv$ All symmetry operators of the molecule.

The spin Hamiltonian for the problem is given by

$$\mathcal{H} = \mathcal{H}^{(0)} + \mathcal{H}^{(1)} + \mathcal{H}^{(2)} , \tag{2}$$

where

$$\mathcal{H}^{(0)} = \sum_{i=1}^{2} \frac{\gamma_i}{2\pi} I_i^z H_i^z ,$$

$$\mathcal{H}^{(1)} = 3J_{0/g} \sum_{P} P(I_1 \cdot I_2) + 9J'_{1/g} \sum_{P} P(I_{1a} \cdot I_{2a}) + 27J_{1/g} \sum_{P} P(I_{1a} \cdot I_{ib}),$$

$$\mathcal{H}^{(2)} = 18J_{/g} \; {}_{P} P(I_1 \cdot I_{1b}) + 9\, J'_{/g} \sum_{P} P(I_1 \cdot I_{1a}).$$

Here $\mathcal{H}^{(0)}$ represents the Zeeman energy in the Paschen-Back high-field case, and $\mathcal{H}^{(1)}$ and $\mathcal{H}^{(2)}$ the interaction between equivalent and nonequivalent nuclei, respectively; g is the dimension of the group.

Since the necessary and sufficient condition for the spectrum to be independent of the interaction between equivalent nuclei is that these couple equally to all other nuclei in the system,[6, 7] the terms in J'_1 do not have to be considered, but those in J_0 and J_1 must be taken into account.

The spin functions obtained from Eq. (2) are exact eigenfunctions of the terms in J_0 but not of those in J_1, J, and J'; therefore $^{(2)}$ and $_1{}^{(1)}$ mix the states with the same total spin angular momentum and symmetry.

In the case presented here the experimental results can be explained by using the approximations

$$\text{(a)} \quad |\delta_0 - \delta_1| >> \text{all } J's, \tag{3}$$

$$\text{(b)} \quad |J_0| > |J| \geq |J - J'| \geq |J'| > |J_1|.$$

Since J_1 is very small, beyond the limits of resolution, the spectra can be analyzed by obtaining the steady-state functions with respect to $^{(2)}$. The terms in $^{(2)}$ are given by the following expressions.

---

[6] H. S. Gutowsky, D. N. McCall, and C. P. Slichter, J. Chem. Phys. 21, 279 (1953).

[7] J. A. Pople, W. G. Schneider, and H. J. Bernstein, High-Resolution Nuclear Magnetic Resonance (McGraw-Hill Book Co., New York, 1959).

A. Diagonal elements:

$$\left\langle \Gamma(m_0, m_1) | \mathcal{H}^{(2)} | \Gamma(m_0, m_1) \right\rangle$$

$$= 1/3\, m_0 m_1 (2J + J'), \text{ for } m_0 = \pm 3/2, \tag{4}$$

$$= 1/3\, m_0 m_1 (2J + J') \text{ for} \left\{ \begin{matrix} m_0 = \pm 1/2 \\ \\ \Gamma = A_1 \times A_1,\ E \end{matrix} \right\} ,$$

$$= 1/3\, m_0 m_1 (2J + J') \mp \ell\, 1/3 (J - J'), \text{ for} \left\{ \begin{matrix} m_0 = \pm 1/2 \\ \\ \Gamma = (E \times E)_{A_1},\ (E \times E)_{A_2} \end{matrix} \right\} .$$

B. Off-diagonal elements:

$$\left\langle \Gamma(m_0, m_1)_i | \mathcal{H}^{(2)} | \Gamma(m_0, m_1)_j \right\rangle$$

$$= 0, \text{ for } m_0 = \pm 3/2$$

$$= f_{ij}(\Gamma, \ell_1, \ell_2) \times (J - J'), \text{ for } m_0 = \pm 1/2,$$

where

$$\ell_1 = 2 m_a - m_b - m_c,$$

$$\ell_2 = m_b - m_c \quad (\text{and } m_i \equiv z \text{ component of angular momentum for the methyl groups});$$

f_{ij} is a function of the species and linear in ℓ_1 and ℓ_2.

Experimental Results

A. The proton NMR spectrum of S-$(CH_3)_3C_6H_3$ at 60 Mc is shown in Fig. IE. 7-2. The value of $2J + J'$ is obtained by identifying the transitions $\Delta m_1 = \pm 1$, $\Delta m_0 = 0$ ($m_0 = \pm 3/2$), which occur at the exact frequency

$$\nu^1 = (\gamma_1/2\pi)\, H_1 \pm (1/2)(2J + J').$$

These are lines 1 and 2 in Fig. IE. 7-2; the separation between them gives

$$|2J + J'| = 2.24 \pm .05 \text{ cps}.$$

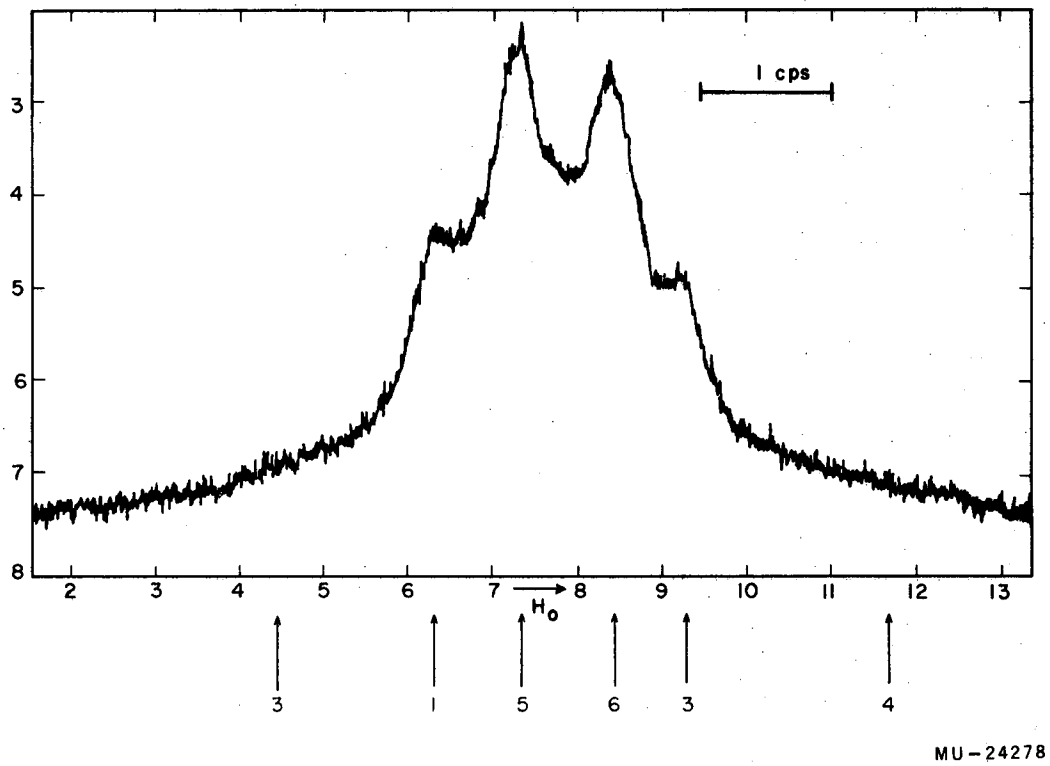

Fig. IE. 7-2a. Proton NMR spectrum of $(CH_3)_3$ in mesitylene at 60 Mc.

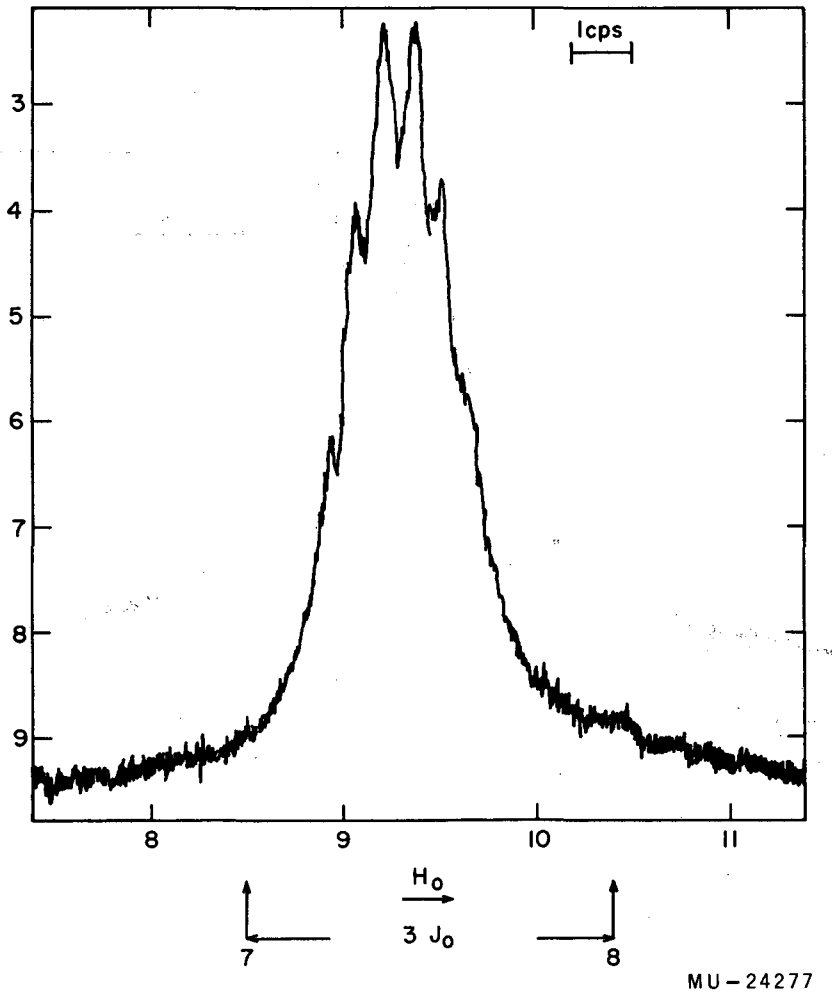

Fig. IE. 7-2b. Proton NMR spectrum of C_6H_3 in mesitylene at 60 Mc.

From the separation between the sets of forbidden lines, (3 and 4) and (7 and 8) the value of J_0 is obtained:

$$J_0 \approx (1/6)\left[\overline{(\nu_4^1 - \gamma_3^1)} + \overline{(\gamma_8^0 - \gamma_7^0)}\right] = 2.2 \pm .2 \text{ cps.}$$

The value of J' must be estimated, since the sets of lines (5 and 6) are not resolved. Nevertheless it is shown in the next section that J and J' arise from π-electron coupled nuclear hyperfine interaction with a ratio which depends on the type of approximation:

$$\left|\frac{J}{J'}\right| \approx \left(\frac{N_0^\pi}{N_p^\pi}\right)^2 = 4 \qquad (5) \qquad \text{(present calculation)}$$

$$\text{or} \quad \left|\frac{J}{J'}\right| \approx 2.$$

Here N^π is the bond order for the corresponding carbon atoms in the aromatic hydrocarbon. The spectrum was calculated for the two cases $J' = 1/4\ J$ and $J' = +\ 1/2\ J$, with $J_1 = 0$.

The best fit is obtained with $J' = +\ (1/2)J$, as shown by the calculated spectrum in Fig. IE. 7-2.

The NMR parameters for the spectrum are given by

$J' = +\ (1/4)J$	$J' = -(1/4)J$
$J = \pm\ 1.00$ cps	$J = \pm\ 0.90$ cps
$J' \approx \pm\ 0.25$	$J' = \mp\ 0.45$
$J_0 = \pm\ 2.2 \pm .2$	
$J_1 \leqslant 0.2$ cps	
$\delta_0 = -0.763 \pm .005$ ppm from TMS.	
$\delta_1 = -5.241 \pm .005$ ppm from TMS.	

The values observed here are higher than those reported by Hoffman[8] after correcting his analysis.

B. The fluorine NMR spectrum of $(CF_3)_3C_6H_3$ at 56.4 Mc is shown in Fig. IE. 7-3. The proton spectrum has not been resolved. Although the features of the parent hydrocarbon are observed, the spectrum is not well resolved, since the value of J_1 is higher here. The value of $2J + J'$ is obtained by identifying the transitions $\Delta m_1 = \pm 1$, $m_0 = \pm 3/2$, which give

$$2J + J' = 5 \pm .5 \text{ cps.}$$

[8] R. A. Hoffman, Mol. Phys. 1, 326 (1958).

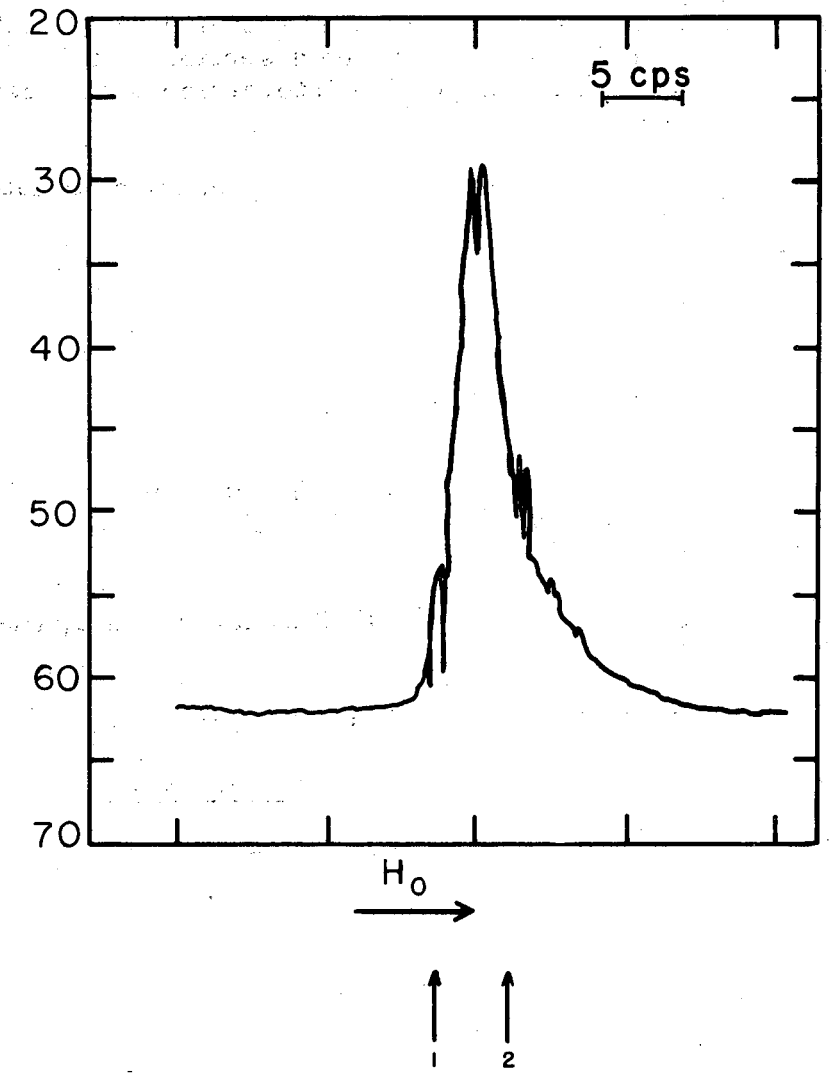

Fig. IE. 7-3. Fluorine NMR spectrum of $(CF_3)_3C_6H_3$ at 56.4 Mc.

Hyperfine Coupling Constants

The electron-coupled nuclear hyperfine interaction, correct to second order in the Ramsay theory,[4] is given by

$$J_{(N,N')} = -(2/3)\, h \sum_n \left\langle {}^1\psi_0 \left| \mathcal{H}_N \right| {}^3\psi_n \right\rangle \left\langle {}^3\psi_n \left| \mathcal{H}_{N'} \right| {}^1\psi_0 \right\rangle / (E_n - E_0). \quad (5)$$

Here through the electron-nuclear spin interactions $\mathcal{H}_{N'}$ excited triplet states ${}^3\psi_n$, are virtually mixed into the ground state ${}^1\psi_0$, $\mathcal{H}_N$ is given by

$$\mathcal{H}_N = \delta_0 \sum_k \delta(\vec{r}_{kN})\, \vec{S}_k ,$$

where δ_0 is a constant, $\delta_0 = 8\pi/3\, g_e g_N \beta_e \beta_N$.

The long-range nuclear interactions may be explained as π-electron coupled.[5] In the aromatic hydrocarbon the σ and π-electron systems interact only through a second-order mechanism, which has been demonstrated by the proton splitting of the ESR spectrum of aromatic free radicals.[9]

The expression obtained for the π-electron coupled nuclear hyperfine interaction is given by

$$J_{N,N'} = -(2/3)h\, Q_H\, Q_{CH_3} \sum_{n,n'} (a_N a_{N'})^n (a_N a_{N'})^{n'} / \Delta\epsilon^{\pi}_{n,n'} (1 - \Delta^2_{n,n'})^2, \quad (6)$$

where Q_H and Q_{CH_3} are empirical constants determined from the ESR spectra of aromatic free radicals,[9, 10]

$$Q_H = -64 \text{ Mc},$$

$$Q_{CH_3} = +75 \text{ Mc}.$$

Here $\Delta_{n,n'}$ is a correction factor to Q_H and Q_{CH_3} since for the free radicals the σ - π exchange energy is between doublet states while here it occurs between a singlet and a triplet state,

$$\Delta_{n,n'} = \Delta\epsilon^{\pi}_{n,n'} / \Delta\epsilon^{\sigma} ,$$

where $\Delta\epsilon_\sigma$ is the excitation energy from bonding to antibonding states for the C-X fragment localized M. O.;[11] a^n_N and $a^{n'}_N$ are the coefficients for the

---

[9] H. M. McConnell and D. B. Chesnut, J. Chem. Phys. 28, 107 (1958).

[10] A. D. McLachlan, Mol. Spectroscopy 1, 233 (1958).

[11] M. Karplus, J. Chem. Phys. 33, 1842 (1960), has used the same correction in calculating the π-electron coupled hyperfine interactions in aliphatic hydrocarbons.

carbon $2p\pi$ atomic orbital, bonded to the X nucleus, (X=N, N') in the L. C. A. O. expression for the Hückel M. O.'s, i.e.,

$$\pi^i = \sum_\ell a_\ell^{(i)} \phi_\ell, \quad \phi_\ell = C\,(2p\pi).$$

It is observed that for the alternate hydrocarbons Eq. (6) leads to the expression obtained by McConnell[5] in the ground-state approximation except for the correction factor:

$$J_{N,N'} = +(2/3)h\, Q_H\, Q_H Q_{CH_3}\, 4\Lambda_{N,N'} / \left\langle \Delta\epsilon (1 - \Delta^2)^2 \right\rangle . \qquad (7)$$

In the work described here, however, the average energy approximation cannot be used. The Hückel M. O.'s for the S-$(CH_3)_3 C_6H_3$,[12,13]

$$\Delta\epsilon^{\sigma} = 4.6\,\beta_0 \quad (11.8 \text{ ev}),$$

$$\beta_0 = 2.56 \text{ ev} \quad (\text{spectroscopic value}^{14}),$$

yield the following values for the coupling constants:

$$J = -0.93 \text{ cps},$$
$$J_1 = -0.38 \text{ cps},$$
$$J' = -0.41 \text{ cps},$$
$$2J + J' = -2.27 \text{ cps}.$$

The calculated $2J + J'$ is in agreement with the experimental results, but J_1 is too high.

---

[12] C. A. Coulson and V. A. Crawford, J. Chem. Soc. (1953) 2052; V. A. Crawford, ibid. (1953) 2058, 2061.

[13] H. C. Longuet-Higgins, et al., Proc. Roy. Soc. (London) 67A, 795 (1954); ibid 68A, 81 329 (1955).

[14] R. S. Mulliken, J. chim. phys. 46, 497 (1949).

8. TEMPERATURE-DEPENDENT CHEMICAL SHIFTS IN NMR SPECTRA OF GASES*

Charles H. Sederholm and Leonidas Petrakis

Recently, several examples have been reported by Gutowsky,[1] G. V. D. Tiers,[2] and others[3] of an NMR chemical shift of proton and fluorine resonances resulting from an isotopic substitution in the vicinity of the nucleus under consideration. In all cases thus far reported, the resonance of a particular atom moves to a higher field, greater magnetic shielding, when an atom in the immediate vicinity is replaced by a heavier isotope.

It has been postulated that this effect is a result of a change in the dynamic state of the molecule due to the increased effective mass for all vibrations in which the substituted nucleus participates, resulting in lower zero-point energies for these modes and thus a change in the average electronic wave function.

Gutowsky has made a semiquantitative calculation based on such a model[1] which gives the proper direction for the shift and a fair agreement with the magnitude. By measuring the chemical shift that accompanies the change of the dynamic state of a molecule when some of its vibrational modes are thermally excited, we hoped to experimentally substantiate this explanation of the isotope shift.

The investigation was done at 60 Mc and on gaseous samples in order to avoid any temperature-dependent solvent effects. The chemical shifts, from methane, of eleven compounds were measured as a function of temperature. The slopes of the best straight lines through the experimental points are tabulated below.

Compound	$\frac{d(\nu_0 \delta \text{ methane})}{dT}$ (cps per ^{o}C)	$\nu_0 \delta$ methane$_{(25^{o}\text{ C.})}$ (cps)
HBr	0.0000±.0005	-260.5
C_2H_6	0.0000±.0005	-44.7
C_3H_6	-0.0080±.0027	-3.9
C_4H_8	-0.0071±.0009	-113.9
C_5H_{10}	-0.0035±.0009	-86.9
$C(CH_3)_4$	-0.0061±.0014	-49.2
$Si(CH_3)_4$	-0.0125±.0015	-8.4
$Sn(CH_3)_4$	-0.0102±.0025	-5.9
C_2H_2	-0.0087±.0014	-80.1
CH_3CCCH_3	-0.0047±.0008	-87.7
C_2H_4	+0.0038±.0015	-310.6

*To be submitted for publication in J. Chem. Phys.

[1] H. S. Gutowsky, J. Chem. Phys. 31, 1683 (1959).

[2] G. V. D. Tiers, J. Am. Chem. Soc. 79, 5585 (1957); J. Chem. Phys. 29, 963 (1958).

[3] T. F. Wimmett, Phys. Rev. 91, 476A (1953).

Almost all organic compounds have resonances in an interval of 600 cps at 60 Mc. On this basis it seems unlikely that the chemical shift of an upper vibrational state of a compound from its ground vibrational state should be more than 100 cps. Let Δ designate this chemical shift. Assuming $\Delta(HBr) \leqslant 100$ cps, one readily calculates that the $d\nu/dT$ of HBr should be $\leqslant 0.0001$ cps per ^{o}C, where ν is the resonance frequency at 14,092 gauss. It is assumed that in the gaseous phase no other effect causes a $d\nu/dT$ of comparable magnitude. If this is true, gaseous HBr can be used as a temperature-independent standard from which to measure temperature-dependent chemical shifts. Because of experimental difficulties, it is more convenient to use CH_4 as a standard rather than HBr. It can be seen from the data above that if HBr is temperature-independent, so is methane.

Let Δ_i be the shift associated with exciting the ith vibrational mode of a molecule, δ^0 the shift from methane of the ground vibrational state, ν_i the frequency associated with the ith vibrational mode, ν_0 the experimental rf frequency, and g_i the degeneracy of the ith mode. We can then write

$$\nu_0\delta = [\nu_0\delta^0 + \sum_i g_i \exp(-h\nu_i/KT)(\Delta_i + \nu_0\delta^0)]/[1 + \sum_i g_i \exp(-h\nu_i/KT)], \quad (1)$$

where δ is the chemical shift from methane. If all the vibrational modes with sizable Δ's have ν's greater than 200 cm^{-1}, and the temperature range under consideration is near 50 ^{o}C, this can be simplified to

$$\nu_0\delta \approx \nu_0\delta^0 + \sum_i g_i \Delta_i \exp(-h\nu_i/KT), \quad (2)$$

and therefore

$$\frac{d(\nu_0\delta)}{dT} \approx \sum_i \Delta_i g_i \frac{h\nu_i}{KT^2} \exp(-h\nu_i/KT), \quad (3)$$

That is, the $d(\nu_0\delta)/dT$ due to the various modes of vibration are additive.

The question of degeneracy is somewhat complicated by the following consideration. Consider, for example, a single hydrogen atom vibrating against a carbon skeleton. There is a Δ_i associated with exciting this mode of vibration. Now consider two hydrogen nuclei attached to the same carbon atom. In order to achieve the same observed chemical shift of the two hydrogen nuclei, one would have to excite both the symmetric and antisymmetric stretching modes. The Δ_i associated with either of these two modes would be approximately 1/2 of the Δ_i associated with the stretching mode of a single hydrogen atom. If one wishes to assign a single Δ to a given kind of vibrational mode, one must collect terms in the sum of Eq. (3) which deal with a given kind of vibration--e.g., CH_3 parallel deformation or CH_2 deformation--and consider them as a single contribution. One should then use an average of the individual frequencies, assign a degeneracy of 1 to the mode, and assign a Δ_i^* to this average mode. In the case of a single group, Δ_i^* become equal to the chemical shift brought about by exciting all the modes of a given kind in that group. These Δ_i^* do not depend upon the symmetry of the molecule, but only upon the type of motion involved.

Over the temperature range studied it is impossible to gain much information about Δ_i^* for any mode the frequency of which is above 2000 cm^{-1}, as these modes are always so lightly populated that the term in the sum of Eq. (3) associated with them is less than our experimental error unless Δ_i^* is unreasonably large. Therefore, although exciting such modes as the CH stretching mode is probably very effective in causing a chemical shift, the temperature dependence caused by this mode is too small to be measurable in the temperature range under consideration.

The temperature dependence of the chemical shift in ethane is zero to within our experimental accuracy. This may come about as an exact, accidental cancellation of two or more temperature-dependent terms with opposite sign. This, however, seems unlikely, particularly in view of the fact that all the $[d(\nu_0\delta)/dT]$'s are of the same sign except in the case of ethylene, an anomaly that can readily be explained. In the case of ethane, we have therefore assumed that each individual term in the sum in Eq. (3) is zero to within our experimental accuracy. It also seems reasonable to assume that to a fair degree of accuracy, the Δ_i^* for a given set of modes determined from one molecule should be applicable in other molecules with similar modes. Making these two assumptions, one may calculate from the data given above the following values for Δ_i^* for several vibrational modes.

Compound	Vibrational mode	Shift (cps)
Methane	CH bending modes	$\lvert\Delta^*\rvert \leqslant 10$
Ethane	CH_3 $\perp$ deformation	$\lvert\Delta^*\rvert \leqslant 17$
	CH_3 $\parallel$ deformation	$\lvert\Delta^*\rvert \leqslant 13$
	CH_3 wag	$\lvert\Delta^*\rvert \leqslant 3$
	C-C stretch	$\lvert\Delta^*\rvert \leqslant 3$
Cyclopropane	CH_2 rock, wag, and twist	$\Delta^* = -14$
Cyclobutane	CH_2 rock, wag, and twist	$\Delta^* = -16$
Cyclopentane	CH_2 rock, wag, and twist	$\Delta^* = -9$
Tetramethylmethane	Skeletal bends	$\Delta^* = -0.3$
Tetramethylsilane	Skeletal bends	$\Delta^* = -0.8$
Tetramethyltin	Skeletal bends	$\Delta^* = -0.6$
Acetylene	CH bending mode	$\Delta^* = -17$
Dimethylacetylene	Skeletal bends	$\Delta^* = -1.2$
Ethylene	Twist	$\Delta^* = +36$

The reason that the CH bending modes in acetylene have a larger Δ_i^* than the CH_2 bending modes in the cyclic compounds is probably that in acetylene, exciting the CH bending modes destroys the symmetry and therefore causes extra paramagnetic shielding due to the asymmetric magnetic susceptibility of the pi electrons. This is probably also the case in the skeletal bending modes of dimethylacetylene. The large positive Δ_i^* for the twisting mode in ethylene is probably due to the delocalization of the pi electrons and subsequent increase in electron density at the protons.

It is seen from the data above that a sizable chemical shift is observed when one changes the dynamic state of a molecule by exciting vibrational modes. This chemical shift is of the order of magnitude that would be nedessary to substantiate the explanation of the isotopic shift offered by Gutowsky.

9. LINE WIDTHS FOR THE PARAMAGNETIC RESONANCE OF Mn^{++} IN AQUEOUS SOLUTION*

Robert G. Hayes and Rollie J. Myers, Jr.

The properties of the aqueous solutions of metal ions have received considerable attention in these laboratories. As part of this general interest we have examined the paramagnetic resonance of several transition-metal ions in aqueous solution both at room temperature and above. In particular, we have been interested in systems in which the ionic fields have essentially cubic symmetry, since the mechanism responsible for width (T_2) in complex ions of lower symmetry with a unique axis is well known.

In the course of this investigation we observed the widths of the Mn^{++} resonance in H_2O [species $Mn(H_2O)_6^{++}$] and discussed a dependence of width on hyperfine component. The Mn^{++} ion has a six-line spectrum due to the interaction of the electronic moment with the nuclear moment of Mn^{++} ($I = 5/2$). At room temperature these six lines are all of approximately the same width, but as the temperature is raised a difference in widths becomes apparent until finally, at a temperature near the boiling point, it becomes obvious that the widths of the two outermost lines ($M_I = \pm 5/2$) are greatest, followed by the two lines next in from these ($M_I = \pm 3/2$), and that the innermost ($M_I = \pm 1/2$) are narrowest. Further, in the pairs mentioned above, the resonance occurring at lower field ($M_I < 0$) is always slightly less than that occurring at higher field ($M_I > 0$). This effect is not explicable in terms of either of the current hypotheses (see below) because no anisotropy in the hyperfine coupling constant has ever been detected in single-crystal studies of Mn^{++} surrounded by an octahedran of water molecules,[1] and this is the first requirement for dependence of width upon hyperfine component. However, one notes that each observed hyperfine line is a superposition of fine electronic transitions $M_S \rightarrow M_S - 1$ in a system with $S = 5/2$. If a mechanism which could split these fine transitions existed the observed width could be a result of unresolved fine structure in each observed line. Such a mechanism is readily found. One may assume that the observed spectrum is that corresponding to the eigenstates of the isotropic part of the spin Hamiltonian $\mathcal{H} = g\beta \bar{S} \cdot \bar{H} + A\bar{I} \cdot \bar{S}$ with g, A isotropic. The first-order portion of this,

*Partially reported at Northern California Section, American Chemical Society meeting, December 19, 1960.

[1] K. D. Bamers and J. Owen, Repts. Progr. in Phys. 18, 304 (1955).

$\mathcal{H} = g\beta S_z H_z + A I_z S_z$, yields six transitions corresponding to $M_I = -5/2 \ldots 5/2$. The off-diagonal portion, $A/2(I^+S^- + I^-S^+)$, however, splits each of the lines into fine closely spaced fine-structure components, corresponding to the incomplete Paschen-Back effect in atomic spectroscopy. Table I gives the observed width at maximum slope of the six hyperfine transitions and also the spread of the fine-structure components as calculated by second-order perturbation theory.

As is seen, the $M_I = +1/2$ line remains unsplit and is thus the only one of interest for line width studies. We have not been able to resolve the fine structure because the splitting between successive components is less than the width of each component.

Table I. Width and spread of lines in Mn^{++} spectrum.

M_I	$\Delta H_{m.s.}$[a] (gauss)	Calc. spread[b] (gauss)
-5/2	19.2	30.6
-3/2	14.8	21.9
-1/2	11.2	11.8
1/2	10.0	0.2
3/2	11.2	12.8
5/2	16.2	27.1

[a] Line width at maxima of derivative.

[b] Calculated spread of fine-structure components.

We have also measured the temperature dependence of the width of the $M_I = 1/2$ component Mn^{++} in dilute H_2O and D_2O solutions in an attempt to distinguish between McGarvey's[2,3] and Al'tschuler and Valiev's[4] hypotheses of T_2 in symmetrical complexes. McGarvey extends the theory accepted for unsymmetrical complexes to symmetrical complexes, arguing that the weak axial fields observed in the solid complexes[1] persist in the liquid, yielding a term in the spin Hamiltonian $D[S_z^2 - S(S+1)]$, where z refers to an axis fixed in the molecule. He then treats this term as causing transitions, using a treatment similar to that by Bloembergen, Purcell, and Pound.[5] This yields an expression for the width of the form

[2] H. M. McConnell, J. Chem. Phys. 25, 709 (1956).

[3] B. R. McGarvey, J. Phys. Chem. 61, 1232 (1957).

[4] S. A. Al'tschuler and K. A. Valiev, Soviet Physics--JEPT 8, 661 (1959).

[5] N. Bloembergen, E. M. Purcell, and R. V. Pound, Phys. Rev. 73, 679 (1948).

$1/T_2 = C\tau_c$, under appropriate conditions, where τ_c is the correlation time for tumbling and is approximately proportional to the viscosity of the solvent. According to this hypothesis the line width is a monotonically decreasing function of temperature. On the basis of the observation by Kozyrev et al.[6] that the line width in Mn^{++} solutions increased again for $T \geqslant 100\ ^{o}C$, Al'tschuler and Valiev proposed that relaxation in these complexes was the result of vibronic interaction. They used an expression of the type used to treat relaxation in solids, replacing the expansion of the vibrational coordinates of the complex in phonon operators by a correlation function for the vibrational amplitudes, i.e., assuming the vibrational motion to be classical. They thus arrived at an expression of the form $1/T_2 = CT^{-1/2}\ \mathrm{ctnh}\ \frac{\hbar\omega}{kT}$, where ω is a mean vibrational frequency. This expression has a minimum at $T \doteq \frac{\hbar\omega}{1.05\,k}$. Our studies of Mn^{++} in D_2O and H_2O indicate that McGarvey's mechanism is probably correct. The line widths in D_2O are consistently approximately 10% greater in D_2O, in which viscosity is somewhat greater. The hypothesis of Al'tschuler and Valiev would yield somewhat smaller line widths in D_2O than in H_2O.

We should be able to extend our studies above 100 °C and investigate the increase in width reported in that temperature range. It is possible that the mechanism of Al'tschuler and Valiev dominates at these temperatures. However, it seems to us more probable that relaxation at these temperatures is controlled by exchange of ligand within the complex, since Connick and co-workers have estimated the mean lifetime of a water molecule in the first coordination sphere of Mn^{++} to be $\leqslant 10^{-7}$ sec at 300 °K.[7] This is only an order of magnitude less than the observed line widths (in megacycles) at the same temperature, and so will surely contribute appreciably at higher temperatures. It is expected that ligand exchange will yield a "strong collision" type of relaxation mechanism familiar in, for instance, microwave spectroscopy with a T_2 approximately equal to the mean lifetime between collisions. The lifetimes at elevated temperature are now under investigation,[8] and we await the results.

These studies are being continued. It is planned that a number of Cr^{3+} complexes, in which ligand exchange is unimportant, be investigated next, followed perhaps by some other systems (e.g., Fe^{3+}) in which relaxation seems anomalous.

---

[6] V. I. Avvakumov, N. S. Garif'yanov, B. M. Kozyrev, and P. G. Tishkov, Soviet Physics–JEPT 10, 1110 (1960).

[7] R. E. Connick and R. E. Paulson, J. Chem. Phys. 30, 759 (1959); Diane Stover, Rate of Elimination of Water Molecules from the First Coordination Sphere of Paramagnetic Cations as Determined by Nuclear Magnetic Resonance Measurements of O^{17} (Thesis), Lawrence Radiation Laboratory, Report UCRL-9265, July 8, 1960.

[8] Robert E. Connick (Lawrence Radiation Laboratory), private communication.

10. ASYMMETRIC ROTOR DIRECTION COSINE ROUTINE

John A. Howe

A computer routine to calculate asymmetric rotor direction cosine matrix elements has been completed. These quantities are required in the analysis of microwave absorption spectra of asymmetric tops.

To date, this routine has been used in analyzing data for 1-chloro-2-fluorethylene. In this case, a near degeneracy gives rise to a sizable second-order correction to the quadrupole hyperfine energies, so that a value of the off-diagonal component of the coupling tensor can be directly calculated. This value can in turn be used to calculate the chlorine 3p lone-pair defect arising from conjugation with the double bond; the value obtained is 0.04 electron.[1]

Future uses for this routine are envisaged in treating the Stark effect of this and of similar molecules, and in calculating second-order quadrupole energies.

[1] John A. Howe, The Microwave Spectrum of cis 1-chloro-2-fluorethylene, J. Chem. Phys. 34, 1247 (1961).

11. CURRENT INVESTIGATIONS ON GENERAL PHYSICAL CHEMISTRY TOPICS, 1961

Kenneth S. Pitzer

1. Nuclear magnetic resonance and electron spin resonance measurements on hydrogen bonding systems.

2. Measurement of the thermal properties of the various isotopic species of hydrogen and of methane at low temperatures and high pressures, and interpretation of the various phase transitions or other anomalies.

3. Theoretical treatment of quantum-mechanical tunneling in collisions leading to chemical reaction.

4. Theory predicting real fluid properties from characteristics of component molecules.

Chalres H. Sederholm

The strange NMR coupling constants between fluorine atoms on adjacent, saturated carbon atoms are being investigated.

Rollie J. Myers, Jr.

1. Paramagnetic resonance studies of transition-metal ions. (With R. G. Hayes.)

2. Paramagnetic resonance of selected hydrocarbon negative ions. (With R. G. Hayes.)

3. A study of the hydrogen atom oxygen molecule reaction. (With N. Edelstein.)

4. Color centers in calcite and other minerals.

John A. Howe

1. Investigation of halogen lone-pair conjugation continues, with further experimental and computational work on both cis and trans 1-chloro-2-fluorethylene.

2. Investigation of the near-ultraviolet absorption spectrum of propargyl aldehyde H—C≡C—CHO has begun.

METALLURGY AND CERAMICS

II A. INFLUENCE OF MICROSTRUCTURE ON THE PHYSICAL PROPERTIES OF SOLIDS

1. SOLID-SOLUTION STUDIES

Earl R. Parker

Earlier work on single crystals[1] had revealed several important facts not previously understood, namely that

(a) in single crystals the dislocations responsible for flow originate at external surfaces,

(b) surface dislocations are generated just as easily in alloy crystals as in pure metals (i. e., solute atoms do not pin surface sources),

(c) dislocations, once generated, move just as easily through the alloy lattices as they do through a crystal of the pure metal,

(d) dislocations piled up at internal interfaces, such as subboundaries, are markedly influenced by the presence of solute atoms (i. e., the greater the concentration of solute atoms, the more resistant to penetration the boundary becomes to piled-up dislocations), and

(e) solution hardening in single crystals is entirely due to the interaction of solute atoms with internal barriers such as subboundaries.

The investigation has been extended to studies of the behavior of polycrystalline materials. Copper was selected as the base material; thus, direct comparisons could be made between the behaviors of the polycrystalline and single-crystal specimens.

The study of polycrystalline specimens is much more involved than that of single crystals because of the complexities introduced by grain size and grain boundary structure (i. e., the extent and kind of preferred orientation). The usual practice of producing a range of grain sizes--i. e., by heating a fine-grained material to a series of higher temperatures--does not produce random grain orientation. Grain growth occurs in a preferential manner, with the higher-energy boundaries tending to disappear more rapidly than those of low energy. The larger-grained specimens thus contain a disproportionate number of lower-energy boundaries. Thus a "growth texture" results which makes a direct evaluation of grain size, as such, impossible because each successively larger grain size would have a less random grain structure. This factor has been generally ignored by investigators in the past, but it must be taken into account and controlled for both solution hardening and creep studies. Both properties depend upon the nature of the grain boundaries. For example, low-angle boundaries would collect dilute atmospheres and would be weak at room temperature, whereas high-angle boundaries would collect more solute atoms and would be stronger because of this characteristic and because of the more complex geometry.

---

[1] C. D. Wiseman, E. R. Parker, and T. H. Hazlett, Substitutional Solid-Solution Strengthening of Copper Alloys, University of California Minerals Research Laboratory Technical Report 16, AECU-3870, June 1957.

Polycrystalline specimens, unlike the single crystals, have definite and high elastic limits. Furthermore, the yield stress varies with the amount and kind of alloy present. The main source of dislocations seems to be the grain boundaries, and these regions are strongly pinned by solute atoms so that the yield strength varies with grain size, grain orientation, and the kind and amount of the foreign atoms present.

Recent preliminary experiments have shown that solid-solution hardening is structure-sensitive and that the magnitude of the hardening is dependent upon the thermal history of the material.[2] The yield strength of a copper alloy containing 10 atomic % of aluminum could be increased 50% by cooling rapidly in helium from 550 °C and then reheating to 550 °C. This surprisingly great increase in strength was attributed to the reconcentration of solute atoms in the grain boundaries, after having been "dissolved" out of them by the higher temperature treatment. These results have been verified, but the explanation of the observed effect is not yet certain. If the interpretation is correct, a new field of alloy investigation has been opened.

[2] K. Kennedy and E. R. Parker, Investigation of Factors Controlling the Mechanical Properties of Alloys, University of California Materials Research Laboratory Technical Report 17, TID-6128, May 1960.

2. ON THE STABILITY OF THE DISLOCATION SUBSTRUCTURE IN QUENCHED ALUMINUM*

Richard R. Vandervoort and Jack Washburn

The equilibrium concentration of vacant lattice sites in a crystal decreases with decreasing temperature according to the approximate relation

$$C_v = \exp(-U_{fv}/kt),$$

where C_v is the fraction of the total number of lattice sites that are not occupied by an atom, and U_{fv} is the energy of formation of a vacancy. Therefore, when a metal is cooled, vacant lattice sites must be eliminated. There are only three ways excess vacancies can be removed: (a) migration to an external surface; (b) precipitation on an edge dislocation line, or (c) clustering to form small voids or prismatic dislocation loops as proposed by Seitz.[1]

Resistivity measurements suggest that when the cooling rate is rapid enough, the concentration of vacancies present at some higher temperature can be frozen in.[2] As long as the temperature is then kept low enough to prevent migration no change in vacancy distribution can take place.

* Brief form of published paper, Phil. Mag. 5, 49 (1960).

[1] F. Seitz, Phys. Rev. 79, 890 (1950).

[2] J. E. Bauerle and J. S. Koehler, Phys. Rev. 107, 1943 (1957).

When an aluminum specimen which has been quenched from 600 °C rapidly enough to retain the high temperature vacancy concentration is reheated to successively higher temperatures, the resistivity increment due to excess vacancies disappears in two distinct stages. The first stage of recovery which accounts for 80% of the total resistivity increment lies in the temperature range from 190°K just below room temperature. It is probably due to disappearance of individual vacancies by formation of clusters. Direct electron microscope observations have shown that this thermal history does, in fact, produce vacancy clusters which collapse to form small dislocation loops 200 A to 600 A in diameter.[3] A dislocation density as high as 10^{10} cm/cm^3 can be produced in this way. Therefore, the resistivity increment remaining at room temperature may be due to the dislocations. The effect of the same thermal history on mechanical properties has been investigated by Maddin and Cottrell.[4] They observed a large increase in room-temperature yield strength, which must also be associated with the presence of prismatic dislocation loops.

The second resistivity drop took place on heating into the temperature range between 100 and 200 °C. The activation energy for the process was found to be 1.31 ev.[5] This suggests that second-stage recovery may be associated with the disappearance of prismatic dislocation loops. Dislocation density could be greatly reduced by migration of vacancies from loops to other sinks, or by growth of the largest loops at the expense of smaller ones. Small amounts of plastic deformation at room temperature also cause a drop in resistivity.[6] This suggests that loops can be swept out by moving dislocations even at room temperature. The experiments reported here were undertaken to obtain direct evidence concerning the mechanisms of this second-stage resistivity decrease and of quench hardening. Changes in dislocation substructure in quenched aluminum specimens caused by reheating to successively higher temperatures or resulting from various amounts of cold work after quenching, were observed by electron transmission microscopy.

Aluminum sheet specimens 0.005 cm thick, of nominal purity 99.995%, were quenched from 600 °C into iced brine. The first series of specimens was then heated for 10 minutes to either 100, 125, 150, 175, or 200 °C. The second series was cold rolled at room temperature to 2.5%, 5%, 10%, 15%, or 45% reduction in thickness after quenching. A thicker specimen was cold rolled to 98% reduction in thickness. All specimens were then thinned by electropolishing in a solution of 20% perchloric acid–80% absolute alcohol to obtain fragments about 1000 to 1500 A thick. The thin foil fragments were examined in an RCA - 2E electron microscope operating at 50 k v with either a 50-mil or a 25-mil aperture. The results can be summarized as follows:

---

[3] P. B. Hirsch, J. Silcox, R. E. Smallman, and K. H. Westmacott, Phil. Mag. 3, 897 (1958).

[4] R. Maddin and A. H. Cottrell, Phil. Mag. 46, 735 (1955).

[5] T. Federighi, Phil. Mag. 4, 502 (1959).

[6] M. M. Winterberger, 1958, Vacancies and Other Point Defects in Alloys (The Institute of Metals, London 1957), 201.

a. Dislocation loops formed by condensation of excess vacancies in quenched 99.995% aluminum began to disappear on heating for 10 minutes to 125 °C and were completely eliminated by heating for 10 minutes to 200 °C.

b. The process was not homogeneous throughout the specimen. Clear areas began to grow at about 125 °C and the proportion of specimen volume that was free of loops increased with increasing temperature of treatment.

c. In the regions still containing loops after heating into the upper part of the range, coarsening took place by growth of the larger loops at the expense of the smaller ones.

d. Elimination of the high dislocation density associated with quenched-in loops probably explains the second-stage resistivity drop observed by Panseri and Federighi.[7]

e. Irregular kinked dislocation lines appeared during the disappearance of loops, and then tended to straighten out and disappear again after the loops had been eliminated.

f. Moving dislocations combined readily with the loops at room temperature. Irregular kinked dislocation lines were produced. A plastic deformation of 5% reduction in thickness by rolling was sufficient to sweep out all the loops--resulting in a decrease in total dislocation density.

This area of research, presently supported by other AEC contract, is to be transferred to LRL in February 1961.

[7] C. Panseri and T. Federighi, Phil. Mag. 3, 1223 (1958).

3. TENSILE BEHAVIOR OF LITHIUM FLUORIDE*

Donald B. Hoover and Jack Washburn

Plastic properties of lithium fluoride and magnesium oxide have become of interest for two reasons:

(a) the true cause for brittleness of nearly all ionic-covalent crystals is not completely understood;

(b) these materials have provided a unique opportunity to correlate properties of individual dislocations with plastic deformation and the nucleation and propagation of cracks.

In lithium fluoride and in other materials having the NaCl structure, it has been found that the grown-in dislocations are usually immobile. Slow cooling from high temperature allows formation of impurity atmospheres or even precipitates on all elements of the existing dislocation substructure.

* Brief version of a paper prepared for publication.

When a stress is applied, slip starts by nucleation of fresh dislocation half loops at the concentrations of most severe surface stress. Dislocation half loops expand across the slip plane and multiply to form wide bands of slip. Because fresh dislocation half loops can be intentionally introduced by local surface deformation, it is possible to create isolated loops to study the properties of individual dislocations, or to influence the distribution of plastic strain by causing growth of many slip bands instead of only a few.

The behavior of individual dislocations has been extensively investigated in lithium fluoride.[1] The mechanism of slip-band growth has also been clarified by electron-transmission microscopy of deformed magnesium oxide.[2]

In spite of the wealth of information concerning the mechanism of plastic deformation in these materials, there have been few attempts to correlate the properties of individual dislocations and the growth of slip bands with macroscopic plastic behavior as revealed by the stress strain curve. Gilman and Johnston[3] have suggested that a yield hump at the beginning of plastic deformation can be explained by the stress dependence of average dislocation velocity if reasonable assumptions are made concerning the increase in number of moving dislocations with increase in strain. Therefore, breakaway of dislocations from impurity atmospheres may not always be involved when this type of yield drop is observed.

The experiments presented here were undertaken to determine the effect of slip distribution on the shape of the stress-strain curve. Tensile tests were performed on specimens which had been carefully polished and therefore deformed by growth of relatively few slip bands. These were compared with specimens in which many mobile surface half loops had been introduced prior to testing.

The results of these experiments can be summarized as follows:

a. When a LiF crystal is loaded in tension along a [100] direction, four slip systems are symmetrically oriented relative to the tension axis. It was found that in any one region of the specimen the growth of slip bands was confined to only two orthogonal systems. This behavior can be rationalized on the basis of the types of dislocation reaction that take place at orthogonal and nonorthogonal slip-band intersections. At the latter the interaction

$$\frac{a}{2}\,[110] + \frac{a}{2}\,[0\bar{1}1] \rightarrow \frac{a}{2}\,[101]$$

leads to formation of dislocation segments that do not lie in their plane of easy glide. Electron-transmission microscopy of deformed magnesium oxide shows that these immobile segments lead to formation of dense dislocation tangles.

---

[1] J. J. Gilman and W. G. Johnston, Dislocations and Mechanical Properties of Crystals (John Wiley and Sons, Inc., New York, 1958), p. 116.

[2] J. Washburn, J. Groves, A. Kelly, and G. K. Williamson, Phil. Mag., 5, 991 (1960).

[3] W. G. Johnston and J. J. Gilman, J. Appl. Phys. 30, 129 (1959).

b. When a specimen deforms by growth of only a few slip bands, the stress-strain curve has a yield hump followed by an increase in strain at almost constant stress. Above about 2% plastic strain the stress begins to increase linearly with increasing strain. If many surface sources are introduced, the crystal deforms by growth of a great number of slip bands. No yield hump is observed and deformation proceeds at significantly lower stress. This behavior can be explained on the basis of the properties of individual dislocations. A given strain rate can be obtained by motion of a few dislocations at high velocity or by motion of a larger number at lower velocity. The velocity-stress relationship for individual dislocations has been measured for lithium fluoride by Gilman and Johnston.[4]

The most likely explanation for the constant-stress region of the stress-strain curve is that during this interval of strain there is rather little interaction between growing slip bands. They all extend entirely across the specimen and their number remains constant. The increase in strain corresponds to widening of the bands. Therefore the number of moving dislocations, their velocity, and the stress all remain constant.

This research has been supported by O. S. R. contract.

[4] W. G. Johnson and J. J. Gilman, J. Appl. Phys. 30, 2 (1959).

4. INTERNAL STRESSES IN CERAMICS*

Richard M. Fulrath

The existence of stresses on individual crystals in a polycrystalline ceramic were postulated by Coble.[1] Model ceramic systems[2] were used to experimentally determine the existence of these microstresses by back-reflection x-ray diffraction. The elastic strains responsible for these stresses are produced by the thermal expansion coefficient difference of the phases of a multiphase ceramic or the anistropic thermal expansion in a single-crystal-species polycrystalline ceramic.

The x-ray diffraction technique used to investigate microstresses in metals cannot be applied directly to ceramic systems when the x-ray

---

* To be published in Conference on the Mechanical Properties of Engineering Ceramics (Interscience Publishers, Inc., New York, 1961).

[1] R. L. Coble, "Effect of Microstructure on the Mechanical Properties of Ceramic Materials;" pp. 213-228 in Ceramics Fabrication Processes, W. D. Kingery, Editor (Technology Press of Massachusetts Institute of Technology and John Wiley and Sons, Inc., New York, 1958).

[2] R. M. Fulrath, Internal Stresses in Model Ceramic Systems, J. Am. Ceram. Soc. 42, 9 (1959).

penetration allows diffraction to include crystals below the surface of the specimen. With penetration of x rays into the volume of the sample the microstructure determines the applicability of x-ray diffraction to measurement of internal stresses. Platy crystals develop a biaxial stress system when dispersed in a matrix whose thermal expansion coefficient differs from that of the crystals. Specific crystallographic planes must be used to detect and measure the internal stresses. Other crystal particle shapes are not amenable to x-ray diffraction analysis under the above conditions. The above limitations were experimentally determined by using aluminum oxide crystals of various sizes and shapes hot-pressed into a matrix of glass.

Techniques were developed for examination of the microstructure of these glass-crystal compacts to aid in the internal stress analysis.

Ceramic systems in which the crystalline phase is opaque to x rays may be analyzed by the x-ray diffraction technique developed for analysis of internal stresses in metals. Microstructural considerations are secondary in such systems. Specimens of hot-pressed thorium oxide particles and glass were used to experimentally verify this analysis.

This work has been supported by the Air Force, Office of Scientific Research, but is to be transferred to LRL in October 1961.

5. MECHANICAL PROPERTIES SINGLE CRYSTALS OF MAGNESIA IN COMPRESSION*

Charles O. Hulse and Joseph A. Pask

Stress-strain curves of single crystals of magnesia were obtained in compression in the [100] direction at temperatures of -196 to 1200 °C; curves were also obtained at different rates of loading at room temperature. The crystals show considerable ductility at all temperatures. The macroscopic yield drops, apparently exponentially, from an extrapolated value of 53,000 psi at absolute zero to about 4500 psi at temperatures of 900 °C and higher.

Heat treatment has an appreciable effect on the yield stress. Crystals heated to 1000 °C and quenched showed a 50% decrease in the yield stress at room temperatures. It is theorized that some of the impurities had diffused away from the dislocations, allowing greater freedom of movement.

The resistance of magnesia single crystals to deformation increases with the number of slip systems and bands activated because of the barriers to dislocation movements which occur at slip-band intersections, i.e., work

*C. O. Hulse and Joseph A. Pask, Mechanical Properties of Magnesia Single Crystals in Compression, J. Am. Ceram. Soc. 43, 373 (1960).

hardening occurs. At about 2 to 3% strain, stress concentrations begin to be relieved by small internal cracks which are not easily propagated. This effect is extensive before final macroscopic failure of the crystal occurs.

This research problem, supported by the NASA, is included in these reports in order to give a reasonably complete representation of the type of research being considered in the Ceramics Group.

6. MAGNESIA WHISKERS*

Charles O. Hulse

In the process of studying the mechanical properties of single crystals of magnesia deformed in compression, workers observed whiskers growing on the fracture fragments, as shown in Fig. II A. 6-1. These whiskers normally extended perpendicularly from {100} crystal faces. They were typically from 1 to 3 microns in "diameter" and of varying lengths up to about 700 microns. Electron diffraction experiments verified that they were single crystals of magnesia. Figure II A. 6-2 shows an electron microscope picture of the end of a whisker with an additional smaller whisker on its end which has yet another smaller whisker on its end.

The whiskers were generally very flexible although a few were apparently brittle. They were subjected to bending stresses on a microscope stage and from the radii of curvature and the "diameters," outer fiber stresses were computed. The ultimate strengths were of the order of millions of pounds per square inch; the maximum strength observed was 3,500,000 psi. These observed strengths are of the order of the maximum theoretically possible for this material as calculated from the published elastic constants and using theoretical shear strength estimations in the literature. Figure II A. 6-3 shows a bent whisker, this particular one having a kink in it of about 20 deg before bending. Kinks were very uncommon.

The problem of explaining how the whiskers formed was complicated by the fact that they formed very rapidly at room temperatures in directions perpendicular to the applied compressive stresses. Single crystals were deformed in compression on a microscope stage and it was observed that whiskers appeared to be pulled out either lengthwise or sideways between the expanding faces of a widening crack.

Other workers have shown that magnesia slips on {110} planes in ⟨110⟩ directions. When edge dislocations on these planes must intersect similar dislocations on an orthogonal plane, flow is more difficult and

---

*A paper by this title has been accepted for publication in J. Am. Ceram. Soc.

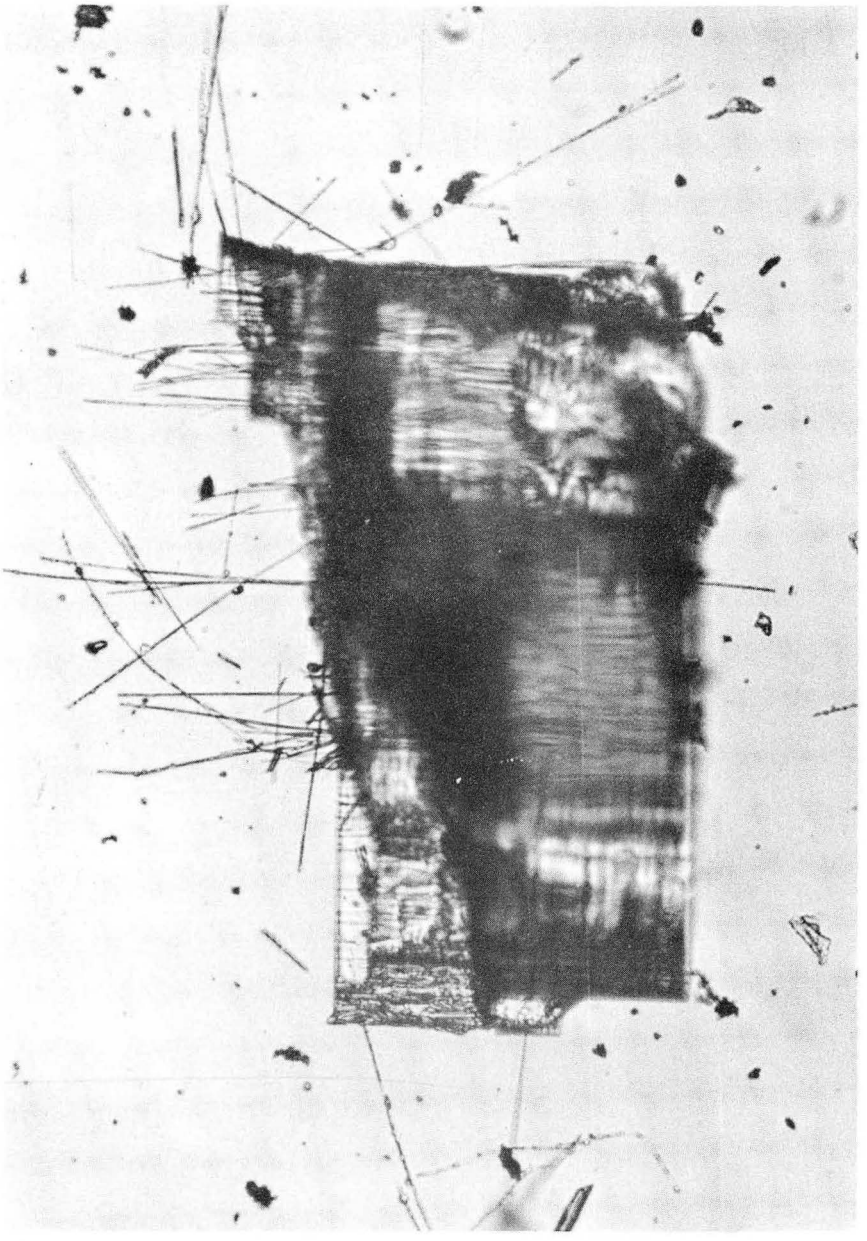

ZN-2823

Fig. IIA. 6-1. Magnesia whiskers on fragments of a crystal deformed to failure.

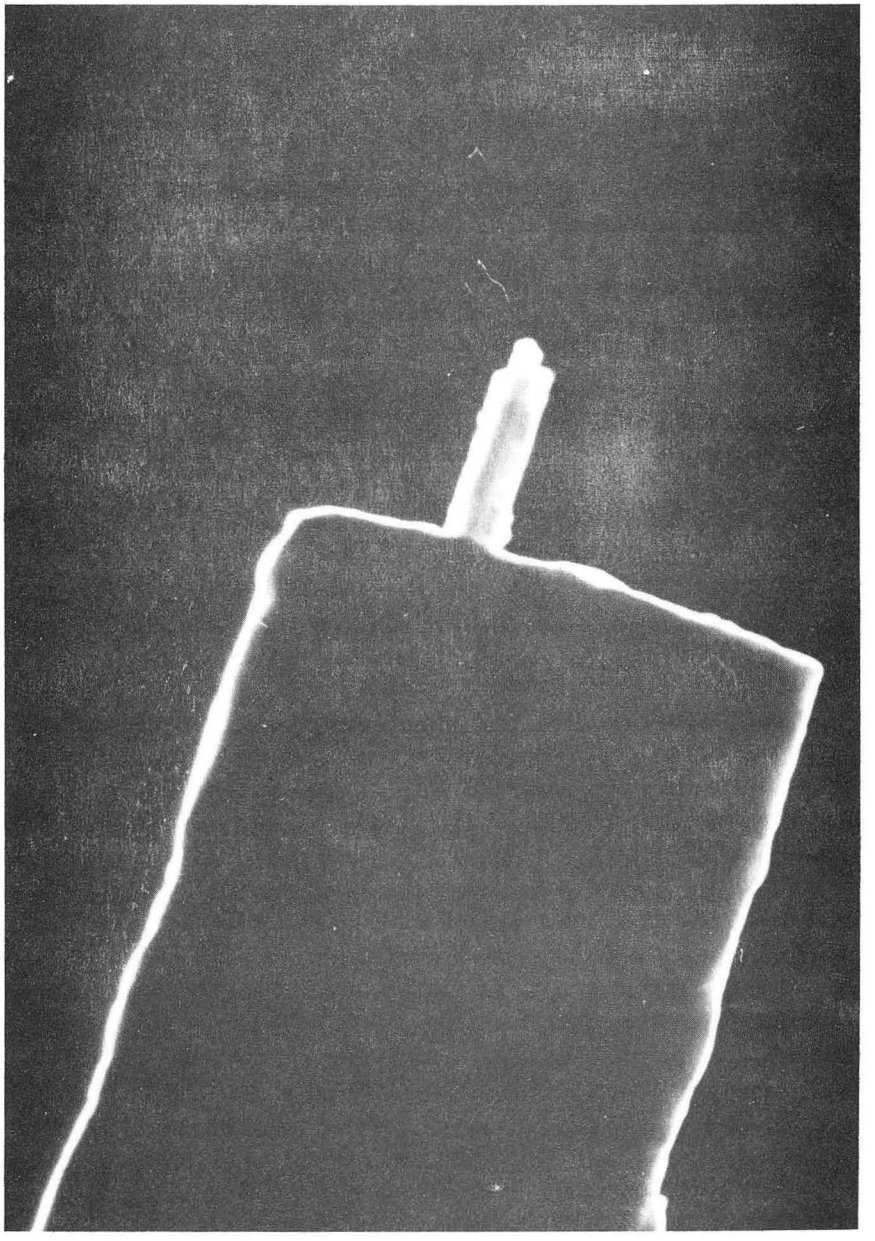

ZN-2824

Fig. IIA. 6-2. Electron microscope picture of the tip of a magnesia whisker.

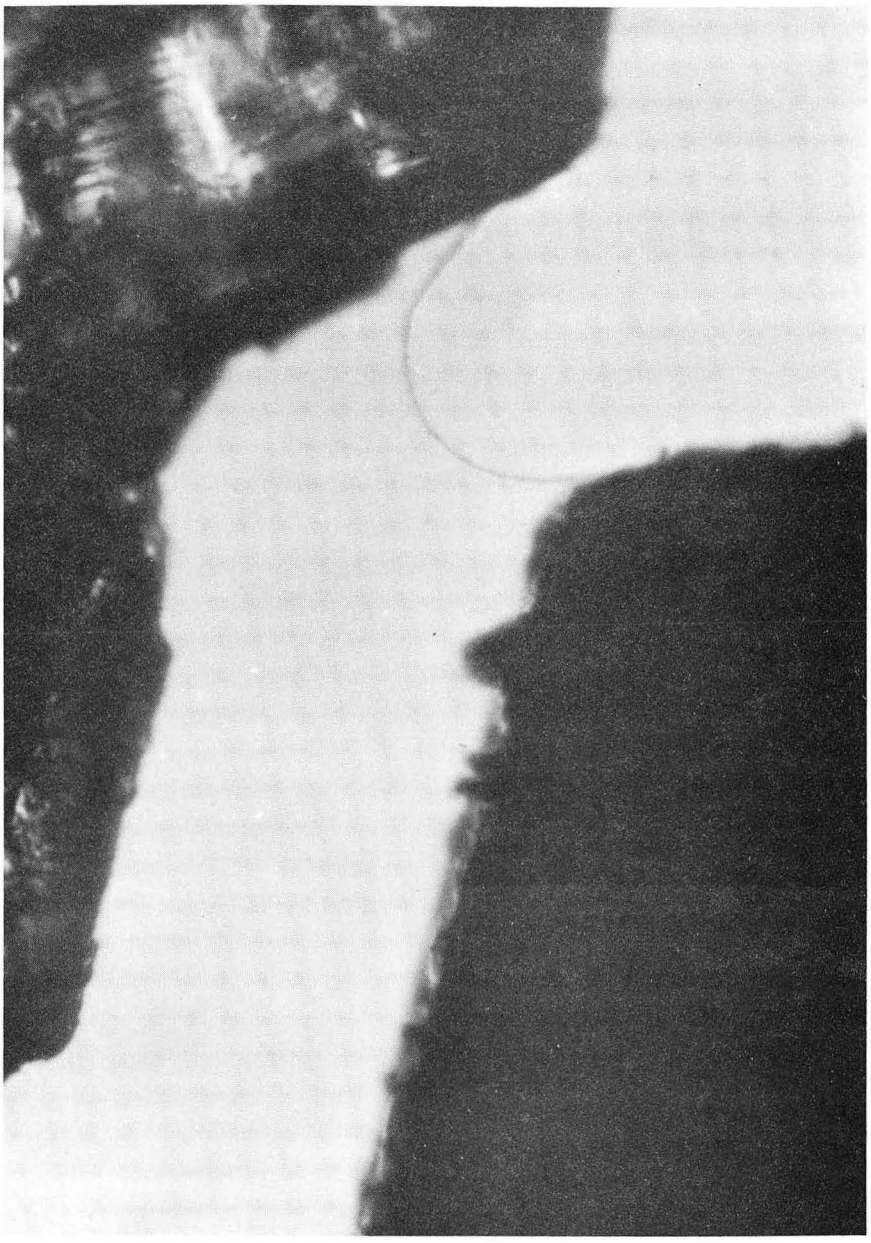

ZN-2821

Fig. IIA. 6-3. A bent magnesia whisker which had a kink of about 20 deg before bending.

dislocations "pile up" against these other bands. The internal stresses due to these pile-ups are sufficient in many cases to nucleate fractures. It was suggested that commensurate compressive forces could also be obtained in similar volumes due to the same pile-ups of edge dislocations of appropriate sign. These pile-ups lead to "hydrostatic" pressure which can then be mechanically relieved by a process of prismatic punching in the ⟨100⟩ direction. The fracture process itself then provides conditions which aid in the production of longer whiskers.

Studies were made to verify that the fracture process was not the essential step in the formation of the whiskers even though it could contribute to their formation. Whiskers were observed to be coming out of {100} fracture faces with no fracture associated with their base. Crystals were chemically polished and, during deformation under the microscope, whiskers were observed to appear on these polished faces. A paper on this subject has been accepted by the Journal of the American Ceramic Society. Some confirming experiments are being done before final publication to verify that the whiskers observed on chemically polished faces are not necessarily associated with a crack in that face.

This research problem, supported by the NASA, is included in these reports in order to give a reasonably complete representation of the type of research being considered in the Ceramics Group.

7. EFFECT OF INTERFACIAL REACTIONS ON THE DENSIFICATION OF CRYSTAL-GLASS SYSTEMS*

Joseph A. Pask

The effects of interfacial reactions on densification of crystal-glass systems were investigated for the model systems of $Na_2Si_2O_5$ glass and SiO_2(quartz) and $Na_2Si_2O_5$ glass and α-Al_2O_3. Only a eutectic exists in the former system. Carnegieite ($NaAlSiO_4$) forms in the latter system. In both cases the solid phase is partially wet by the glass at temperatures at which the glass is mobile.

Mixtures of powders of 50% by volume of each combination were prepared; this amount of glass, when molten, is sufficient to fill all the voids in any haphazard packing of the crystalline phase. Upon heating complete densification of such a system should be achieved because of the interfacial tension forces. The SiO_2 system showed such densification at about 750 °C when the glass ceased to behave as a solid and became sufficiently mobile to cause the crystalline phase to collapse. The α-Al_2O_3 system, however, did not show any appreciable densification below about 1400 °C. X-ray

*Brief form of paper to be published in Proceedings of Seventh International Ceramic Congress, England 1961.

diffraction analyses showed the appearance of carnegieite as low as 750 °C. The carnegieite apparently formed on the alumina surfaces and produced a bridging effect at the alumina-alumina contact points retaining the original alumina framework. This condition was maintained up to the eutectic temperature between carnegieite and alumina, at which point the particles became free to move to a lower potential energy state, and densification occurred.

Theoretical packing characteristics and shrinkages of mixtures of crystal and glass powders, using a 50% by volume packing coefficient, were determined. A check was obtained between calculated and experimentally obtained values.

8. RESEARCH IN PROGRESS IN MICROSTRUCTURE, 1961

Jack Washburn

1. Clustering of Quenched-In Vacancies in Copper

Precipitation of thermal vacancies after quenching produces small prismatic edge-dislocation loops in copper and other metals. The intermediate steps between a random dispersion of single vacant lattice sites and the final dispersion of dislocation loops is not clear. Electrical resistivity, length change, and small-angle x-ray scattering are being measured to determine the mechanism of formation of loops in quenched copper.

2. Plastic Properties of Body-Centered Cubic Metals

The effect of temperature of deformation, orientation, and amount of strain on the dislocation substructure in molybdenum single crystals is being studied by transmission-electron microscopy. It is hoped that these experiments will provide the basis for an improved theory of strain hardening of body-centered cubic materials.

Joseph A. Pask

1. Controlled microstructures in the LiF-MgF_2 system and their correlation with mechanical properties. Growth of single crystals of LiF and MgF_2.

2. Mechanical properties of magnesia single crystals and polycrystalline samples at temperatures up to 1750 °C in compression.

3. Determination of activation energy for and mechanisms of creep in single crystals of magnesia in compression.

4. Experiments on development of microstructures in glass-crystal systems under various interfacial energy conditions.

5. Mechanisms and kinetics of MgF_2 and water vapor reactions.

6. Interfacial energies and adherence of glass to metal.

Earl R. Parker

1. Continued investigation of cause of solution hardening; measurement of changes in grain boundary energy produced by alloying elements.

2. Measurement of Bordoni peaks for Cu and Al at low frequencies (approximately 1 cps--all previous work has been in the kilocycle range).

3. Search for Bordoni peak in high-purity iron. (Has never been found, but it should exist in high-purity material.)

4. Measurement of yield strength of high-purity iron at temperatures near absolute zero. (Suspect high values reported in literature due to impurities.)

Richard M. Fulrath

1. The Development and Observation of Ceramic Microstructures (with Robert B. Langston).

2. Diffusion by Grain Boundary Migration Under Thermal Cycling (with Perry L. Studt).

3. The Flexural Strength of Multiphase Ceramics (with Leonard N. Grossman).

4. A Dynamic Method of Measuring Reaction Heats by Differential Calorimetry.

5. The Effect of Dispersed Ductile Spheres on the Strength of Brittle Matrices (with Loren A. Jacobson).

Lawrence Himmel and M. Guinan

1. Dispersed Phases

This study is concerned with the influence which finely dispersed particles of a second phase exert on the properties of metals and alloys. By use of a combination of techniques, including thin-film transmission-electron microscopy, efforts are being made to establish the manner in which the presence of the dispersed phase modifies the deformation behavior of the matrix as well as its subsequent response to heat treatment (i.e., recovery and recrystallization). The materials under investigation consist of oxide particles of controlled size which are randomly dispersed in a silver or copper matrix; these metal-oxide systems are thermodynamically stable and are produced by the internal oxidation of dilute solid-solution alloys.

Work began in June 1960. Since then, our activities have been concentrated on the design and construction of various pieces of equipment, and on the development of techniques for specimen preparation and handling. For example, construction of equipment for studying dislocation damping phenomena in the frequency range from 10 to 100 kc and at temperatures from 4 °K to approximately 1200 °K is now nearing completion. Apparatus for precision electrical resistivity measurements (normal and magneto-resistivity) at temperatures from 4 °K to roughly 1000 °K is also under construction. For controlled heat-treating operations and other applications, a portable high-vacuum and high-purity inert gas supply system is also being assembled.

Attempts are being made to establish the conditions (temperature, time, oxygen pressure, solute concentration) under which uniform oxide dispersions of controlled particle size (in the range from 10 to 100 A) can be obtained by internal oxidation. This work is being carried out with Ag-Al_2O_3, Al-MgO, and Al-CdO alloys. Replica techniques for characterizing the structure of these alloys are also being developed. In addition, seeding techniques for growing dilute silver alloy single crystals of controlled orientation are being investigated. Preliminary attempts have also been made to prepare thin foils of internally oxidized silver alloys for examination by transmission-electron microscopy. It is expected that the efforts devoted to specimen preparation will be greatly intensified during the coming year.

As soon as the equipment now under construction is completed and calibrated and satisfactory specimens become available, the following specific experiments will be undertaken:

a. A study of the effectiveness of oxide dispersion as pinning points for dislocations in silver. This will involve dislocation damping measurements on pure silver, dilute silver alloys, and internally oxidized alloys, combined with thin-film transmission microscopy of plastically strained crystals.

b. A study of Bordoni damping in internally oxidized silver alloys.

c. A study of the effect of oxygen in solid solution on the stacking fault energy of silver. This will involve direct measurements of the radius of curvature of extended dislocation nodes in vacuum-annealed and oxygen-saturated silver, as well as a study of the dislocation structures produced in these two materials by quenching from high temperatures.

d. A study of the effectiveness of the oxide-metal interface as a sink for vacancies. This will involve quenching experiments on both high-purity silver and internally oxidized alloys. The kinetics of annealing out of the quenched-in vacancies will be followed by electrical resistivity measurements, and the corresponding structural changes will be studied by thin-film microscopy.

e. A study of the influence of oxide dispersions on the development of Kirkendall-type porosity associated with chemical interdiffision processes in copper alloys. This work is now in progress.

f. A comparison study of the mode of deformation of high-purity silver and internally oxidized silver alloys. Single crystal specimens will be deformed in tension to various points along the stress-strain curve and the resulting dislocation structures will be studied by thin-film microscopy.

This work, primarily funded by separate AEC contract, is to be transferred to LRL May 1, 1961.

II B. KINETICS OF DISLOCATION MECHANISMS

1. MECHANISMS OF DEFORMATION AND FRACTURING OF INTERMETALLIC COMPOUNDS

John E. Dorn and Jimmy D. Mote

The purpose of this investigation is to uncover the dislocation mechanisms associated with plastic deformation, ductility, and fracturing in intermetallic compounds.

The need for understanding the mechanical properties of intermetallic compounds has become increasingly important not only because of their strengthening effect when present as second phases, but also because they promise to play an important role as high-temperature materials in their own right.

There are so many intermetallic compounds as to preclude any possibility of investigating the slip mechanisms, dislocation-rate-controlling mechanisms, and mode of fracturing of each individual compound--and, indeed, such a program is not necessary.

It is well recognized that the mechanisms of slip are characterized by the geometric restriction imposed by the slip plane and the Burger's vector. From this point of view, the deformation mechanisms of intermetallic compounds can be elucidated by a study of representative examples of each type of intermetallic compound as revealed by recent advances in the theory of alloying. Although the current investigation contemplates a long-term detailed study of intermetallic compounds, the objectives of the immediate work can be illustrated by a typical example. Following are some of the various types of intermetallic compounds that crystallize in hexagonal lattices:

Type	Structure	Electron/Atoms	R_a/R_B	Example
IA	H. C. P. (ξ)	1.50	1.2	Ag-Al
IB	H. C. P. (ξ)	1.75	1.2	Ag-Zn
IIA	Laues $C_{36}(MgNi_2)$	1.8	1.23	Mg-Ni
IIB	Laues $C_{14}(MgZn_2)$	1.9	1.23	Mg-Zn
III	Hexagonal (NiAs)	2.5	1.6	Fe-Sb
IV	AlB_2	(rings of boron atoms)		Al-B

Those compounds of Types IA and IB crystallize in the close-packed hexagonal structures. These types of structures are principally dictated by the electron-to-atom ratio, the atomic radii and electronegativity playing a secondary role. Whereas Type IA is usually found at an electron to atom ratio of about 3/2, Type IB is usually found near an electron-to-atom of about 7/4. Geometrically, however, Types IA and IB actually constitute the same phase, and this deduction is emphasized by the fact that the close-packed hexagonal phase of Ag-Al extends from electron-to-atom ratios of slightly below 3/2 to somewhat above 7/4. As the electron-to-atom ratio increases the axial ratio decreases from that for close packing--i. e., 1.63--

to values of about 1.59. Consequently, the plastic behavior of most Types IA and IB close-packed hexagonal intermetallic compounds might be characterized by the example of the Ag-Al compounds.

During the current fiscal year a preliminary study of the hcp Ag–33 atomic % Al intermetallic compound was completed. This investigation was carried out in an attempt to uncover the operative strain-rate-controlling dislocation mechanisms in Ag–33 atomic % Al. Experiments were conducted on specially oriented single crystals in tension over a wide range of temperatures. Slip was observed to take place by the $\{0001\}\langle 11\bar{2}0\rangle$ and $\{\bar{1}100\}\langle 11\bar{2}0\rangle$ mechanisms; fracture took place across the $\{\bar{1}0\bar{1}2\}$ mechanism.

Basal slip exhibited a strong yield point over the range from 77 to 450 °K, the upper resolved shear stress having the exceptionally high value of 10,500 psi over this entire range of temperatures.

The critical resolved shear stress for prismatic slip decreased from 48,000 psi at 4.3 °K to 23,000 psi at 170 °K, following which it decreased slowly to 21,500 psi at 475 °K; from 475 to 575 °K, the critical resolved shear stress decreased precipitously to 2000 psi; and from 575 to 750 °K it decreased less rapidly to a low value of about 500 psi.

Prismatic slip over the temperature range 4.3 to 170 °K was shown to be controlled by the thermally activated mechanism of nucleation of kinks in dislocations lying in Peierls potential troughs. Over the temperature range 170 to 475 °K, as well as over the entire region of basal slip, where yield point phenomena were observed and over which the critical resolved shear stress for slip was insensitive to temperature, the critical resolved shear stress was shown to be determined by short-range ordering (or clustering). The precipitous decrease in the critical resolved shear stress over the temperature range 475 to 575 °K was tentatively ascribed to a decrease in the degree of short-range ordering (or clustering) and also the effect of fluctuations in the degree of order. It is at present uncertain whether or not these effects are also responsible for the data over the temperature range 575 to 700 °K.

The results of this preliminary investigation revealed several important areas which require further experimental and theoretical scrutiny. These are enumerated as follows:

1. X-ray determination of the degree of short-range order (or clustering), to shed more light on the ordering energy, estimated in the preliminary investigation, from purely mechanical tests, to be -760 cal/mole. The degree of short-range order is determined from the background intensity of diffraction patterns obtained by using strictly monochromatic x rays. The short-range-order coefficients are evaluated from the intensity distribution by means of a harmonic analysis, after corrections for Compton and thermal scattering have been made.

Determinations of the degree of short-range ordering in crystals of cubic symmetry have been made by using this technique; however, it has not been applied to crystals of hexagonal symmetry. Although the mathematical analysis for the case of hexagonal symmetry is more formidable,

the data should reveal more interesting details of the short-range ordering phenomena because of the asymmetry of the structure.

A study of stacking faults will also be made, since they can be evaluated from the shifts of the diffraction peaks.

The equipment necessary for obtaining the data has been designed and is to be placed in operation early in 1961.

2. Theoretical formulation of the effect of fluctuations in the degree of order and composition on the plastic behavior at temperatures just above one-half of the melting temperature (475 to 575 ^{o}K). In order to understand the kinetics of processes controlled by short-range ordering it is necessary to understand not only the kinetics of short-range ordering, but also the kinetics of fluctuations in short-range order. Since the currently available models for short-range ordering assume "smeared" equilibrium conditions, it is necessary to formulate a new theory which will reveal some of the details of the fluctuations in short-range order and consequently its effect on the plastic behavior of materials.

3. Experimental studies of the effect of stress and temperature on the creep rate in the temperature range where fluctuations in order and composition are known (in terms of the preliminary investigation) to affect the plastic behavior.

REPORTS AND THESES

1. J. Mote, K. Tanaka, and J. E. Dorn, Effect of Temperature on Yielding in Single Crystals of the Hexagonal Ag-Al Intermetallic Phase, First Technical Report, I E R, June 1, 1960.

2. W. L. Barmore, Activation Energies for Prismatic Slip in Single Ag-Al-Zn Crystals at Intermediate Temperatures (M. S. thesis) University of California, Berkeley, California.

This investigation was initiated under AEC Contract AT(11-1)-34, Project 46. The transfer to LRL was made December 1, 1960.

2. THE EFFECT OF STRAIN RATE ON DIFFUSION

Jimmy D. Mote, Ahmed R. Wazzan, and John E. Dorn

The major objective of the current investigation is to determine the effect of strain rate on the concentration of vacancies in metals at elevated temperatures. In particular, the effect of strain rate on the self-diffusivity of Ni is being evaluated. These results are being correlated with current concepts of vacancy creation during plastic deformation. Future investigations will be initiated to explore the effect of substructure on diffusion, and the effect of edge and screw dislocations on vacancy generation will be investigated.

Experiments are being conducted to determine the effect of a constant tensile strain rate on the diffusivity of Ni^{63} in Ni. Single crystals of high-purity Ni are produced by a modified Bridgman technique. The crystals are carefully machined to the approximate dimensions 0.1 in. thick, 1/2 in. wide, 4 in. long. The tensile specimens are electroplated with radioactive Ni^{63}. The surface activity of the specimen is determined by means of a flow counter, the specimen is given a static diffusion anneal, and the surface activity is again determined. This procedure is repeated until the static diffusivity is determined. The same procedure is followed with the specimen undergoing a dynamic diffusion anneal until the dynamic diffusivity is determined. These data have been obtained at a series of fixed strain rates for two different temperatures.

The results indicate that the coefficient of self-diffusion is given by the relationship

$$D = Ae^{-Q/RT}, \qquad (1)$$

where

D = coefficient of self-diffusion,
A = constant,
Q = activation energy for self-diffusion,
T = absolute temperature,
R = gas constant.

The values obtained for D show a variation from crystal to crystal of as much as 40%. Visual observation of the crystals indicates that there may be some correlation between the diffusivity and the substructure. This idea will be discussed under proposed extension of the work.

These experiments were carried out in a range where the expression for the diffusivity ratio, $D_{\dot{\epsilon}}/D$, may be valid:*

$$(D_{\dot{\epsilon}}/D - 1) = A(\dot{\epsilon}, T)\exp(-K_2 t) + \frac{K_1[1 - \exp(-K_2 t)]}{K_2 n_v}\dot{\epsilon} \qquad (2)$$

*Derivation of this equation will be given in a report to be published.

Where K_1 = constant,

K_2 = constant,

$D_{\dot{\epsilon}}$ = diffusivity in crystal being strained,

D = diffusivity in unstrained crystal,

$\dot{\epsilon}$ = strain rate,

n_v = number of vacancies in the crystal.

The data are yet insufficient to evaluate K_1 and the form of the function $A = A(\dot{\epsilon}, T)$, but the trend suggests that (a) A decreases with temperature at a constant strain rate, and (b) A increases with increasing strain rate at constant temperature.

REPORTS AND THESES

1. A. Messner, R. Benson, and J. E. Dorn, "Self-Diffusion in Nickel Single Crystals," Transactions, ASM (to be published.

2. A. Messner, Self-Diffusion in Nickel Single Crystals, M. S. Thesis, University of California, Berkeley, California.

3. RESEARCH IN PROGRESS IN DISLOCATION MECHANISMS, 1961

John E. Dorn

1. Additional experiments are currently being conducted to elucidate the effect of strain rate on the diffusivity of Ni^{63} in Ni single crystals. With these additional data an attempt will be made to evaluate the constant K_1 in Eq. (2) and to determine the form of the function $A = A(\dot{\epsilon}, T)$. Theoretical considerations of the mode of generation and annihilation of vacancies in nickel single crystals will be undertaken.

2. The effect of temperature on the creep rate, over the temperature range 440 to 710 °K, for a mean creep rate of 6×10^{-2} per hour, has recently been determined. This work is continuing and the results for a different creep rate will be completed soon. In addition, the effect of incremental stress changes on the creep rate will be determined over this same range of temperatures. The results of these experiments will be analyzed in terms of the maturing theoretical analysis on the effect of fluctuations in short-range order.

3. Experimental studies are being made of the activation energy for creep in the temperature range above 575 °K, to provide preliminary data for uncovering the operative dislocation mechanisms. These studies will provide data indicating whether (a) the rate-controlling process in this range is an extension of that process operative in the region 475 to 575 °K or (b) some new process is responsible for the plastic behavior.

4. Experimental studies are in progress on the plastic behavior of polycrystalline Ag–33 atomic % Al over a wide range of temperatures, to uncover the effects of grain boundaries on the mechanical behavior. The experimental phases of this work are complete and a detailed analysis of the results is now being conducted. It is expected that the results will be reported early in 1961.

5. Hot hardness tests on Ag-Al alloys of varying composition are being conducted over a wide range of temperatures. These data will reveal the most interesting compositions for further investigation.

II C. ELECTRON MICROSCOPY

1. A STUDY OF FATIGUE DEFORMATION BY REFLECTION ELECTRON MICROSCOPY*

Gareth Thomas, N. P. Sandler, and I. Cornet

Electron microscopy techniques have been used since 1952 for the study of metal surfaces deformed in fatigue.[1] Initially replica techniques were used to view extrusions.[1-7] Out of this work intense interest arose in the nature of holes, intrusions, and microcracks formed during cyclic stressing, which led to the development of taper section techniques for their examination.[8-10] More recently taper sections have been utilized for direct transmission electron microscopy in the study of fatigue surfaces.[11, 12] Meanwhile, there appears to have been a neglect of a simpler technique for viewing a fatigued metal surface; namely, reflection electron microscopy. However, this may be due to difficulties in adapting the electron microscope for reflection. In the investigation presented here a Hitachi H. U. 10 electron microscope has been used to study surface effects resulting from fatigue deformation. This microscope is provided with a tilting head and goniometric specimen holder to facilitate its operation in reflection. Although the resolution in reflection is only of the order of 200 A, because of the shadows cast by any material projecting out of the metal surface, considerable enhancement of contrast is obtained.

---

*Published as Technical Note in J. Inst. Metals 89, 253 (1960-1961).

[1] W. J. Craig, Proc. Am. Soc. Testing Materials 52, 877 (1952).

[2] P. J. E. Forsyth, J. Inst. Metals 82, 449 (1953-54).

[3] M. S. Hunter and W. G. Fricke, Jr., Proc. Am. Soc. Testing Materials 54, 717 (1954).

[4] P. J. E. Forsyth and C. A. Stubbington, J. Inst. Metals 83, 395 (1954-55).

[5] P. J. E. Forsyth and C. A. Stubbington, J. Inst. Metals 83, 173 (1955).

[6] M. Hempel, International Conference on Fatigue of Metals (Inst. Mech. Engrs., London (1956) 543.)

[7] A. H. Cottrell and D. Hull, Proc. Roy. Soc. (London) (A) 242, 211 (1957).

[8] W. A. Wood, and R. L. Segall, Bull. Inst. Metals 3, 160 (1957).

[9] W. A. Wood, Phil. Mag. 3, 692 (1958).

[10] J. C. Grosskreutz and C. M. Gosselin, J. Appl. Phys. 31, 1127 (1960).

[11] R. L. Segall and P. Partridge, Phil. Mag. 4, 912 (1959).

[12] P. B. Hirsch, P. G. Partridge, and R. L. Segall, Phil. Mag. 4, 721 (1959).

In the work reported here, coarse-grained polycrystalline specimens of super-high-purity aluminum (99.996%) were electropolished and fatigued to failure at a stress of 8,000 psi in plane bending. The surfaces of the fatigued samples were observed under oblique light, approx 8 deg, in the light microscope. Figure II C. 1-1 illustrates a typical photomicrograph taken from the specimens. Sections were then carefully cut from the fatigued specimens and mounted in the electron microscope set at a tilted illumination of 7 deg with the specimen inclined at 10 to 15 deg to the electron beam. The microscope was set up for use with the double condenser lens at a beam diameter of 20 μ; Fig. II C. 1-2 shows an electron micrograph taken from the same specimen as that shown in Fig. II C. 1-1. On comparison of these figures it is clear that better contrast is obtained with the reflection electron microscope, and because of the increased depth of focus obtained by using electron illumination it is possible to derive more information regarding the shape and distribution of the extrusions.

During examination in the electron microscope the surface was observed to fluoresce, indicating that it was charging up in the electron beam, as might be expected if aluminum oxide were present. It is concluded, therefore, that the whole surface of the specimen is covered with an oxide layer. The steps observable in Fig. II C. 1-2 are parallel to the top edge of the specimen, and conform to the slip steps and deformation of the underlying metal. Large extrusions extending out of the slip bands are visible over much of the metal surface.

On the tips of these extrusions fluorescence indicates the presence of oxide films either retained at the advancing edge or formed after extrusion. The transparency of the edges shows that their thickness is of the order of 1000 A, and even the base of the extrusion is so thin that it is barely opaque to the beam. From this, one deduces that the shape of the extrusion is lenticular. One would suppose that the restriction at the edges due to the tenacious oxide film imposes lateral compression in the extrusion, causing it to bulge into a lens shape. Thus much more information about the nature of one extrusion is made available using the reflection technique, since extrusions are just barely detectable in the light microscope (Fig. II C. 1-1). A view at a shallower angle is shown in Fig. II C. 1-3.

Similar observations have been made on copper, and there is evidence that the extrusions split apart in this metal. Fluorescence in copper specimens make imaging a serious problem; in fact, it is essential to use a charge neutralizer in the microscope specimen chamber, otherwise, focusing is impossible.

This work was partially supported by the Office of Naval Research.

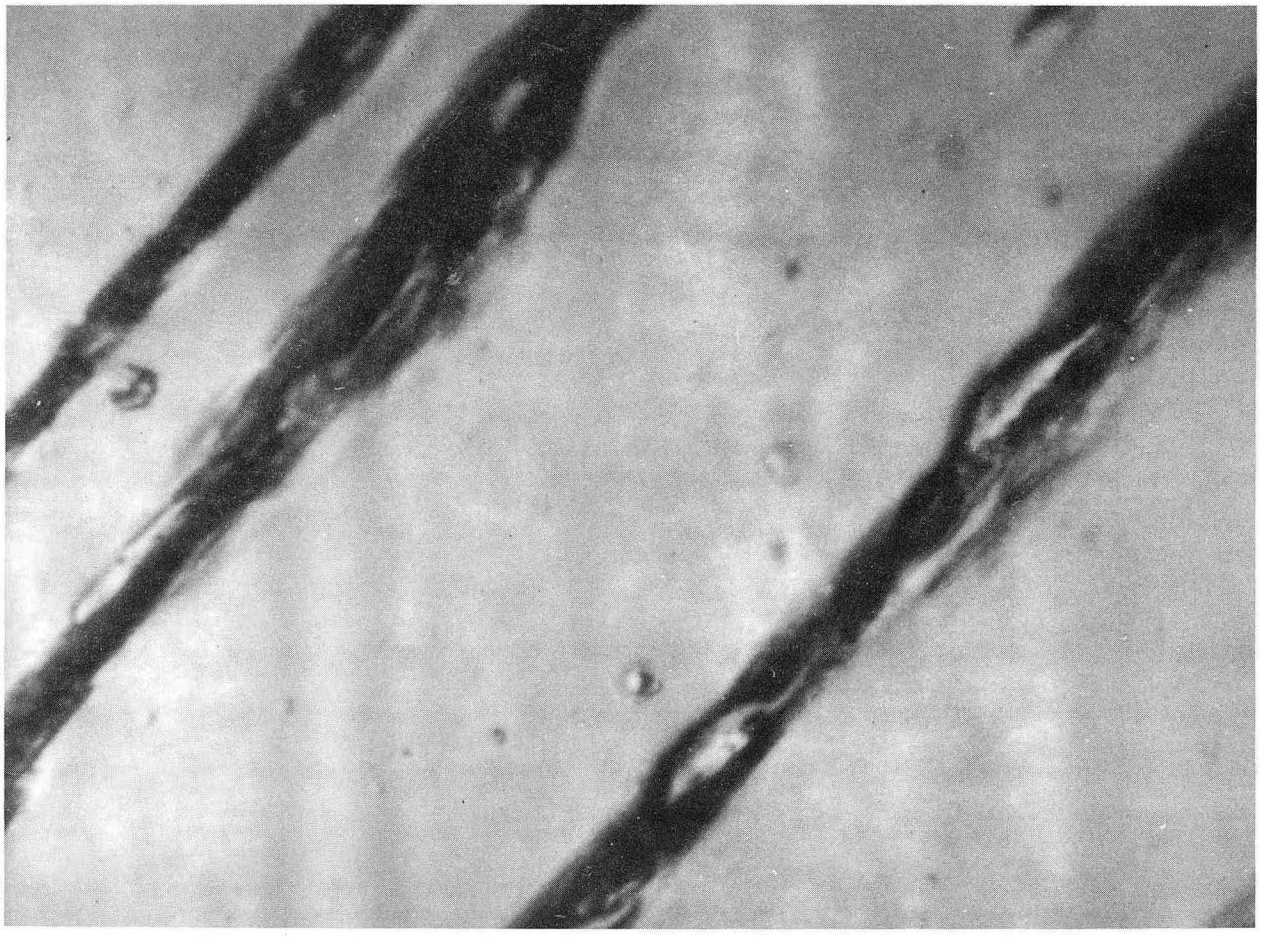

ZN-2829

Fig. IIC. 1-1. Optical micrograph of fatigued aluminum, showing extrusions. 1500 ×.

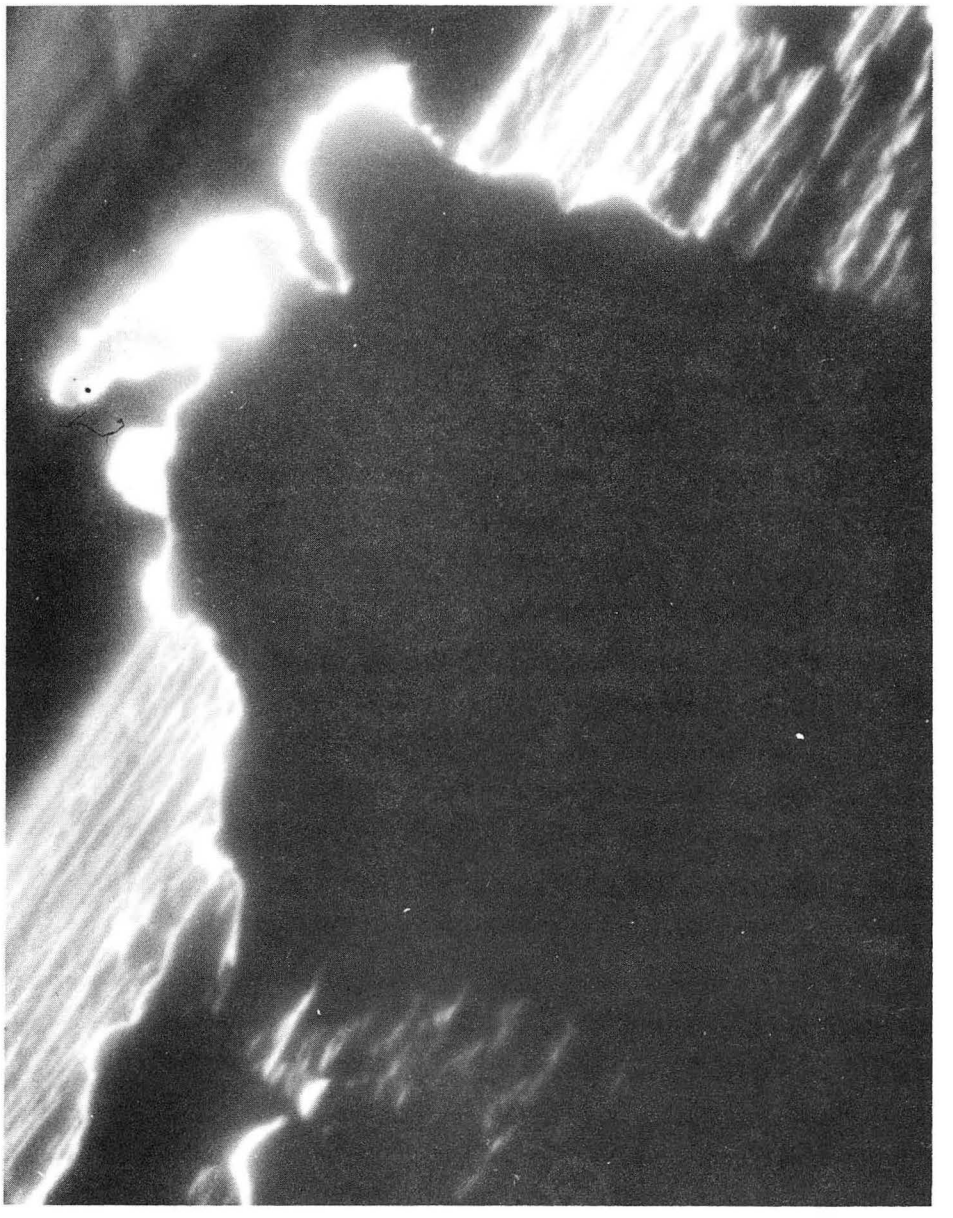

ZN-2826

Fig. IIC. 1-2. Electron micrograph (reflection) of same specimen shown in Fig. IIC. 1-1, showing extrusions with fluorescence at their tips. Linear magnification 6000 ×. Image foreshortened in viewing direction in reflection.

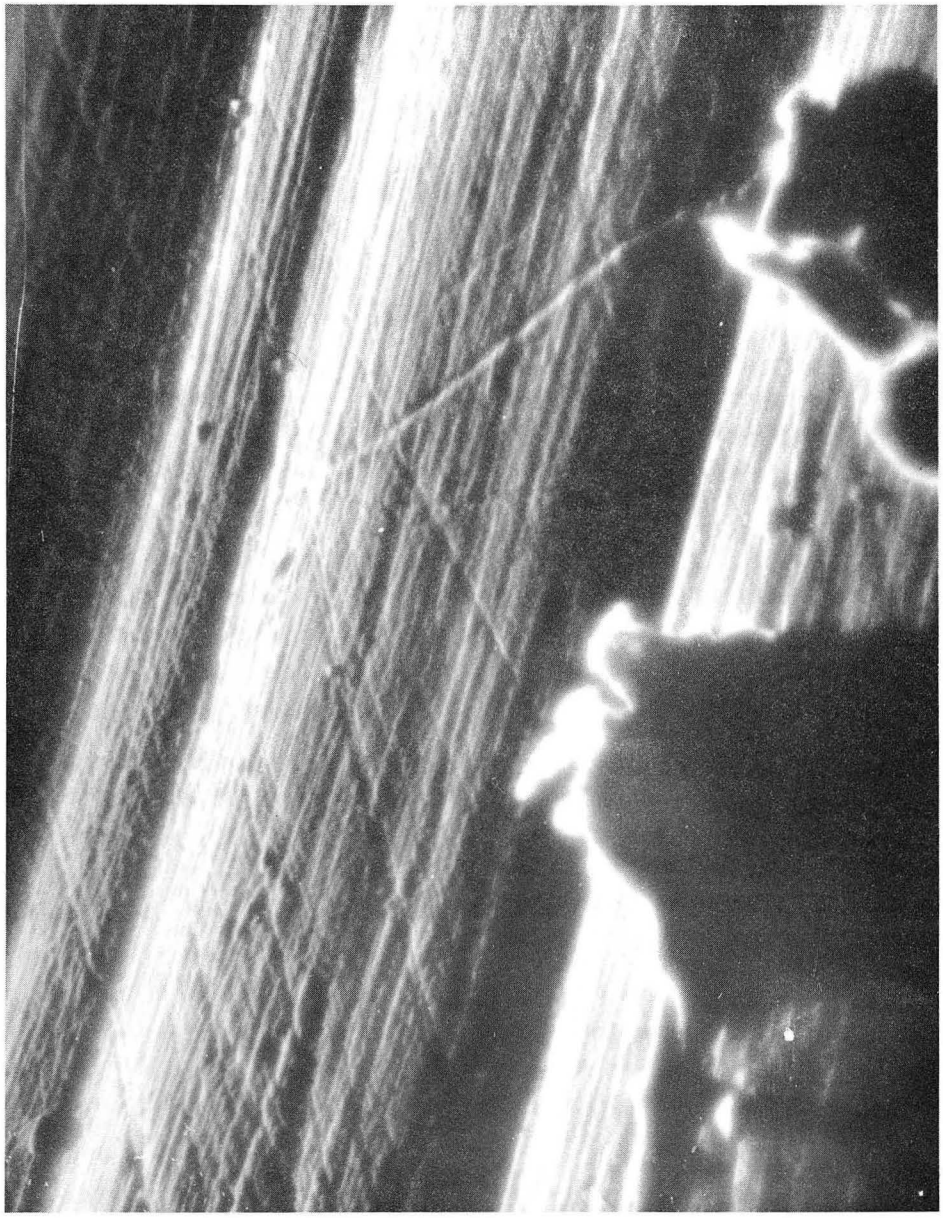

ZN-2825

Fig. IIC. 1-3. Area similar to Fig. IIC. 1-2. Taken at a shallower angle. Linear magnification 3000 ×.

2. A SPECIMEN-TILTING DEVICE FOR USE IN THE HITACHI H. U. 10 ELECTRON MICROSCOPE*

M. Conrad Huffstutler, Jr. and Gareth Thomas

With the development in recent years of electron microscopes capable of resolving details of 10 A or less and having facilities incorporated to permit the use of a fine-focus electron beam (approx 10 μ diameter), direct transmission through metal foils about 1000 A thick has become a widely used research technique. In transmission the illuminating beam is diffracted when Bragg's law is realized, and a focused electron diffraction pattern is formed in the back focal plane of the objective lens. However, the spherical aberration of the objective lens is too large to allow low-order Bragg reflections to be recombined in the final image except in the case of crystalline materials of lattice spacings greater than about 10 A.[1] In the case of metals, therefore, it is not yet possible to obtain direct images of their lattices, and the contrast in the image is produced by an entirely different mechanism which does not aim at revealing the atomic structure. By insertion of objective apertures of suitable sizes, the Bragg reflections are cut out so that only the straight-through and small-angle scattered electrons pass through. In this way the bright-field image is formed. Contrast in the image thus results from differences in the intensities of electrons scattered into Bragg reflections and is called "Bragg contrast." Reversal of contrast (dark field) is obtained by tilting the illumination system or moving the objective aperture so as to include a Bragg reflection. Because of the variation of depth periodicity in the intensity oscillations of the direct and diffracted waves, discontinuities of structure on an inclined plane (e.g., wedge-shaped crystals, grain boundaries, stacking faults) give rise to interference fringes. Defects that result in lattice displacements (e.g., dislocations) produce a phase variation in the diffracted beam and also give rise to Bragg contrast.[2] Unfortunately, the geometric relationships of the diffracting areas relative to the through beam are frequently unfavorable for optimum contrast, and the specimen must be tilted to improve the situation. A further advantage of tilting is that it permits one to determine Burger's vectors of dislocations.[2] In many cases first observation of a specimen yields little information, but tilting often brings the features of interest into contrast. Tilting also makes it possible to illuminate grains that were originally dark, and vice versa, since the orientation of the grain determines whether or not the diffracted beam passes through the objective aperture.

Because proprietary tilting devices are not available for many electron microscopes, a tilting unit was designed and incorporated into a Hitachi H. U. 10 electron microscope.

---

*Details of this unit were published in the Rev. Sci. Instr. January, 1961.

[1] J. W. Menter, Proc. Roy. Soc. (London)(A) 236, 119 (1956).

[2] P. B. Hirsch, A. Howie, and M. J. Whelan, Phil. Trans. Roy. Soc. (a) 252, 499 (1960).

A convincing demonstration of the usefulness of the tilting device is shown in the fugures. This was taken from a thin foil of magnesium prepared by electropolishing. In Fig. II C. 2-1 the grain A appears dark, whereas in Fig. II C. 2-2 after a 2-deg tilt it appears light. Note also how the contrast has changed in other areas of the foil, particularly the extinction contours B and the fringes at the wedge boundary C, and that the dislocation visible at D in Fig. II C. 2-2 is invisible after tilting.

3. OBSERVATIONS OF DISLOCATIONS IN MOLYBDENUM AND MAGNESIUM*

Gareth Thomas, Ray Benson, and John Nadeau

A. Molybdenum

Specimens in the form of rolled sheet 99.9% pure and 100 μ thick were annealed for 12 hours at 1500 °C in a silicon carbide tube furnace at a pressure of 10^{-4} mm Hg. These were then deformed in tension 1 to 5% at room temperature and foils were prepared by electropolishing in 98% H_2SO_4.

Figure II C. 3-1 shows the microstructure after annealing; very few dislocation lines are visible (the black lines are thickness-extinction contours). Figures II C. 3-2 and II C. 3-3 show typical dislocation arrangements after a strain of a few per cent. These form networks consisting mainly of screw-dislocation subboundaries. Such networks can form as a result of two possible interactions on (110) planes, namely

$$\frac{1}{2}\, a\,[111] + \frac{1}{2}\, a\,[\bar{1}1\bar{1}] = a\,[010] \qquad (1)$$

or

$$\frac{1}{2}\, a\,[11\bar{1}] + \frac{1}{2}\, a\,[1\bar{1}1] = a\,[101]. \qquad (2)$$

Case 1 would be preferred because the a[010] dislocation has a lower energy than the a[101] dislocation.

At higher strains, the density of dislocations in the networks increased, and there was a tendency for smaller networks to form inside the subboundaries. This behavior is quite like that of face-centered cubic metals of intermediate stacking-fault energy.

The dislocations were never observed to move while the specimen was being examined in the electron microscope, which suggests that they may be pinned (e. g., by impurity interstitial atoms). More work is being done to check this. The dislocations were never extended, and stacking faults were never observed.

---

*Work reported in Proceedings of the Symposium on Electron Microscopy, Holland, 1960 (in press).

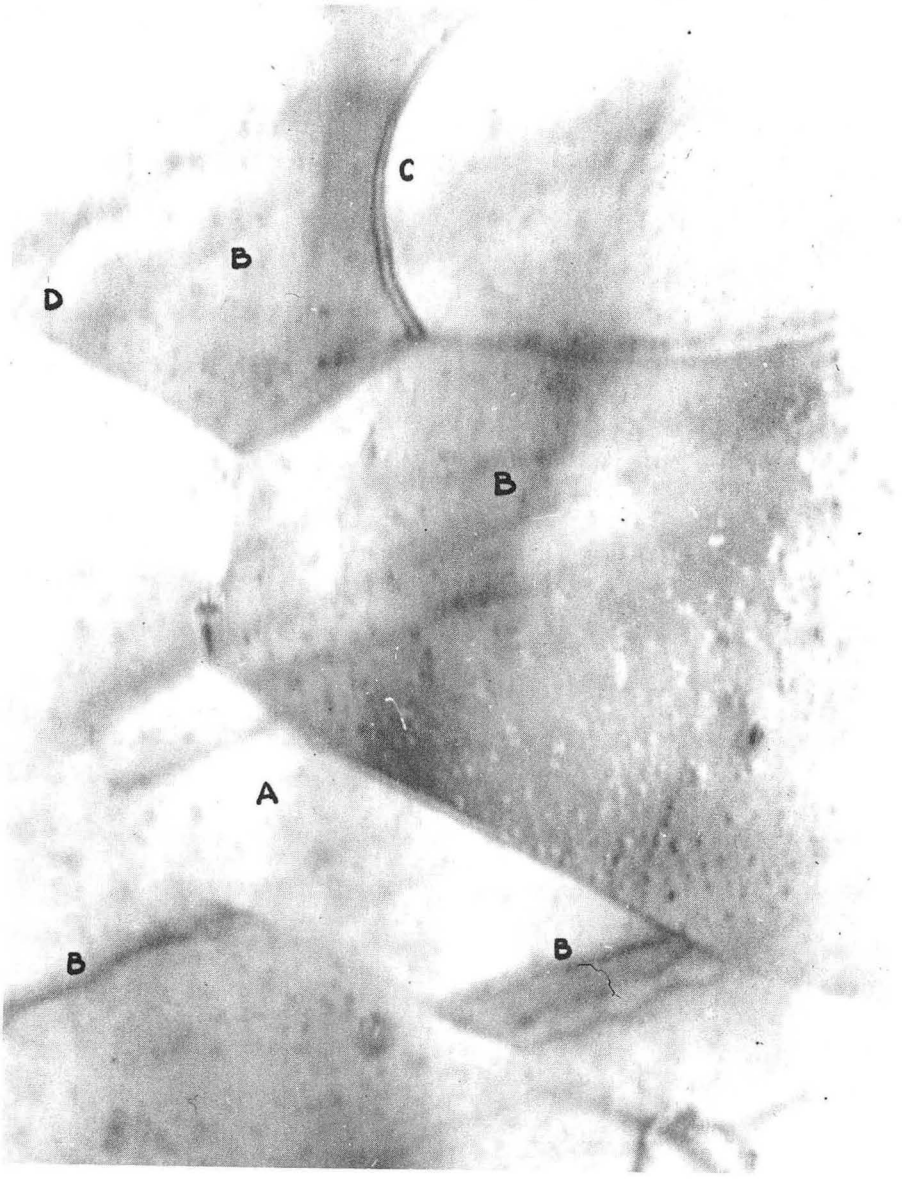

ZN-2828

Fig. IIC. 2-1. Thin foil of magnesium.

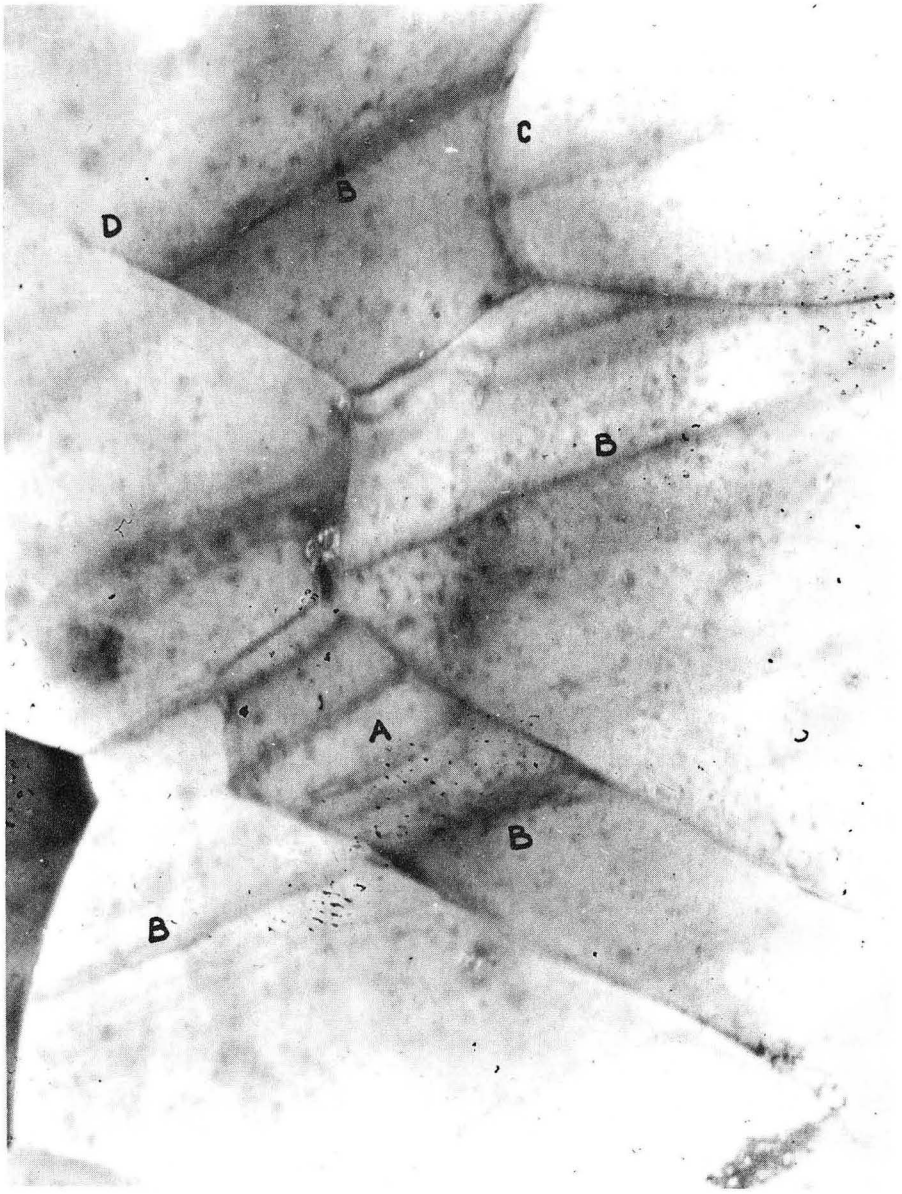

ZN-2827

Fig. IIC. 2-2. Same as IIC. 2-1, but tilted 2 deg.

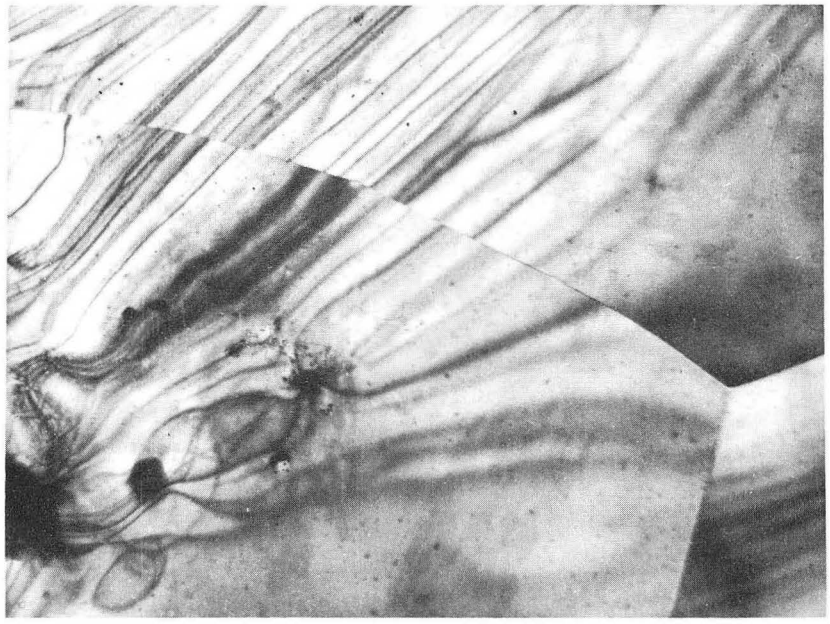

ZN-2807

Fig. IIC. 3-1. Mo after annealing at 1500 °C; × 10,000.
Black lines are extinction contours.

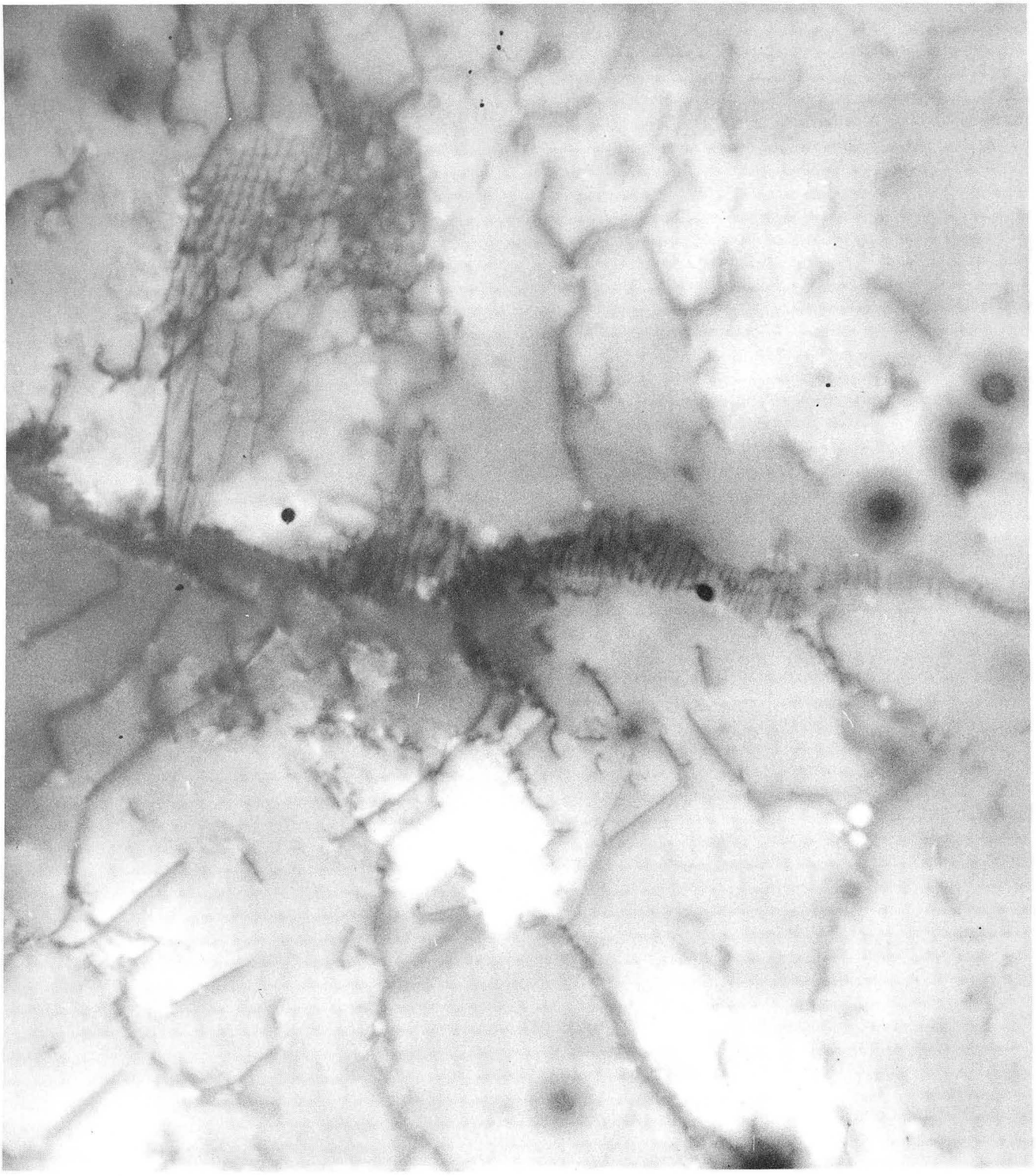

ZN-2814

Fig. IIC. 3-2. Mo deformed 2%; × 40,000.

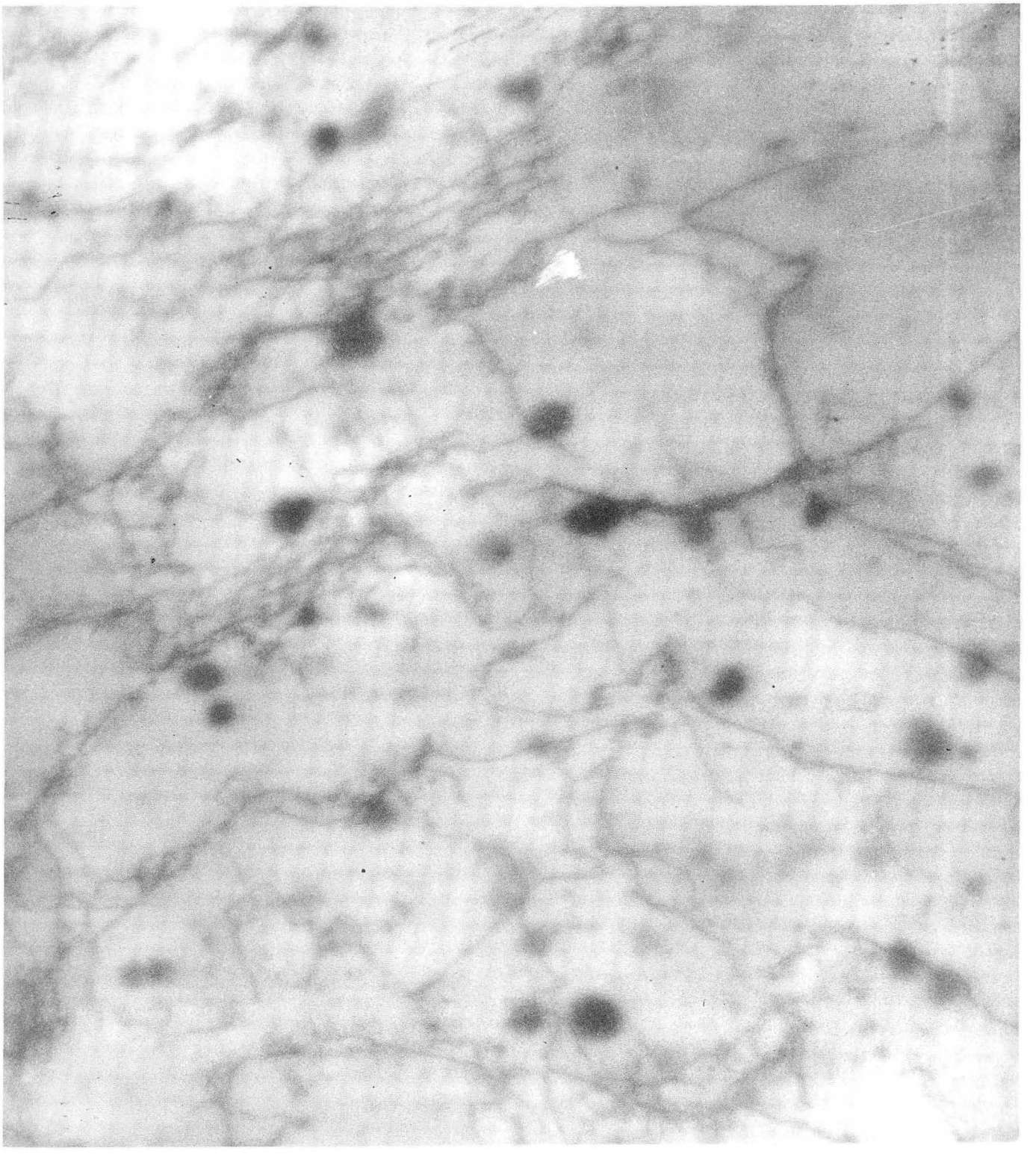

ZN-2813

Fig. IIC. 3-3. Mo deformed 3%; × 40,000.

Some specimens were annealed at 300 °C for a few hours after a 3% strain. The structure changes to that shown in Fig. II C. 3-4, viz., a system of closed dislocation loops. This indicates that a considerable amount of climb has taken place during annealing, corresponding to the first stages of recovery.

Work hardening in this material is attributed to the interactions between glide dislocations and the forest in the networks.

B. Magnesium

Specimens 99.98% pure were annealed in dry helium at 620 °C and furnace-cooled. Some specimens were quenched into ice at -15 °C. The annealed specimens were deformed at room temperature by rolling and by tensile straining. Foils were prepared by electropolishing in ethanol–perchloric acid electrolyte.

The dislocations were observed to be very mobile and to glide easily in the basal planes to form networks. However, these networks broke up during examination, indicating that recovery takes place near room temperature.

In certain cases pyramidal slip was observed, i.e., glide on $\{10\bar{1}1\}/\langle 11\bar{2}0\rangle$ slip systems. An example is shown in Fig. II C. 3-5.

No dislocation loops were observed in quenched specimens even after many different experiments. This probably means that the mobility of vacancies is so high in magnesium that the quenching rate is too slow to trap vacancies in supersaturation.

As was found in molybdenum foils, the dislocations in magnesium were not extended, and stacking faults were never observed. From this it is concluded that magnesium probably has a high stacking-fault energy.

4. CRYSTAL STRUCTURE OF β' $Cu_{0.75}Al_{0.25}$ *

Gareth Thomas and M. Conrad Huffstutler, Jr.

X-ray diffraction studies, transmission electron microscopy, and selected area diffraction have shown that the structure of copper aluminum martensite is distorted hexagonal with a = 2.57 A, c = 4.21 A. The martensite is twinned on 20 A scale and the presence of twins accounts for the errors in determinations of the lattice constants by other workers.

*Abstract of paper submitted to Acta Crystallographica.

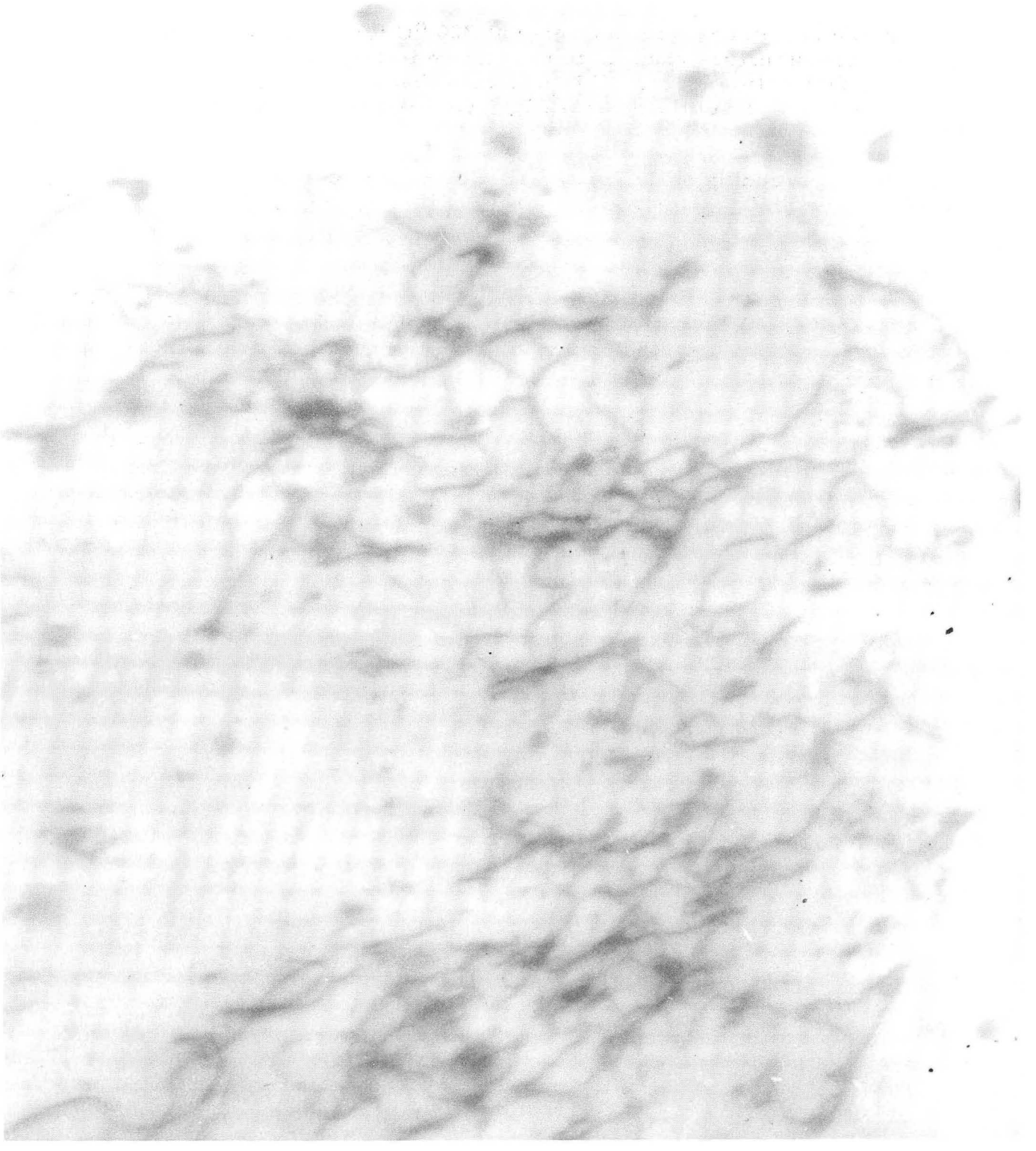

ZN-2812

Fig. IIC. 3-4. Mo deformed 3%, annealed 1 hr at 300 °C; × 40,000.

ZN-2809

Fig. IIC. 3-5. Slip in Mg on pyramidal planes; × 30,000.

5. DIRECT OBSERVATION OF DISLOCATIONS IN MAGNESIUM OXIDE

Jack Washburn

Dislocations have been observed in thin metal foils by electron transmission microscopy for a number of years. It had been the common belief that this technique was applicable only to metals. However, we have recently succeeded in observing dislocations in magnesium oxide, a ceramic material of high melting point. Large crystals, supplied by the Norton Company, were prepared by cleavage followed by chemical polishing, to produce a thin specimen. From the measured separations of the traces of (110) slip planes on the two surfaces of the specimen the thickness was found to be 3000 to 5000 A. As a result of this work it now appears likely that direct observation of defects in a large class of refractory ceramic materials will be possible. The excellent sharpness and contrast with which dislocation arrangements can be studied in magnesium oxide crystals is illustrated by Fig. II C. 5-1.

The technique has been applied to the study of the mechanism of slip-band growth and strain hardening. A full report of this work has been published recently.[1, 2] The most important observations may be summarized as follows.

a. The damage in slip bands which gives rise to strain hardening within the band consists primarily of elongated plus-minus edge dislocation pairs. A mechanism has been proposed for the formation of these elongated edge dislocation loops based on the trapping of long jogs on moving screw dislocations.

b. Direct evidence has been obtained for cross-slip in magnesium oxide. The path taken by some dislocations moving under the influence of thermal stresses, while under observation, showed that motion was not confined to a single {101} slip plane. Double cross-slip took place on a very fine scale, resulting in what appeared to be noncrystallographic glide paths.

c. Dislocation interactions at slip-band intersections have been studied. No clear evidence has been obtained for the occurrence of the dislocation reaction

$$\frac{a}{2}[110] + \frac{a}{2}[1\bar{1}0] \rightarrow a[100].$$

However, the dislocation reaction

$$\frac{a}{2}[110] + \frac{a}{2}[0\bar{1}1] \rightarrow \frac{a}{2}[101]$$

does take place, and leads to the formation of dense dislocation tangles at intersections between nonorthogonal slip bands.

d. An elongated plus-minus edge-dislocation pair is unstable at high temperature. Above about 500 °C edge pairs tend to break up into a string of circular edge dislocation loops. The damage in a crystal deformed at

[1] Phil. Mag., V. 5, p. 192-3 (1960).

[2] Phil. Mag., V. 5, p. 991-9 (1960).

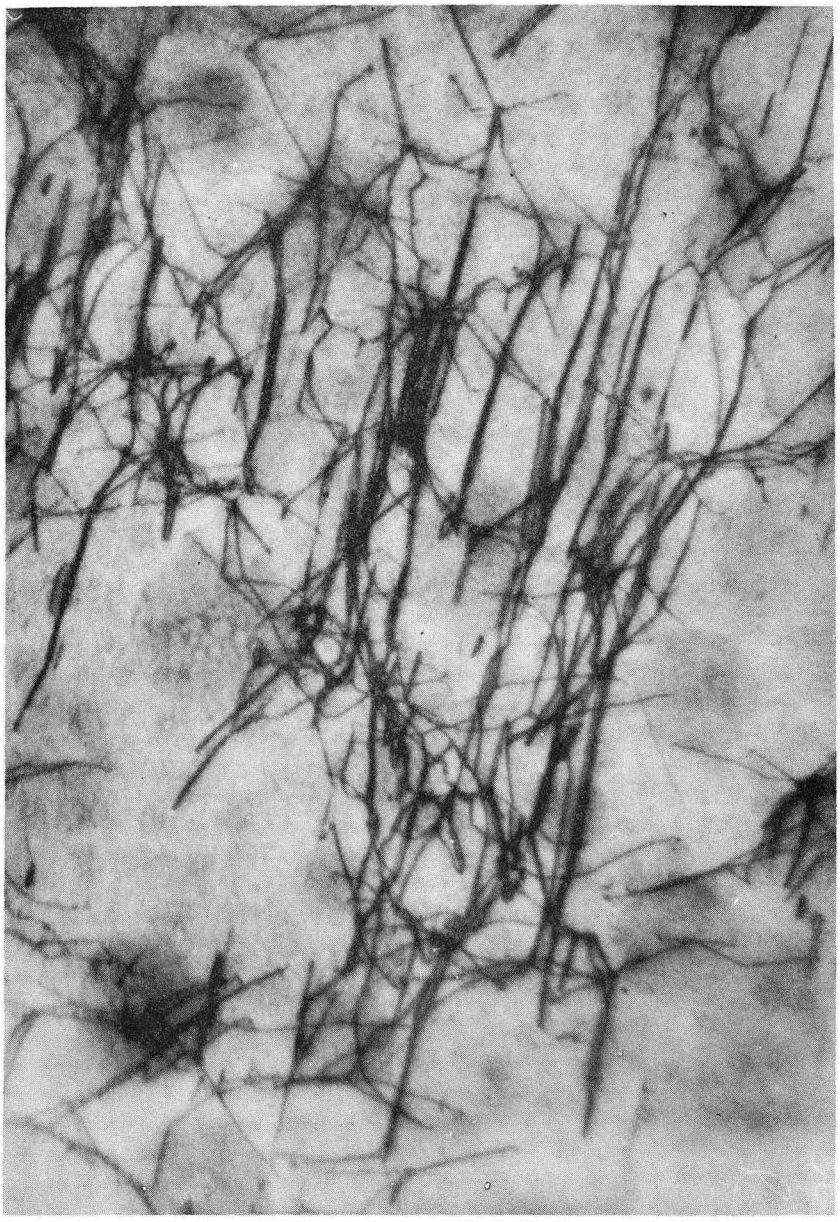

ZN-2822

Fig. IIC. 5-1. Direct observation of dislocations in magnesium oxide.

1000 °C is almost entirely of this type. A few very large elongated loops are still observed. The difference between the dislocation substructures produced by low- and high-temperature deformation seems to be best explained by a much greater glide and climb mobility of jogs on screw dislocations at high temperature.

Electron-transmission microscopy of magnesium oxide promises to further clarify the mechanism of dislocation multiplication in crystals having the sodium chloride structure. It may also lead to a much more satisfactory understanding of the brittleness exhibited by ionic crystals.

Most of the work reported in this abstract was conducted at the Department of Metallurgy at Cambridge University in England during the author's tenure of a National Science Foundation Senior Postdoctoral Fellowship (on leave from the University of California). The experiments were done in cooperation with Dr. A. Kelly, Dr. G. K. Williamson, and Mr. J. Groves.

Work in this area will in the future be funded through LRL.

6. RESEARCH IN PROGRESS IN ELECTRON MICROSCOPY, 1961

Electron Microscope Studies of Alloys

Gareth Thomas

(a) Martensitic Reactions

A study has been made of the diffusionless transformation that occurs in Cu–12% Al alloys when quenched from a high temperature. The transformation is b. c. c. → distorted h. c. p. martensite. The interesting feature is that the martensitic structure is twinned on a very fine scale (see Fig. II C. 6-1.) These twins form on the {1120} planes. From the electron diffraction patterns the c/a ratio has been determined as 1.6. The form of the martensite is similar to that observed in high-carbon and alloy steels. Further studies are to be made on some of these ferrous alloys.

(b) Age Hardening of Alloys

Work on alloys has been concentrated on Cu-Be, which is an age-hardening alloy, and a complete analysis has been carried out for a commercial copper-beryllium alloy containing 2% Be and 0.2% Co.

Hardening is associated with precipitation of thin platelike clusters of Be atoms on {100} planes which give rise to one-dimensional diffraction effects (see Figs. II C. 6-2 and II C. 6-3). The dislocations in this alloy are dissociated. It is hoped to pursue this further, using a wide range of alloys.

ZN-2808

Fig. IIC. 6-1. Cu-12% Al quenched from 850 °C, showing martensite needles with twins; × 80,000.

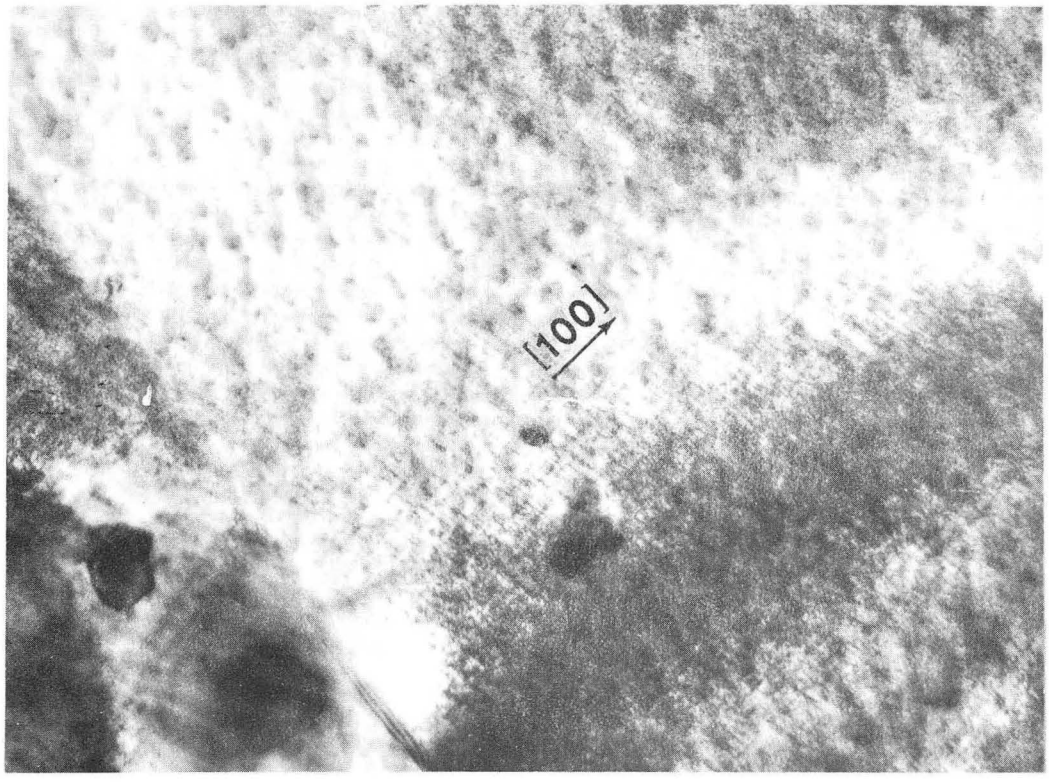

ZN-2810

Fig. IIC.6-2. Cu-2% Be-0.2% Co, aged 1 hr at 100 °C; × 40,000. Note precipitates in ⟨100⟩.

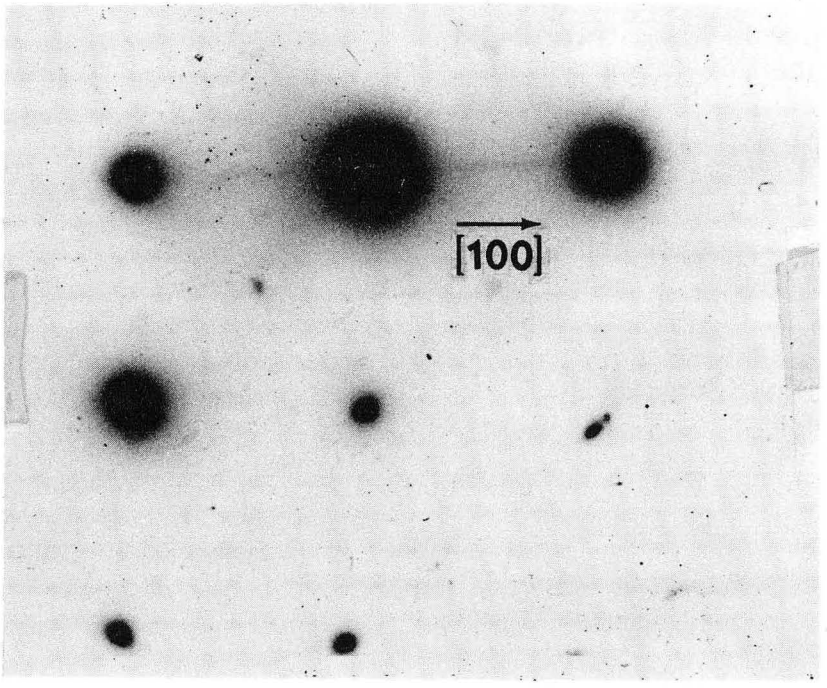

ZN-2811

Fig. IIC. 6-3. Electron-diffraction pattern of alloy shown in Fig. IIC. 6-2. Note streaks parallel ⟨100⟩ .

J. E. Dorn

1. Thin foils have been prepared for viewing by transmission electron microscopy. These experiments will reveal the details of dislocation motion and the interactions of the moving dislocations with each other, and other perturbations of the crystal lattice.

J. Washburn

1. Deformation Substructures in Copper

Specially oriented single crystals of high-purity copper are being deformed in tension and then examined by transmission electron microscopy. The relationship between flow stress and dislocation substructure is being studied.

2. Nucleation of Cracks

Etch-pit observations have shown that cracks are frequently formed in magnesium oxide at the stress concentration where two slip bands cross. Slip-band intersections are being examined by transmission electron microscopy in an attempt to determine whether or not any of the proposed dislocation mechanisms for crack nucleation can be observed.

II D. HIGH-TEMPERATURE REACTIONS

1. THE DISSOCIATION PRESSURES AND HEATS OF FORMATION OF THE MOLYBDENUM SILICIDES*

Alan W. Searcy and A. G. Tharp

The silicon partial pressures for the dissociation of the three molybdenum silicides Mo_3Si, Mo_5Si_3, and $MoSi_2$ have been measured by the Knudsen effusion method. The apparatus and procedures were similar to those described by Searcy and McNees.[1]

Both molybdenum and tungsten Knudsen cells were used. Hole areas were varied by a factor of six to determine whether there was any substantial deviation from equilibrium conditions.

All samples used in these measurements were made by direct synthesis from the elements. Temperatures were measured with a Leeds and Northrup optical pyrometer. Pressures were calculated from the usual Knudsen equation, assuming that only silicon vapor was effusing from the cell.

Preliminary vapor pressure measurements for Mo_3Si showed that the rate of vaporization of silicon decreased with time. This apparently resulted from the impedance to escape of the silicon vapor caused by the residual molybdenum. To minimize this effect the sample was reground to a fine powder after each determination and treated as a fresh sample for the next determination.

Dissociation pressures were measured over the temperature range 2015 to 2280 °K. At the lower temperatures the pressure was very low, an this, combined with the effect described above, caused a considerable scatter in the data. However, variation in the area of the effusion hole did not result in any systematic change in the measured vapor pressures.

Because of the scatter in the data a Third-Law analysis was considered superior to the usual plot of log P versus $1/T$ as a method of determining the heat of dissociation. The value of ΔC_p for the dissociation reaction,

$$Mo_3Si(s) \rightarrow 3Mo(s) + Si(g), \qquad (1)$$

was estimated to be -2.5 cal deg^{-1}. This value was combined with data from Stull and Sinke[2] and from King and Christensen[3] to calculate

---

*Published paper, J. Phys. Chem. 64, 1539 (1960).

[1] A. W. Searcy and R. A. McNees Jr., J. Am. Chem. Soc. 75, 1578 (1953).

[2] D. R. Stull and G. C. Sinke, Thermodynamic Properties of the Elements (American Chemical Society, Washington, D. C., 1956).

[3] E. G. King and A. U. Christensen, Jr., J. Phys. Chem. 62, 499 (1958).

$-(\Delta F_T - \Delta H_{298})/T$ at the various temperatures. From these quantities and the experimental data, values of ΔH_{298} were calculated. The mean ΔH_{298} was found to be 131.9 ± 1.2 kcal.

The dissociation pressures for Mo_5Si_3 were measured at various temperatures ranging from 2050 to 2261 °K. Heat content and entropy data for this compound are not available, but these data can be estimated by assuming that both $(H_T - H_{298})$ and the entropy are additive functions of the constituent atoms, an approximation which is a very good one for both Mo_3Si and $MoSi_2$. Accordingly, then, the values of $-(\Delta F_T - H_{298})/T$ for the reactions

$$3/4Mo_5Si_3(s) \rightarrow 5/4Mo_3Si(s) + Si(g) \qquad (2)$$

$$5/7MoSi_2(s) \rightarrow 1/7Mo_5Si_3 + Si(g) \qquad (3)$$

should be approximately the same as for the reaction

$$Mo_3Si(s) \rightarrow 3Mo(s) + Si(g).$$

From these estimated values and the experimental data, ΔH_{298} for Reaction (2) was found to be 131.1 ± .7 kcal.

For $MoSi_2$, measurements were made over the temperature range 1926 to 2156 °K. From the estimates mentioned previously and the experimental data, ΔH_{298} was found to be 117.2 ± .6 kcal for Reaction (3).

For all three reactions the dissociation pressure can be expressed as a function of the temperature by means of equations of the form

$$\log P = a/T - 5.75 \log T + b$$

in which a and b are constants and 5.75 is equal to $\frac{\Delta C_p}{R}$ for the reaction. To obtain the best values of a and b, the values of ΔH_{298} are combined with the free energy functions to calculate values of log P at each extreme of the temperature range. These two calculated pressures are then used to evaluate a and b. For reaction (1), a = -33.690, b = +28.94; for reaction (2) a = 32,940, b = +28.67; and for reaction (3), a = -29,800, b = 28.62.

The heat of formation of each molybdenum silicide can be calculated by combining the values of ΔH_{298} for the reactions with the heat of sublimation of silicon at 298° K, which is 108.4 ± 3 kcal.[4] The values thus obtained are -23.4 ± 4 kcal for Mo_3Si, -22.6 ± 5 kcal for $(1/3)Mo_5Si_3$, and -13.0 ± 5 kcal for $(1/2)MoSi_2$. Robins and Jenkins[5] have made calorimetric measurements

[4] S. G. Davis, D. F. Anthrop, and A. W. Searcy, J. Chem. Phys., in press.

[5] D. A. Robins and I. Jenkins, Acta Met. 3, 598 (1955).

on a compound identified as Mo_3Si_2, which is presumably Mo_5Si_3.[6] Their results would give -23.4 kcal for the heat of formation of $(1/3)Mo_5Si_3$. For $(1/2)MoSi_2$ they obtained -15.7 kcal as the heat of formation.

This work was supported by the Metallurgy and Materials Branch of the Office of Naval Research and is in an area that will be supported by LRL after August 31, 1961.

[6] B. Aronsson, Acta Chem. Scand. 9, 137 (1955).

2. VAPOR PRESSURE OF SILICON AND THE DISSOCIATION PRESSURE OF SILICON CARBIDE*

Stanley G. Davis, Donald F. Anthrop, and Alan W. Searcy

Elucidation of the vaporization equilibria for silicon and the silicon-carbon phase system is of exceptional interest. Direct determinations of the vapor pressure of silicon have yielded values for the heat of sublimation at 298 °K that range from 90[1] to 105 ± 12 kcal.[2] A mass spectrometer investigation demonstrated that silicon atoms are the principal vapor species at temperatures below 2000 °K.[2]

Experiments by Ruff indicated that carbon is present in silicon carbide vapor at concentrations higher than can be explained as due to elemental carbon molecules and atoms.[3] More recently, Kleman tentatively identified some of the spectroscopic bands obtained by heating silicon in a graphite furnace as bands of SiC_2 molecules.[4]

This paper reports results of Knudsen effusion investigations of both the vapor pressure of silicon in a silicon-carbide-coated graphite Knudsen effusion cell and of silicon carbide–graphite mixtures in a graphite cell. The silicon carbide–graphite mixtures provide silicon carbide dissociation pressure data from which the heat of dissociation of silicon carbide can be calculated. Combination of this heat with the heat of formation of silicon carbide yields an indirectly determined value for the heat of sublimation of silicon.

* Paper accepted for publication in J. Chem. Phys.

[1] L. Brewer, Paper No. 3 in Chemistry and Metallurgy of Miscellaneous Materials: Thermodynamics, edited by L. L. Quill (McGraw-Hill Book Co., Inc., New York, 1950).

[2] R. E. Honig, J. Chem. Phys. 22, 1610 (1954).

[3] O. Ruff, Trans. Electrochem. Soc. 68, 87 (1935).

[4] B. Kleman, Astrophys. J. 123, 162 (1956).

While this work was in progress, detailed information about the vapor species above silicon carbide became available as a result of a mass spectrometic investigation by Drowart, De Maria, and Inghram.[5] Those investigators have measured ion intensities for Si^+, SiC^+, SiC_2^+, Si_2^+, Si_2C^+, $Si_2C_2^+$, Si_3^+, $Si_2C_3^+$, and Si_3C^+ produced by heating silicon carbide in a graphite cell at 2100 to 2300 °K, and have calculated the heat of sublimation of silicon to silicon atoms. This heat of sublimation yields calculated silicon pressures that are lower by about a factor of 10 than the pressures calculated from the direct mass spectrometric measurements by Honig.[2] Better agreement would be expected.

The relative concentrations of gas molecules in a complex vapor mixture cannot be determined by a Knudsen effusion study in which only the total weight loss is measured as a function of time. However, if the relative concentrations of gas molecules are known, total weight-loss measurements can give more precise values for the pressures of the principal gaseous species--in this system silicon atoms--than can a mass spectrometer. The total weight-loss measurements can be corrected for the contributions of the minor vapor species from the mass spectrometric data to yield silicon atom pressures which should be more reliable than silicon pressures obtained from either mass spectrometer or total weight-loss measurements alone.

Since reliable entropy data are available for the dissociation reaction of silicon carbide, the heat of reaction can be calculated most precisely from the individual vapor pressure measurements combined with the known entropy for the reaction. The heat of the reaction SiC(s) = Si(g) + C(s) at 298 °K is thus calculated as 126.0 ± 3 kcal. When this heat is combined with the heat of formation of silicon carbide recommended by Humphrey,[6] the heat of sublimation of silicon is calculated as 112.6 ± 3 kcal.

The evaporation of liquid silicon from a silicon-carbide-coated graphite cell yields the heat of sublimation of silicon directly. The measured pressures above this system were corrected for the concentrations of molecules that should be present in the vapor.[5] The high-temperature heat capacity data of Olette[7] for solid and liquid silicon were used in the calculation of ΔH_{298}. Combination of the measured silicon pressures with known entropies then yields, for the heat of sublimation of silicon to silicon atoms, 108.4 ± 3 kcal at 298 °K.

No explanation has been found for the discrepancy between the heats of sublimation of silicon calculated from the direct vapor pressure measurements and from the silicon carbide dissociation pressure measurements. The excellent agreement of the dissociation pressure measurements with the data of Drowart supports adoption of the conclusion that the vapor pressure

---

[5] J. Drowart, G. de Maria, and M. G. Inghram, J. Chem. Phys. 29, 1015 (1958).

[6] G. L. Humphrey, S. S. Todd, J. P. Coughlin, and E. G. King, Bureau of Mines Report of Investigations 4888, 1952.

[7] M. Olette, Compt. rend 244, 1033 (1957).

data are substantially correct and that the heat of the reaction SiC(s) = Si(g) + C(s) is 126.0 ± 3 kcal at 298 °K. Furthermore, an unpublished mass spectrometric investigation of the evaporation of liquid silicon, reported since the completion of this work, leads to a heat of sublimation of silicon of 107 ± 3 kcal,[8] in excellent agreement with our value of 108.4 ± 3. The best interpretation of the data appears to be to presume that both sets of vapor pressure measurements are substantially correct and that the discrepancy between the heats calculated from the direct and indirect determinations lies, at least in part, in thermal data outside this investigation.

The discrepancy between the values for the heat of sublimation of silicon can be reconciled by the hypothesis that the heat of formation of silicon carbide at 298 °K is more negative than the reported value of -13 ± 1 kcal.[6] From phase equilibria for the condensed phase silicon-carbon system, the heats of formation of both cubic and hexagonal silicon carbide are concluded to be -15.0 ± 2 kcal.

If the heat of formation of silicon carbide is -15 and the heat of sublimation of silicon is 108.4 kcal, the heat of dissociation of silicon carbide to silicon vapor and carbon solid at 298 °K is calculated to be 123.4 instead of 126.0 kcal. The remaining discrepancy most probably lies in the dissociation pressure measurements, but the discrepancy is now within our expected uncertainties.

This work has been funded by separate AEC contracts and will be transferred to LRL, March 1961.

[8] J. Drowart and G. de Maria, quoted by M. G. Inghram in Advance Papers of An International Symposium on High-Temperature Technology, Asilomar, California, October 1959.

3. THERMODYNAMIC PROPERTIES OF C_2*

Robert L. Altman

Recent spectroscopic data[1, 2] indicate that the $^1\Sigma_g^+$ state of C_2 is about 616 cm^{-1} below $^3\Pi_u$ state hitherto considered the ground state.[3] Ballik and Ramsay[2] have also provisionally obtained the molecular constants of a new $^3\Sigma^-$ state whose excitation energy is somewhat higher than the $^3\Pi_u$ state. We have recomputed the thermodynamic properties of C_2. The enthalpy and free energy functions are unaffected by this omission up to 3500 °K. If the uncertain data of the $^3\Sigma_u^+$ state had been included in these calculations, the enthalpy at 4000 °K would be greater by 0.1 kcal/mole and the free energy function by 0.01 eu.

The ground-state partition function was evaluated with the method of Pennington and Kobe.[4]

We have compared these results at 2000 and 2500 °K with other published thermodynamic tables,[5, 6] and note that Pitzer[5] and Altman[6] give values different from those found here.

Drowart et al.[7] have reported heats of sublimation for diatomic carbon of 195.8 kcal/mole *2nd law) and 198.0 (3rd law), based on Pitzer's thermodynamic data. With the new data, these values are reduced to 194.2 and 196.9, respectively, in excellent agreement with Brewer et al.[8]

This work was supported through a contract with the Metallurgy Branch of the AEC.

---

*Brief form of published paper, J. Chem. Phys. 32, 615 (1960).

[1] E. A. Ballik and D. A. Ramsay, J. Chem. Phys. 31, 1128 (1959.

[2] E. A. Ballik and D. A. Ramsay (private communication).

[3] J. G. Phillips, Astrophys. J. 107, 389 (1958).

[4] R. E. Pennington and K. A. Kobe, J. Chem. Phys. 22, 1442 (1954).

[5] K. S. Pitzer and E. Clementi, Large Molecules in Carbon Vapor, UCRL-8675, March 1959.

[6] R. L. Altman, Thermodynamic Properties of Propellant Combustion Products, Rocketdyne Report 669.

[7] J. Drowart, R. P. Burns, G. De Maria, and Mark G. Inghram, J. Chem. Phys. 31, 1131 (1959).

[8] Brewer, Hicks, and Krikorian, J. Chem. Phys. (in press).

4. CHEMICAL CONSIDERATION OF HIGH-TEMPERATURE THERMOELECTRIC POWER DEVELOPMENT*

Alan W. Searcy and David J. Meschi

The maximum theoretical efficiency of any heat engine is limited by the difference in temperature between the hot and cold portions of the thermal cycle. If thermoelectric devices can be adapted for use with very high temperature sources, the over-all efficiency of these devices may possibly be raised to the point where they could compete with more conventional power sources.

There are several ways in which the thermoelectric principle may be applied, but this discussion will be limited to solid semiconductors which may be suitable for use as thermoelectric elements at temperatures above 1500 °K.

To be a semiconductor, a material must have a band gap of a few electron volts. Silicon and germanium are two elements which meet these requirements. There are many group III - group V binary compounds, which have a similar diamond type structure and the same number of valence electrons as silicon and germanium. It is notable that in these, as well as certain other classes of binary compounds, the band gap depends largely on two primary factors: the average row in the periodic table of the atoms in the compound, and the ionic character of the bonds. The higher the average row in the periodic table, and the greater the ionic character, the wider the gap.

As an example of the first principle, an arsenide would have a smaller gap and hence be a better conductor than a nitride of the same element. From the second principle, one would expect that nitrides would be better conductors than oxides.

These simple rules can be applied with reasonable safety only to compounds in which both constituents are in their normal valence states. For instance, they do apply to TiO_2 or BaO, but not to TiO or BaO_2. For these other compounds a cruder rule which can usually be applied is that the band gap decreases as the proportion of metallic constituent is increased (e. g. TiO should be at least as good a conductor as TiO_2).

High temperature thermoelectric elements must obviously be chosen from those materials which are stable at high temperatures. A survey of such materials can be found in High Temperature Technology.[1]

From these materials one may then select those which have thermoelectric properties. In addition to the inherent semiconductors, there are also compounds whose conductivities are too low to be useful in the pure state, but which could conceivably be doped with some material to make them semiconductors. An example of this type of compound is boron nitride.

---

*Published in Thermoelectricity, ed. Paul Egli, John Wiley and Sons, New York, 1960.

[1] High Temperature Technology, I. E. Campbell, John Wiley and Sons, New York, 1956.

All of the compounds referred to hitherto have been binary. There are also possibilities among the more complicated compounds, such as carbonitrides, mixed oxides, etc., but less is known about the high temperature properties of these classes of substances.

In addition to the rather simple considerations mentioned above, one must also keep in mind several other somewhat more complicated factors in designing a high temperature thermoelectric device. To begin with, the couple materials at the junction must be thermodynamically stable with respect to each other, or they must be shielded from each other by the interposition of some suitable material between them. There is available much information on two component systems; but data on ternary systems are somewhat scarcer. However, a judicious use of the data available allows one to make many predictions about the stability of various substances in contact with each other.

Doped semiconductors introduce the additional complication of diffusion. Under the influence of the thermal gradient the doping material would tend to diffuse to one end of the element and establish a concentration gradient as well. It is difficult to evaluate this gradient because at least three different flow processes are involved: thermal, material, and electrical. The solution of this problem would lie in the realm of thermodynamics of irreversible processes. If one ignores the influence of the electrical current, then it is easier to predict at least qualitatively the steady state concentration of the doping material under the influence of a thermal gradient, by the use of thermodynamic data. A main difficulty to be avoided, obviously, is the separation of the doping material as a separate phase in cases of limited solubility.

Good experimental data on this type of problem is lacking, however. If such data were available it would conceivably be possible to pre-dope the element with the same concentration gradient which would correspond to the anticipated steady state conditions. This would result in constant performance characteristics.

Also, from the research view point, it would be interesting to turn the problem around and use the effect of doping materials on the conducting properties of a material as a means of studying diffusion in solid phases.

This work is presently funded by the Office of Naval Research, but will be transferred to LRL in September, 1961.

5. KINETICS OF REACTION BETWEEN BARIUM METATITANATE AND BARIUM CARBONATE TO FORM BARIUM ORTHOTITANATE*

Eric R. McCartney, Joseph A. Pask, and Lieselotte K. Templeton

The solid-state reaction in this system was followed at temperatures of 800 to 1050 °C by gravimetrically measuring the CO_2 evolved during the reaction. The difficulty, normally encountered with powders, of determining the actual reacting surface areas did not materialize in this study because of the formation of a mobile BaO-containing liquid phase on the surfaces of the $BaCO_3$ particles which readily spread over the available surfaces of $BaTiO_3$ and Ba_2TiO_4.

The geometry of the system was found to be responsible for the type of kinetics realized. In general, the reaction rate was faster when the particles of both reactants were finely divided and when reactants with larger amounts of impurities were used. Mixtures of uniformly very finely precipitated $BaTiO_3$ with fine $BaCO_3$ closely followed a first-order rate law. The controlling step here was postulated as being a chemical reaction or nucleation process occurring at the surface of the $BaTiO_3$ particles. However, when one of the reactants was coarse, a product layer was formed through which diffusion had to occur for the reaction to go to completion. Diffusion is actually the rate-controlling step at these temperatures. When the $BaCO_3$ particles were coarse, the fine $BaTiO_3$ particles packed in the void network formed by the $BaCO_3$ particles. The Ba_2TiO_4 product, which has a larger specific volume than $BaTiO_3$, then had an opportunity to expand into the $BaTiO_3$ void network without rupture, resulting in a parabolic rate law. When the $BaTiO_3$ particles were coarse, however, the Ba_2TiO_4 product layer that formed on the surface quickly reached an over-all limiting thickness that was maintained through the balance of the reaction by cracking or flaking, resulting in a zero-order rate law. Materials with a range of particle sizes first exhibited a first-order type of behavior followed by a diffusion-controlled behavior. In this temperature range the diffusion process is the slow step; the first-order relationship is obtained for the fine particles because diffusion distances are small. It is expected that at lower temperatures the chemical reaction process is the slow step.

The initial diffusion step into $BaTiO_3$ prior to the nucleation process was apparently always fast, and thus not a rate-determining step.

The activation energy for the chemical reaction or nucleation process was 56 to 59 kcal/mole; for the diffusion process, 28 to 31 kcal/mole. The purity of the reactants affected the reaction rate but not the activation energy.

This research problem, supported by the Office of Naval Research, is included in these reports in order to give a reasonably complete representation of the type of research being considered in the Ceramics Group.

---

* From Eric R. McCartney, Joseph A. Pask and Lieselotte K. Templeton, The Solid-State Reaction Between Barium Metatitanate and Barium Carbonate to Form Barium Orthotitanate, in Proceedings of Fourth International Symposium on Reactivity of Solids (to be published this spring).

6. GLASS-METAL BONDING: WETTABILITY OF IRON BY SODIUM SILICATE GLASSES

Joseph A. Pask, Richard M. Fulrath, S. Frederick Ravitz, Lucy G. Hagan, Robert W. Cline, and Robert B. Adams

An experimental unit was developed to allow the application of a glass specimen onto a metal or solid surface at elevated temperatures under controlled atmospheric conditions.

Sodium disilicate glass on Armco iron in vacuum at 900 to 1000 °C showed a contact angle of 55 ± 2 deg; the adherence was poor. On magnetite, the contact angle was 2 ± 1 deg, and the adherence was excellent. Behavior of the glass on oxidized iron was affected by its ability to rapidly dissolve large quantities of the oxide. Glass, when dropped onto a lightly oxidized surface, spread toward lower angles and retracted essentially to the 55-deg angle upon solution of the oxide; adherence correspondingly ranged from good to poor. Under some conditions when the glass dropped onto a lightly oxidized surface, it became unbalanced, with one side in contact with oxidized surface and the other with clean metal. The resulting unbalance of forces, with the stronger driving force on the side in contact with oxide, caused the drop to move over the metal surface with only the leading edge in contact with oxide. When the glass dissolved a sufficient amount of iron oxide to cause crystallization of fayalite (Fe_2SiO_4) within it, the contact angle was in the range of 15 to 35 deg and the best adherence was obtained. Vaporization of iron in vacuum at 1000 °C was not retarded by thin oxide films.

Contact angles, and adherence on platinum and iron of sodium disilicate glasses with varying iron additions were also studied at 1000 °C in vacuum. On platinum, the iron concentration in the glass did not affect either the contact angle (about 12 deg) or the adherence, and no devitrification occurred in the glass. On iron, the contact angle decreased with increasing iron content in the glass, ranging from 55 to approximately 22 deg. Adherence was poor with no iron in the glass, and it increased as the iron content and reaction at the interface increased. Polished cross sections of the glass-iron assemblies showed a greater attack of the metal surface as the iron content in the glass increased, according to the reaction

$$Fe + 2\ Fe^{+++} \rightarrow 3\ Fe^{++}.$$

Crystals of fayalite were observed in the glasses as the iron content increased.

This research was primarily supported by separate AEC contract.

Related Papers:

Robert W. Cline, Richard M. Fulrath, and Joseph A. Pask, Fundamentals of Glass-to-Metal Bonding: V. Wettability of Iron by Molten Sodium Disilicate, J. Am. Ceramic Soc. (to be published).

Lucy G. Hagan and S. Frederick Ravitz, Fundamentals of Glass-to-Metal Bonding: VI. Reaction Between Metallic Iron and Molten Sodium Disilicate, J. Am. Ceram. Soc. (to be published).

Robert B. Adams and Joseph A. Pask, Fundamentals of Glass-to-Metal Bonding: VII. Wettability of Iron by Molten Iron Containing Sodium Silicate, J. Am. Ceram. Soc. (to be published).

7. RESEARCH IN PROGRESS IN HIGH-TEMPERATURE REACTIONS, 1961

Alan W. Searcy

1. The equilibrium species in evaporation of molten sulfur have been investigated, and the results are now being analyzed. (With M. Charles Zietz and Maynard Michel.)

2. The vaporization of magnesium oxide has been studied by Knudsen effusion techniques and the transpiration method, and the data are being compared with data obtained from spectroscopic techniques in order to establish the dissociation energy of MgO gas. (With Robert L. Altman.)

3. A phase reported by another investigator to be ThO has been found by us to be a more complex material. The data are being prepared for publication. (With Ray S. Newbury.)

4. A review of high-temperature inorganic chemistry is approaching completion. (Under ONR sponsorship.)

5. The kinetics of free surface evaporation of Zn_2SnO_4 is under investigation. (With Clarence L. Hoenig.)

6. Anomalous evaporization behavior of ZnO is being studied. (With T. C. M. Pillay.) (Under ONR sponsorship.)

7. The experimental limits of techniques of vapor pressure determination by direct force measurements are under study. (With David A. Schulz.)

8. The stabilities of ZnO, CdO, and other oxides are being measured by vaporization techniques. (With D. F. Anthrop.)

9. The vapor pressure of In_2S_3 is being determined. (With Alan R. Miller.)

10. A study of the limiting evaporation rate of metals in vacuum has been initiated to test conflicting theories. (With Zuhair A. Munir.)

11. The kinetics of reactions of gases at very low pressures with tungsten and other metals at high temperatures are being measured. (With D. J. Meschi and H. U. Anderson.) (Presently under ONR sponsorship, will continue under LRL.)

Joseph A. Pask

1. Determination of vapor species above MgF_2 measurement of vapor pressure of MgF_2. (With Eric R. McCartney and Lieslotte K. Templeton.)

2. Kinetics and mechanism of the reaction between MgF_2 (single crystals and powders) and H_2O vapor. (With Eric R. McCartney and Lieselotte K. Templeton.)

3. Theoretical studies of wetting and adherance in glass-metal systems.

REACTOR MATERIALS ENGINEERING

III.1. WORK IN PROGRESS, 1961

T. H. Pigford

Nuclear Field-Cycle Research

Work was initiated on this project in August 1960 at the level of two part-time graduate students. As the funding situation has clarified, additional graduate students have been added, and the level of effort is now at that projected for the remainder of this year. No publications or reports are issued yet.

The program of this first year is devoted mainly to development of basic equipment for the experimental program, literature search and analysis to determine most fruitful directions of experimental approach, and performance of a few screening experiments.

The area of immediate interest is the study of high-temperature solid-gas systems, with particular emphasis on the diffusion of gases in reactor materials at high temperature. Experiments are being designed to isolate and examine the various detailed mechanisms that may contribute to the kinetics of gas release from solids. Uranium dioxide is the first material under investigation. A small high-temperature furnace for gas-permeation studies is nearing completion, and preliminary operation and checking will be commenced soon. Among the first experiments will be the study of permeation of gas into the solid, when exposed in a system pressurized at temperatures up to 1700 °C. Possible equilibrium effects and release rates upon depressurization will be examined. Necessary vacuum equipment and systems for gas purification and analysis are under construction.

Apparatus is being developed to study the preparation of uranium-bearing refractory fuel bodies and coatings by electrophoretic deposition. The application of electrophoresis to inorganic chemical systems has been limited, with little investigation into the specific nature of the charge development on the colloidal particles. The application of electrophoresis has generally been towards the solution of specific problems, and empirically developed compositions of suspending media, suspended material, and surface-active agents are cited in the literature. The specific problem under investigation here is the study of interfacial relations between carbide surfaces and surface-active additives in organic suspending media. A literature survey is being completed, and construction of an electrophoretic cell is under way. A variable-voltage dc generator has been constructed.

A parallel study is under way to examine the performance of these coated materials as possible components of nuclear fuel elements. Thermionic fuel elements are included in the study, and equipment is being developed to study the gas evolution and thermionic-emission properties of these materials.

Preliminary studies* are under way to examine the kinetics of interphase transfer of uranium and fission products from these fuel bodies in the presence of temperature gradients in nonaqueous molten systems. A small laboratory furnace for holding a molten batch at a controlled temperature is being designed.

---

*This portion partially funded through another LRL division, is under the supervision of Professor D. R. Olander.